Molecular Dynamics Simulation of Nuclear Pasta

C.O.Dorso
(UBA, Universidad de Buenos Aires)

in collaboration with

P. Gimenez Molinelli (UBA)
P.Alcain (UBA)
J. Lopez (UTEP)

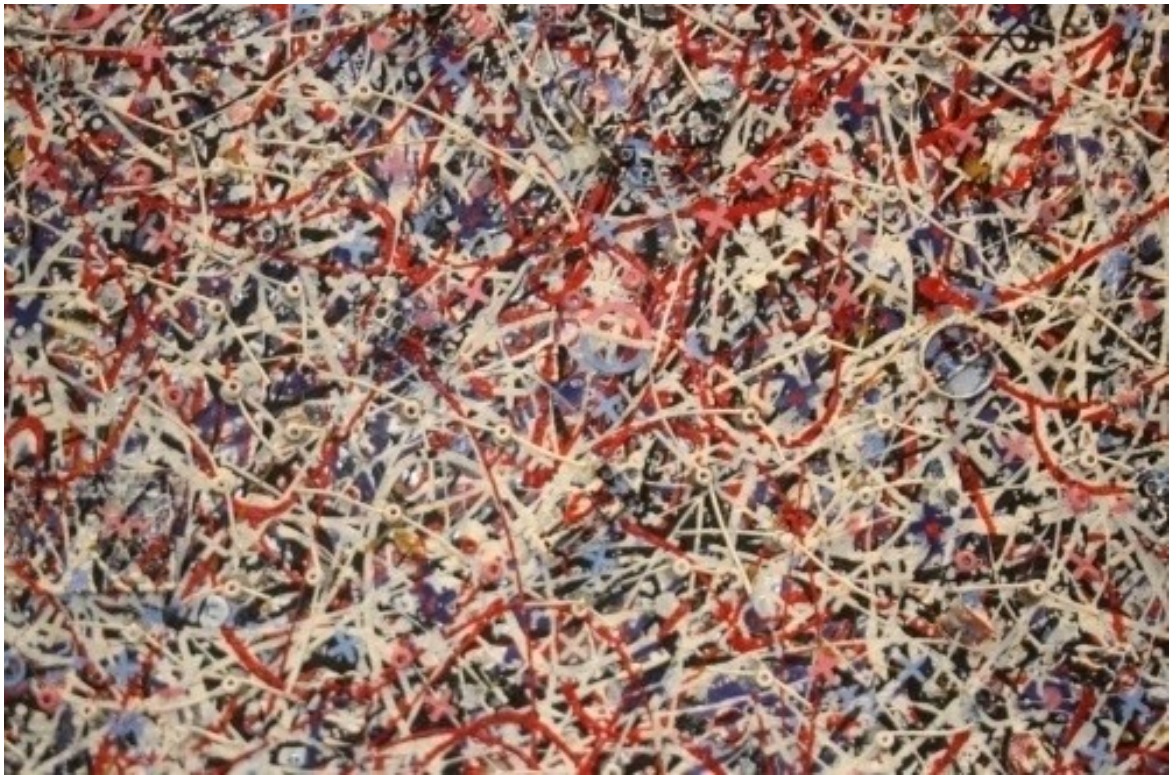

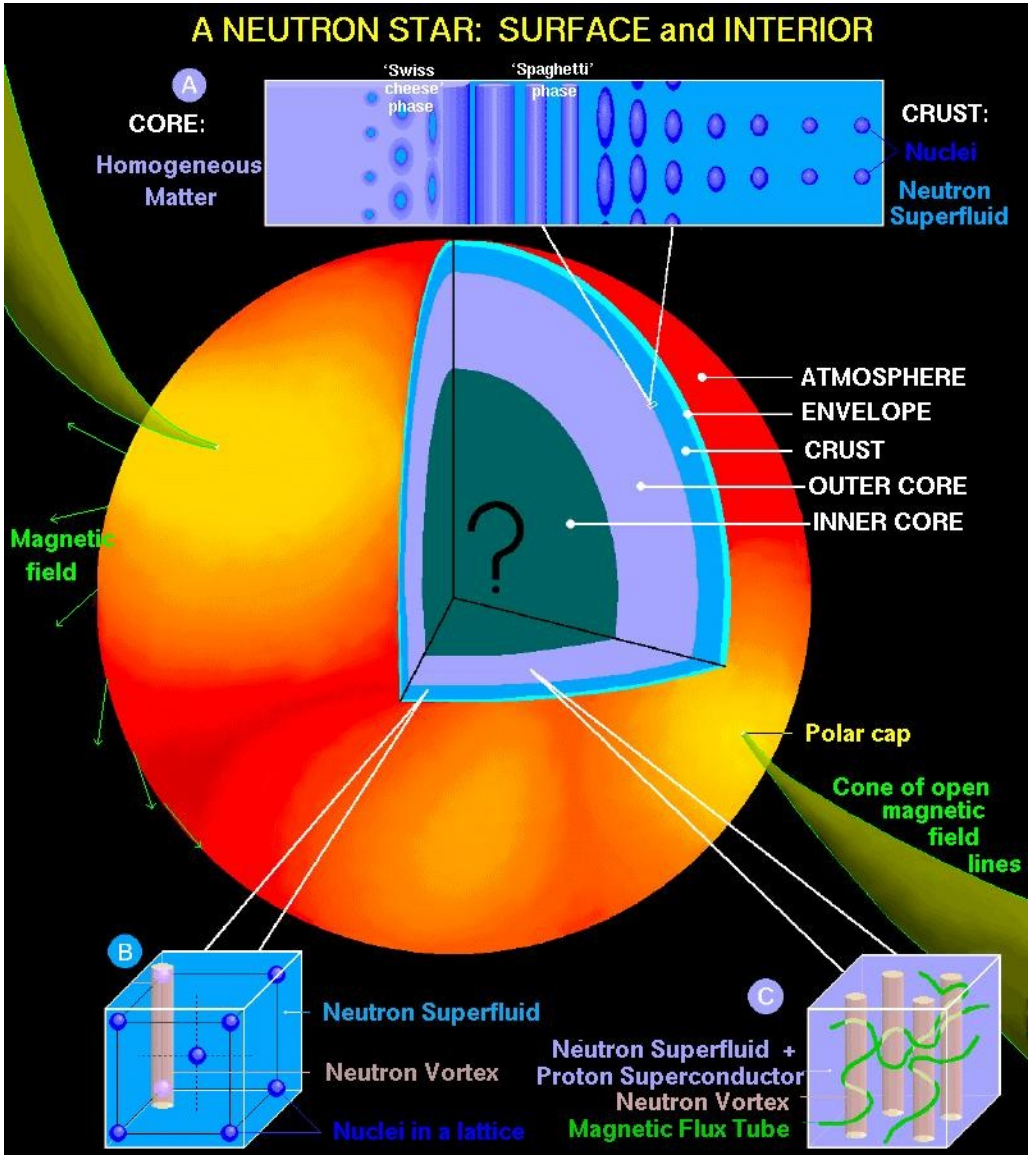

- $M \sim 1.4\ M_{\odot} \rightarrow 2\ M_{\odot}$
- $R \sim 10$ km
- $\rho \sim 10^{6}$ g/cm$^{3} \rightarrow 8 \times 10^{14}$ g/cm^{3}
- $x \sim 0{,}5 \rightarrow 0{,}2$ (?)
- T ~ 1 MeV (10^{10} K)

The Model, finite systems, nuclear collisions

What is nuclear Pasta?

What is the effect of periodic boundary conditions on the calculated morphology of the system?

What is the role of Coulomb interaction?

What is the role of the Debye screening length on the scale of heterogeneities?

Phase Transitions within Pastas?

Neutrino opacity?

Pastasciutta?

Expading (&fragmenting) infinite systems

The model, finite nuclei, fragmentation

CMD Model

Potential

$$V_{np}(r) = V_r\,[exp(-\mu_r r)/r - exp(-\mu_r r_c)/r_c] -$$
$$- V_a\,[exp(-\mu_a r)/r - exp(-\mu_a r_c)/r_c]$$
$$V_{nn}(r) = V_0\,[exp(-\mu_0 r)/r - exp(-\mu_0 r_c)/r_c]$$

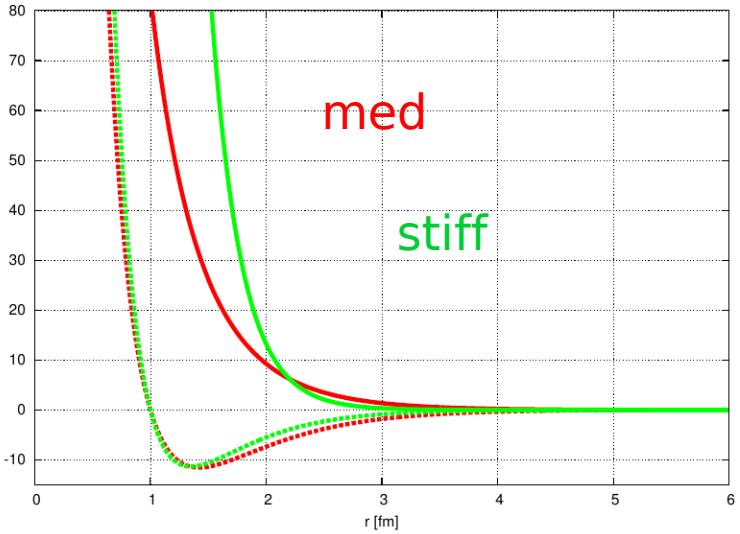

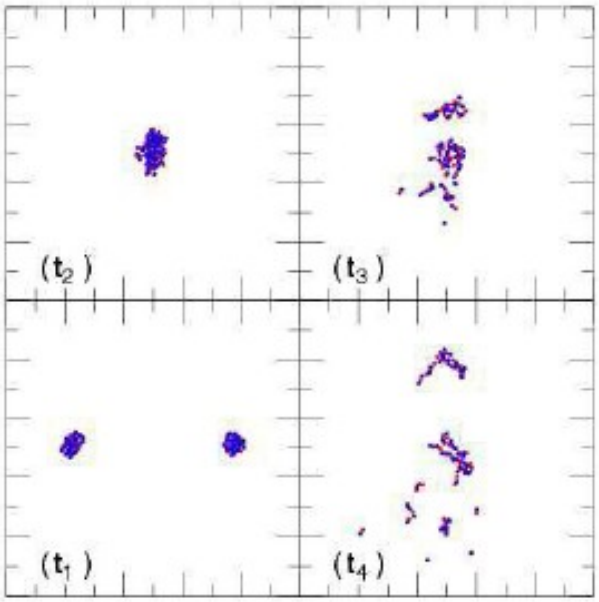

Dynamical evolution

CMD Model

According to original work

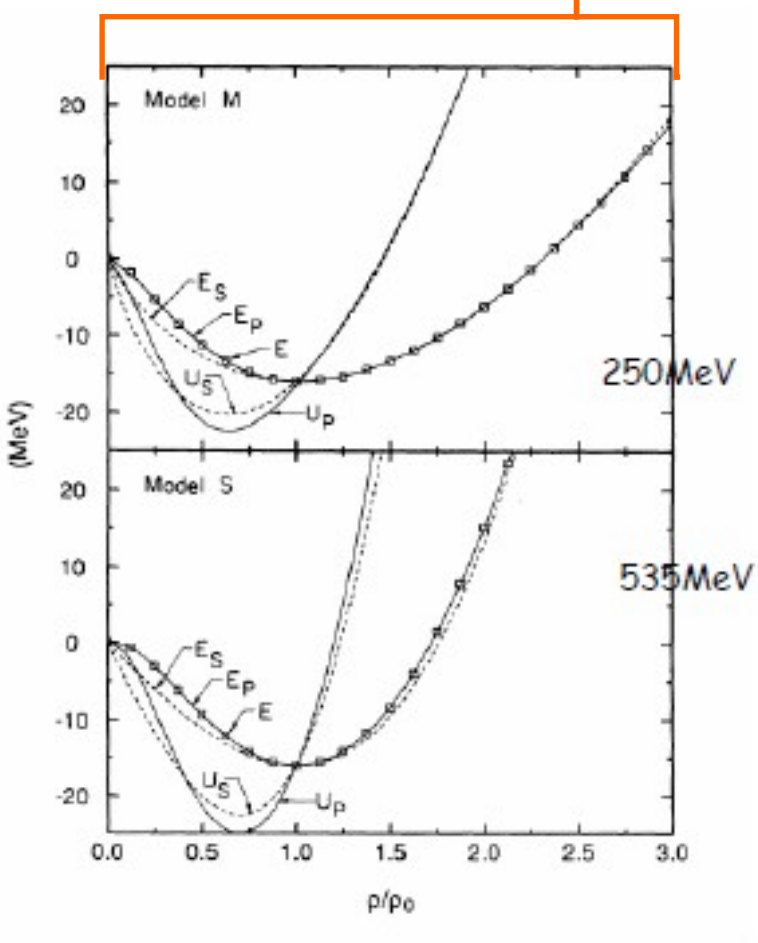

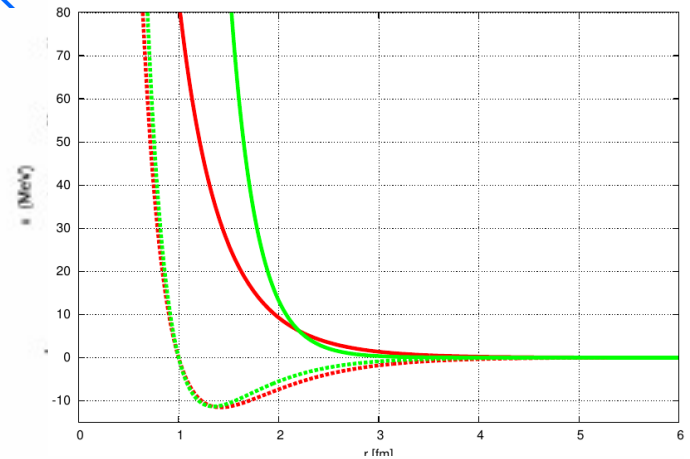

FIG. 1. The interparticle potentials v_{ss} and v_{sp} for the M (solid) and S (dashed) models.

TABLE II. Energies of nuclei (MeV/nucleon) for the M and S models compared to experimental binding energies.

A	Z	E_M	E_S	E_{exp}
2	1	−5.76	−5.67	−1.11
3	1	−7.14	−7.26	−2.83
4	2	−7.91	−7.05	−7.07
5	2	−7.47	−6.22	−5.47
16	8	−10.39	−10.49	−7.98
40	20	−10.44	−10.60	−8.55
90	40	−9.93	−10.25	−8.71
139	57	−9.12	−9.58	−8.38
197	79	−8.38	−8.84	−7.92

PHYSICAL REVIEW C VOLUME 42, NUMBER 1 JULY 1990

Accuracy of the Vlasov-Nordheim approximation in the classical limit

R. J. Lenk, T. J. Schlagel, and V. R. Pandharipande
Department of Physics, University of Illinois at Urbana-Champaign, Urbana, Illinois 61801
(Received 1 March 1990)

CMD Model

Collisions

- Solve equations of motion
  (Verlet, symplectic)
- Recognize clusters
  (MST, MSTE,ECRA)
- Determine mass spectra
- Study critical behavior
- Calculate Caloric Curves , **etc**

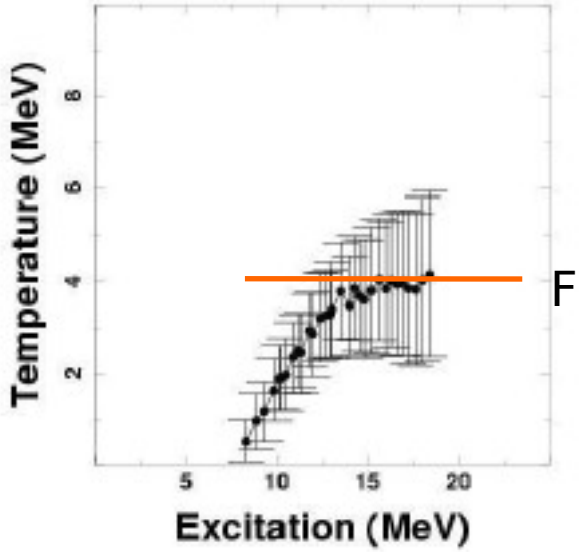

Flat CC

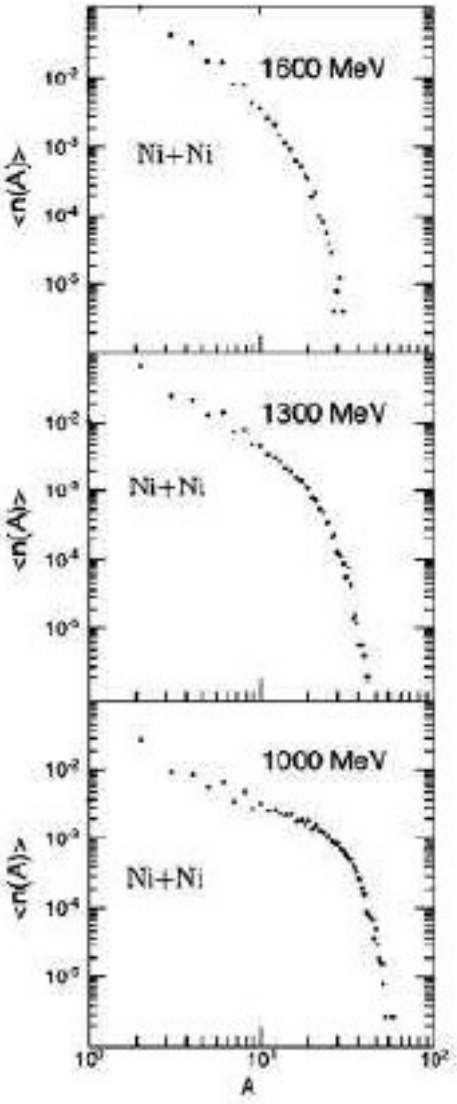

Fragment recognition algorithm

MST Clusters

Given a set of particles i,j,k,…, clusters are defined such that :

$$i \in C \Leftrightarrow \exists j \in C / (r_i - r_j) < r_{clust}$$

With r_{clust} the clusterization radius

With periodic boundary conditions

MSTE Clusters

In this case clusters are defined in the following way:

$$i \in C \Leftrightarrow \exists j \in C / (\frac{p_{ij}^2}{4\mu} - v_{ij}) < 0$$

With μ the reduced mass and p_{ij} the relative momentum

Early Cluster Formation Model

Given a set of particles (i,j,k..) clusters are defined as those partitions C_i that minimize the following expression:

$$E = \sum_{C_i} \left[\left(\sum_{i \in C_i} \frac{p_{ij}^2}{2m} \right)_{c.m.C_i} + \sum_{i<j, \in C_i} v(r_{ij}) \right]$$

This is a highly self consistent problem that has been solved by devising a method in the spirit of simulated annealing (ECRA).
For such a problem a Markov chain in the space of partitions is constructed

C.O.Dorso & J.Randrup Phys.Lett. B 301 (1993) 328

Ca + Ca at 80 MeV/A

QMD

ECRA

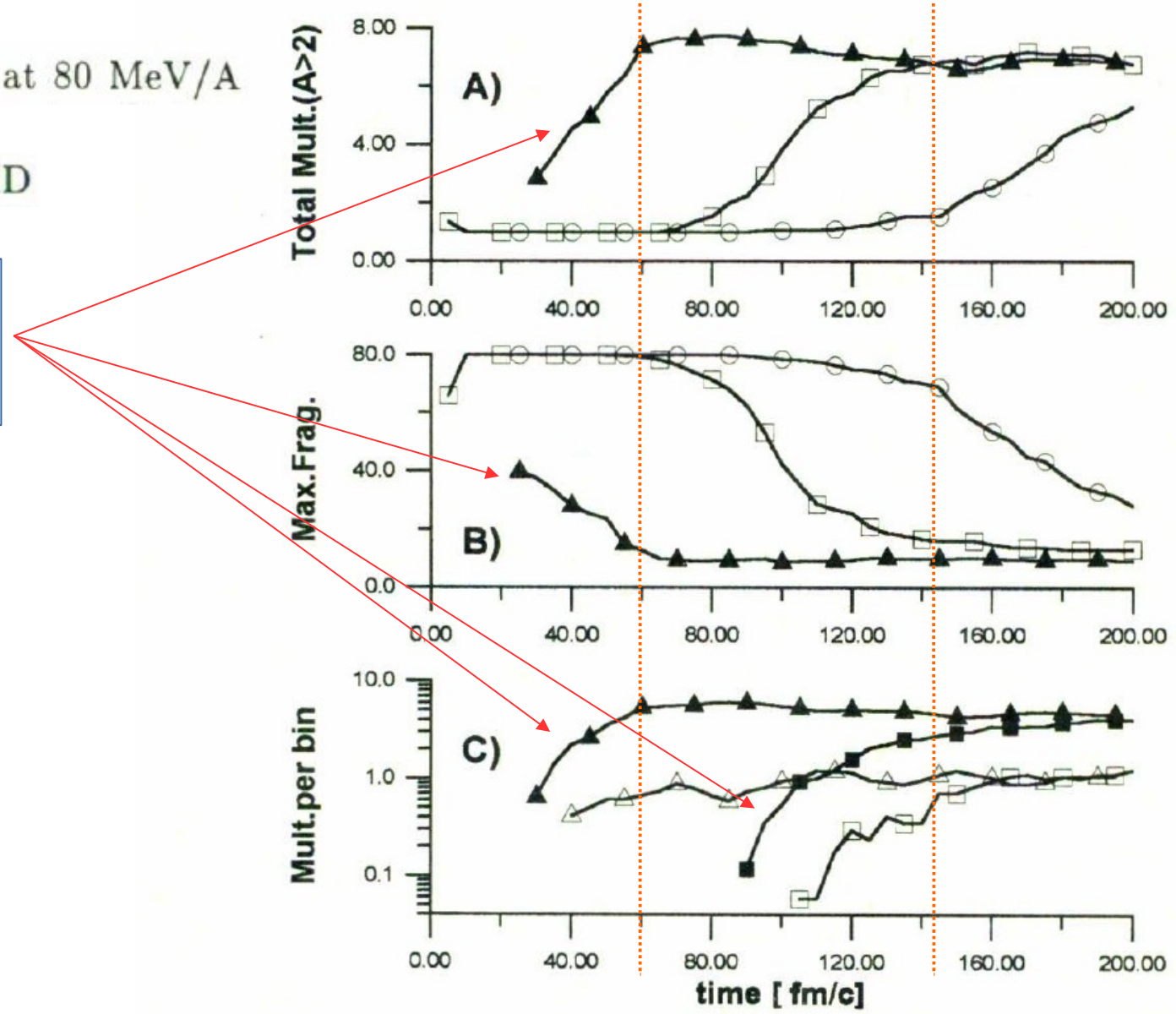

IGURE 1. (a) The total fragment multiplicity $A \geq 3$. (b) The largest fragment. The results from ıe ECRA algorithm are displayed as full lines with full triangles that of the MST algorithm as ıll line with open circles ($R = 6$ fm) and open triangles ($R = 3$ fm) lines, respectively. In (c), we ıow the multiplicity of fragments $3 \leq A \leq 5$ (full triangles denote ECRA results and full squares IST results) and $7 \leq A \leq 9$ (open triangles ECRA, open squares MST) as a function of time.

ECRA Clusters

Early Cluster Formation Model

Given a set of particles (i,j,k..) clusters are defined as those partitions C_i that minimize the following expression:

$$E = \sum_{C_i} \left[\left(\sum_{i \in C_i} \frac{p_{ij}^2}{2m} \right)_{c.m.C_i} + \sum_{i<j, \in C_i} v(r_{ij}) \right]$$

Solved using Puente's approximation

Lennard Jones

$$V(r) = 4\epsilon\left[\left(\frac{\sigma}{r}\right)^{12} - \left(\frac{\sigma}{r}\right)^{6}\right] - 4\epsilon\left[\left(\frac{\sigma}{r_{\text{cut}}}\right)^{12} - \left(\frac{\sigma}{r_{\text{cut}}}\right)^{6}\right], \quad (7)$$

with a truncation distance $r_{\text{cut}} = 3\sigma$, i.e. $V(r > 3\sigma)$

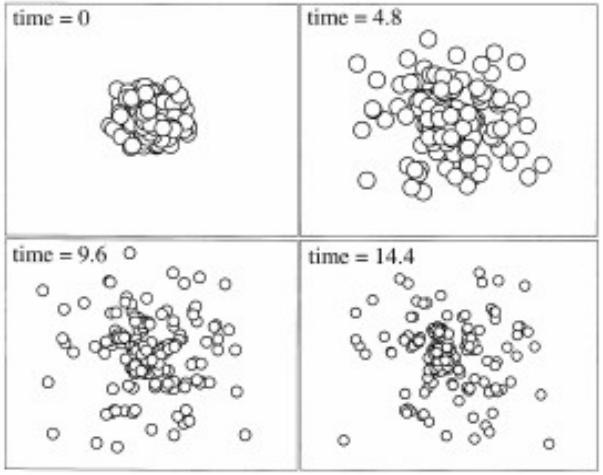

Fig. 1. Four instants corresponding to the disassembly of a typical event with $N = 216$ particles and a total energy per particle of $E/N = 0.3$.

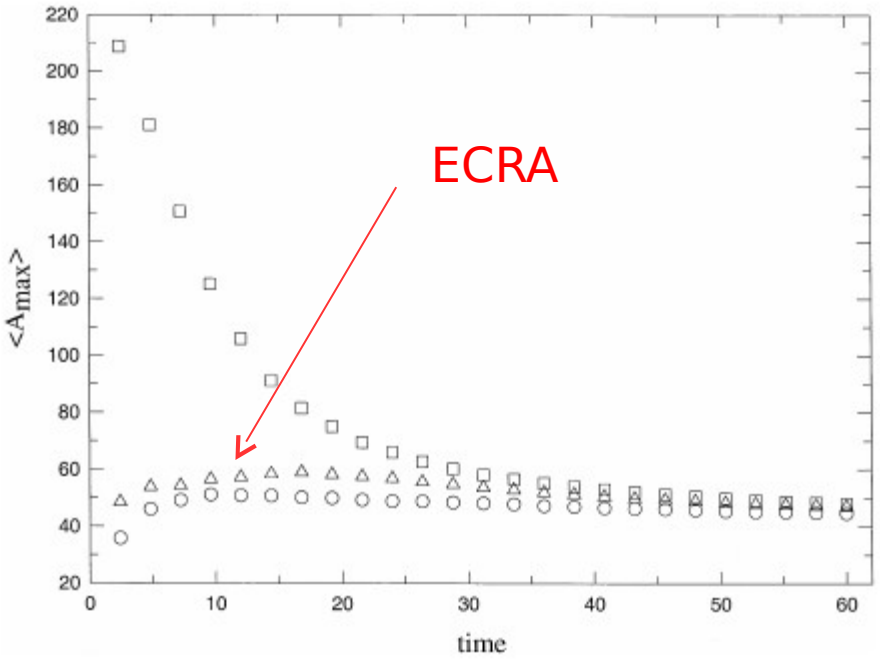

Fig. 2. Evolution of the average particle number of the largest fragment $A_{\max}$. The squares represent the geometrical analysis, whereas the circles indicates the results of the BFMX method. The results of the SA analysis are also shown for comparison (triangles).

Efficient recognition of clusters in molecular dynamics

A. Puente [1]

Departamento de Física, Universitat de les Illes Balears, 07071 Palma de Mallorca, Spain
LPTMS Université de Paris XI, Bât 100, 91405 Orsay Cedex, France

CMD Model

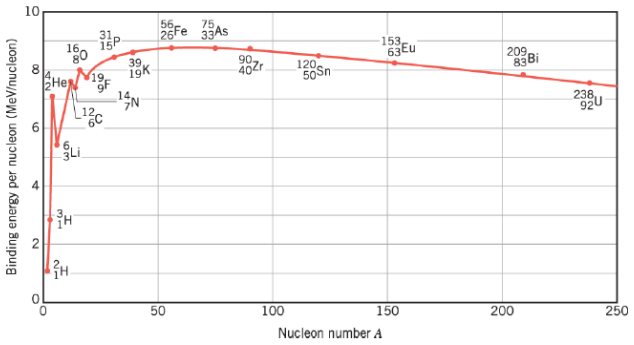

Table 1. Comparison of coefficients obtained for different models.

Coefficient	Stiff	Medium	Experimental
C_v	16.1	17.37	15.75
C_s	−11.73	−14.38	−17.8
C_c	−0.197	−0.226	−0.177
C_{sym}	−34.07	−25.08	−23.7

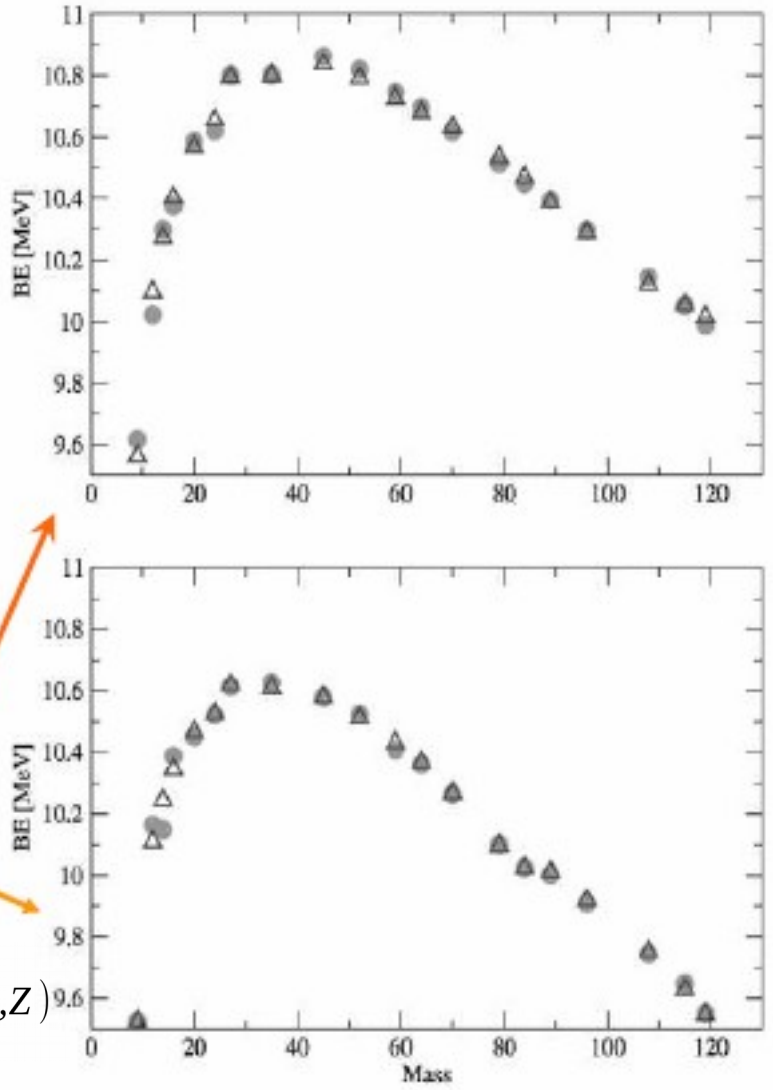

Figure 1. Energies obtained with the mass formula fit (triangles) for the stiff and medium models (top and bottom panels, respectively) together with the corresponding ground states calculated using frictional molecular dynamics (circles).

$$BE = C_v A - C_s A^{2/3} - C_c \frac{Z^2}{A^{1/3}} - C_{sym} \frac{(A-2Z)^2}{A} - \delta(A,Z)$$

Normalized parallel velocity Distribution calculated in the Center of mass for z>3 in Mid-peripheral ^{58}Ni+C reactions

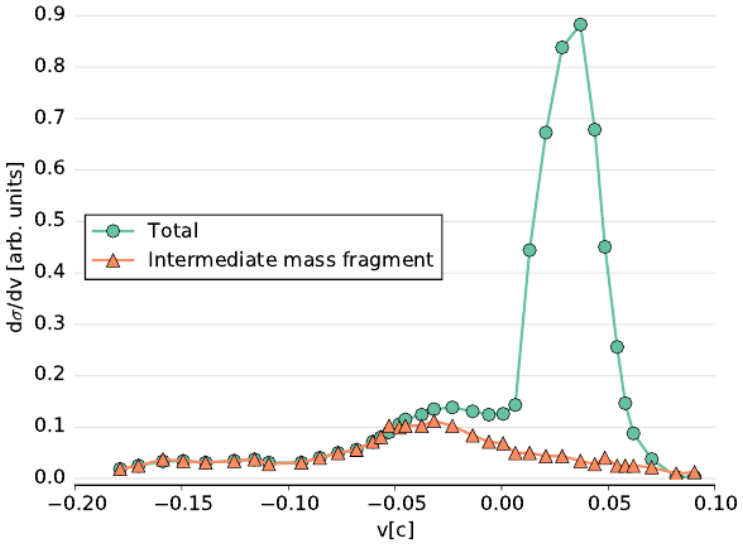

Exp.

(a) $\eta = 0.0001\,\mathrm{fm/c}$

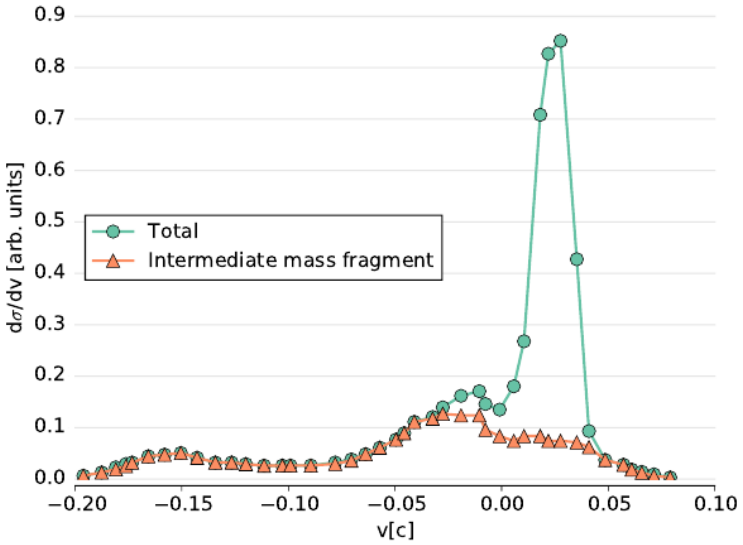

sim.

A Quasi-Classical Model of Intermediate Velocity Particle Production in Asymmetric Heavy Ion Reactions

A. Chernomoretz[1], L. Gingras[2], Y. Larochelle[2*], L. Beaulieu[2], R. Roy[2], C. St-Pierre[2], C.O.Dorso [1]
[1] *Departamento de Fisica, Universidad de Buenos Aires, Buenos Aires, Argentina.*
[2] *Laboratoire de Physique Nucléaire, Département de Physique, Université Laval, Québec, QC, Canada G1K 7P4.*
(January 8, 2014)

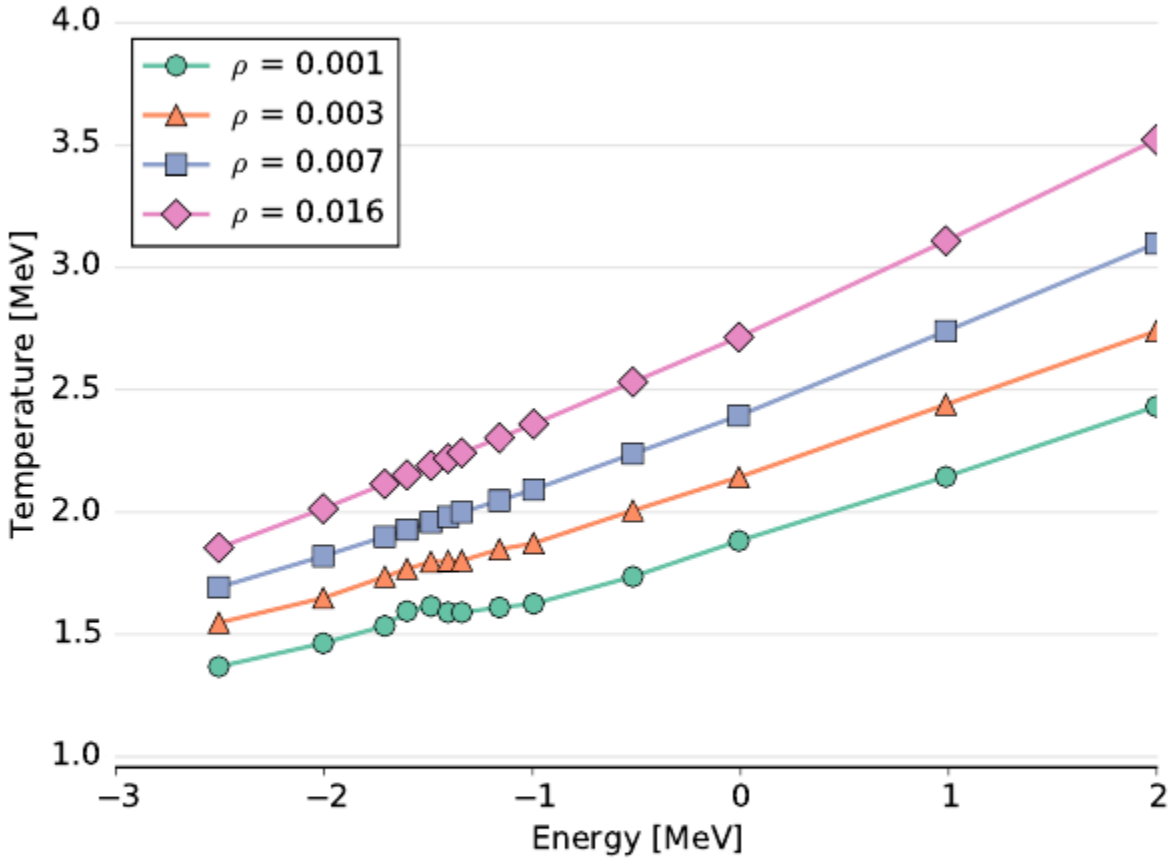

Figure 4: Caloric curve of a system equilibrated at four different densities calculated with CMD.

From nuclei to N Stars

Our work: use molecular dynamics to study "neutron stars"

Solve the dynamics as before but…

Simulate the infinte systems using Periodic boundary conditions

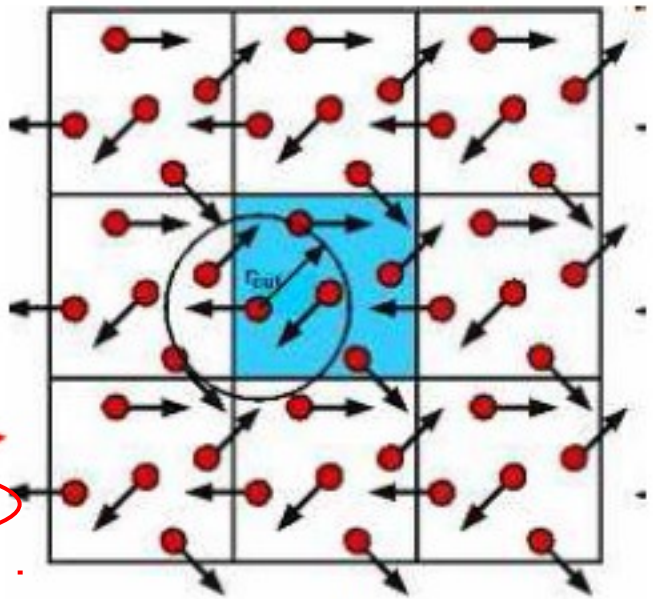

(or Debye)

For Coulomb use Thomas Fermi approximation

$$V_C(r) \approx \frac{e^2}{r}$$

$$V_C^{TF}(r) \approx \frac{e^2}{r}\exp(-r/\lambda)$$

$$\lambda_e = \pi^{1/2}/[2e(3\pi^2 n_e)^{1/3}]$$

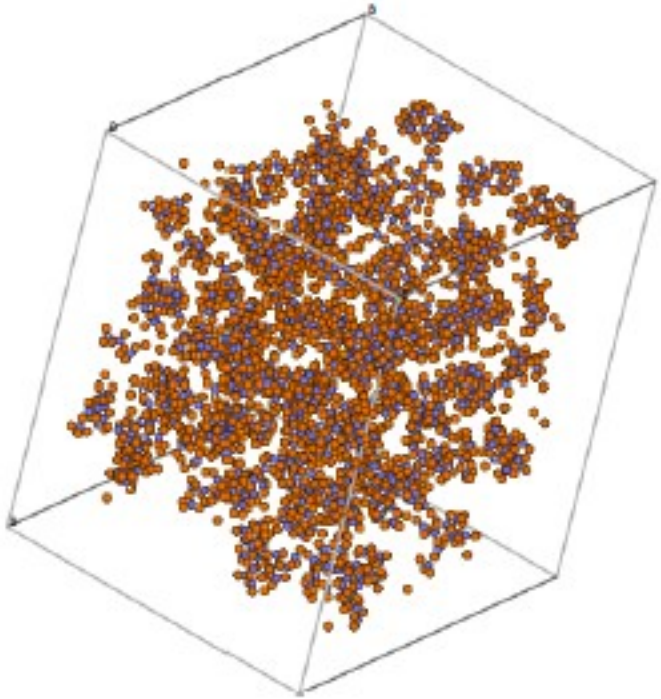

We first study

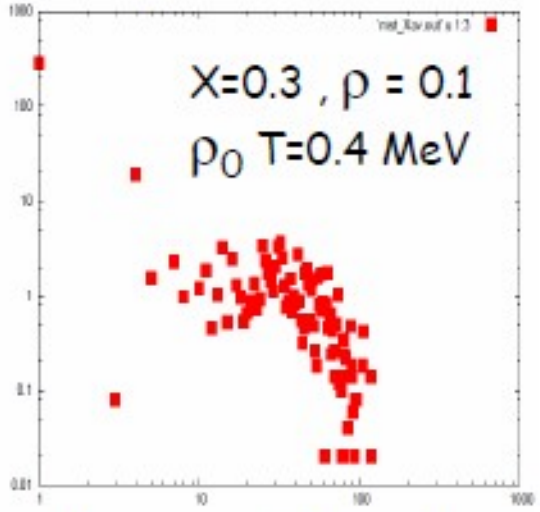

Fragments and their mass distribution

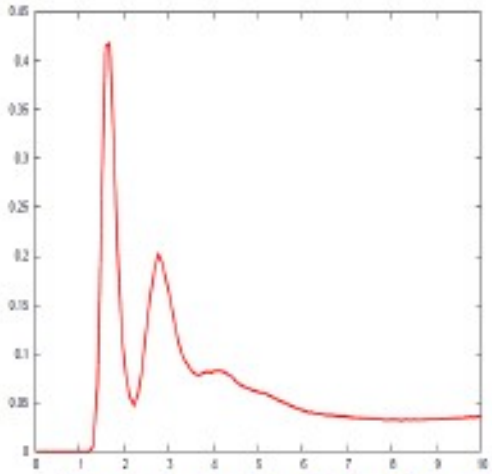

Pair correlation function

Topology (why?)

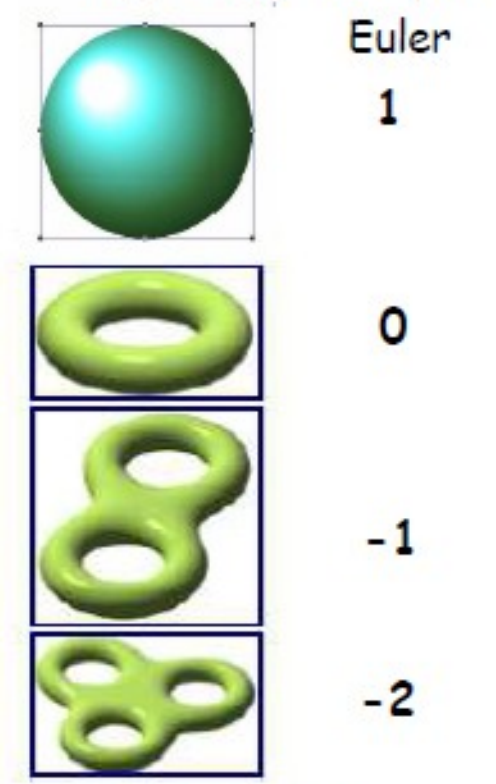

Minkowski functionals

. . .

First results

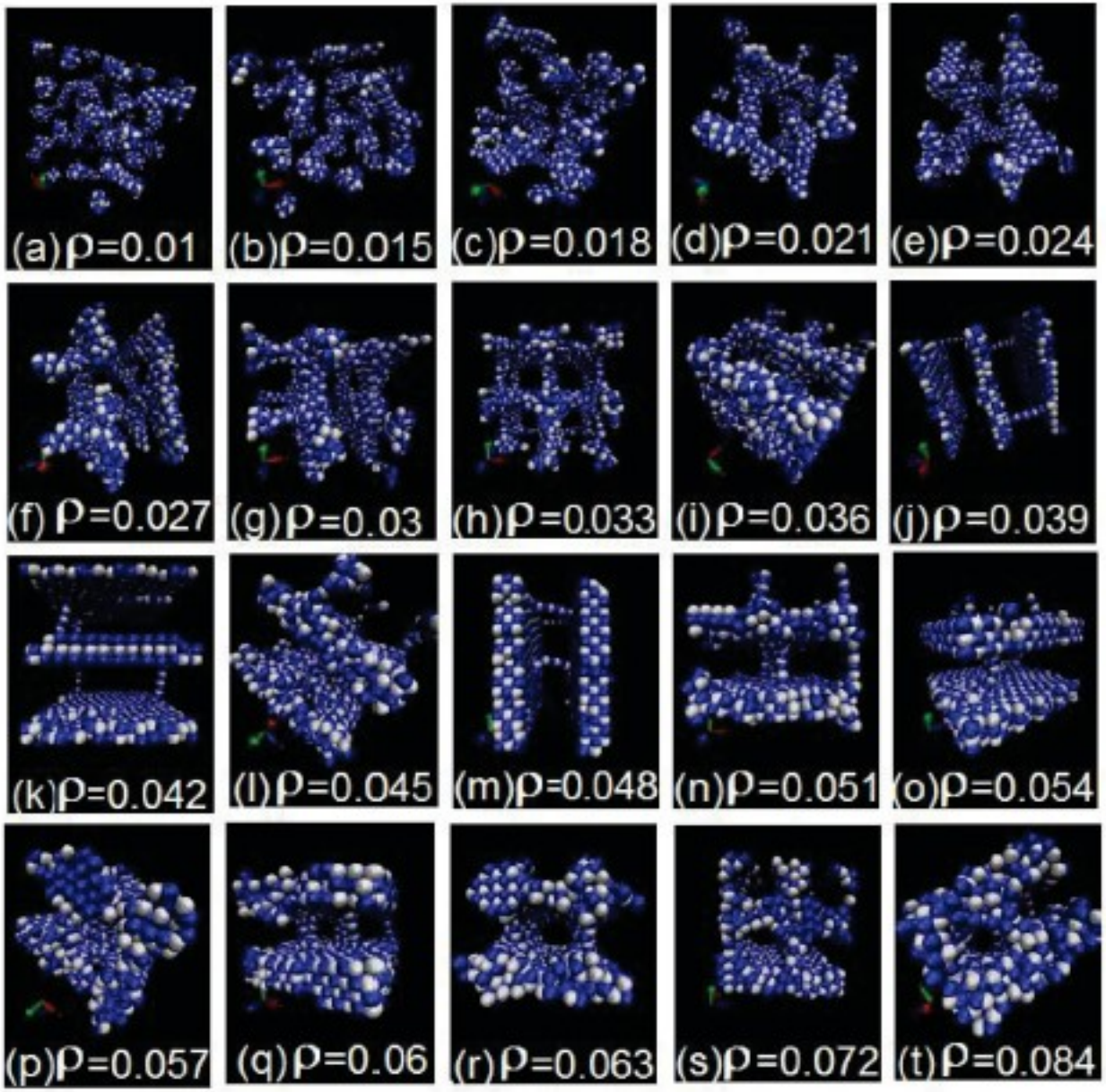

FIG. 1. (Color online) Smörgåsboard of pasta shapes corresponding to the densities shown and to $x = 0.5$ and $T = 0.1$ MeV.

Pasta ! (or pastasciutta)

Gnocci

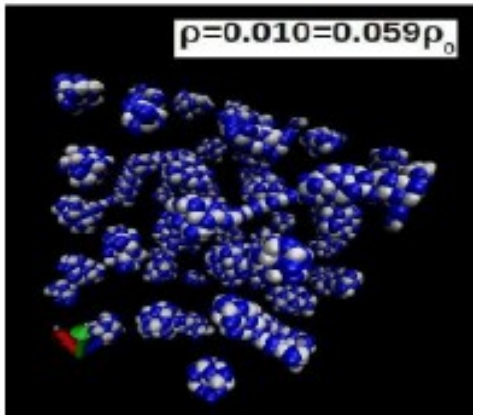

Spaghetti

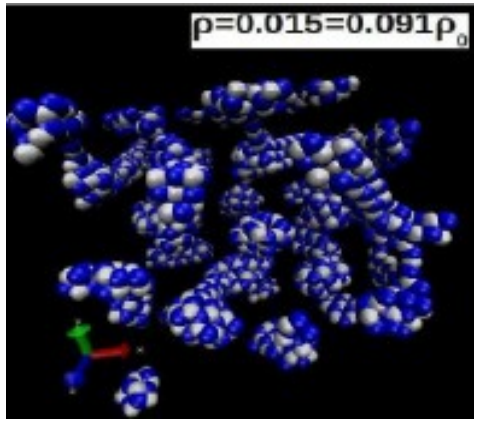

Lasagna

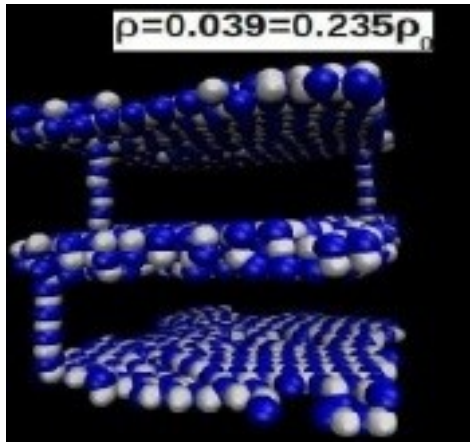

Euler Characteristic

Take out a sheet of paper.

Draw any number of dots on your page. Now connect the dots with lines, subject to the following rules: lines may not cross each other as they move from dot to dot, and every dot on your page must be connected to every other dot through a sequence of lines.

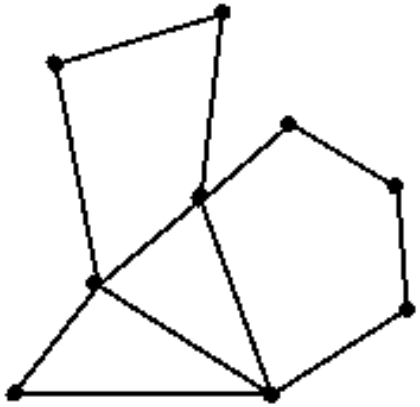

Now count the number dots (D), lines (L), and regions separated by lines (R).
Don't forget to count the outside as a region too.

D=9, L=12, R=5

Compute D-L+R. What do you get?

D-L+R=2. No matter how you started, the number you will always get is 2!

In 3D Convex Polyhedra

The **Euler characteristic** $\chi = V - E + F = 2$

V numbers of vertices (corners)

E numbers of edges

F numbers of faces

Name	Image	Vertices V	Edges E	Faces F	Euler characteristic: $V - E + F$
Tetrahedron		4	6	4	2
Hexahedron or cube		8	12	6	2
Octahedron		6	12	8	2
Dodecahedron		20	30	12	2
Icosahedron		12	30	20	2

In 3D non-convex polyhedra χ can have any value, and thus can be used to characterize the shape

Name	Image	Vertices V	Edges E	Faces F	Euler characteristic: $V - E + F$
Tetrahemihexahedron		6	12	7	**1**
Octahemioctahedron		12	24	12	**0**
Cubohemioctahedron		12	24	10	**−2**
Great icosahedron		12	30	20	**2**

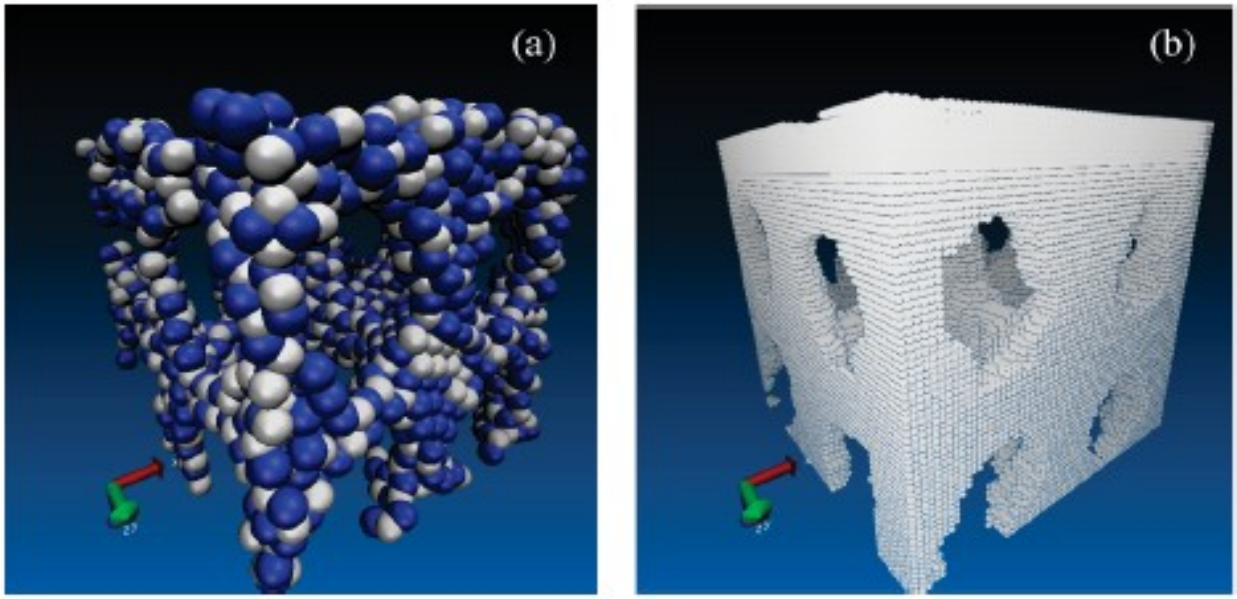

FIG. 8. (Color online) Sample transformation of a nuclear structure to a corresponding polyhedron. The structure corresponds to a case with $x = 0.5$, $\rho = 0.33$ fm^{-3}, and $T = 0.1$ MeV.

$$V = n_c, \quad A = -6n_c + 2n_f,$$
$$2B = 3n_c - 2n_f + n_c, \quad \chi = -n_c + n_f - n_e + n_v,$$

TABLE I: Classification Curvature - Euler

	Curvature < 0	Curvature ~ 0	Curvature > 0
Euler > 0	Anti-Gnocchi		Gnocchi
Euler ~ 0	Anti-Spaghetti	Lasagna	Spaghetti
Euler < 0	Anti-Jungle Gym		Jungle Gym

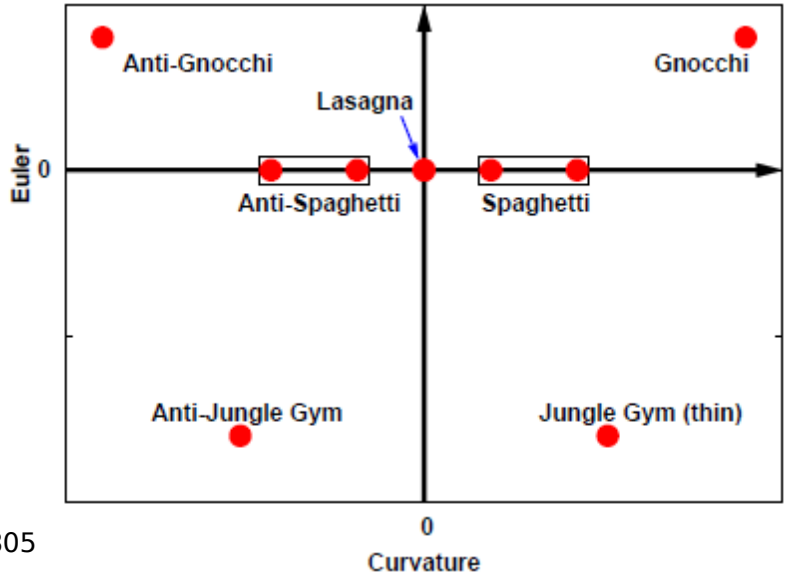

Topological charcaterization of neutron stars crust
C. O. Dorso, P. A. Giménez Molinelli, and J. A. López, Phys. Rev. C **86**, 055805

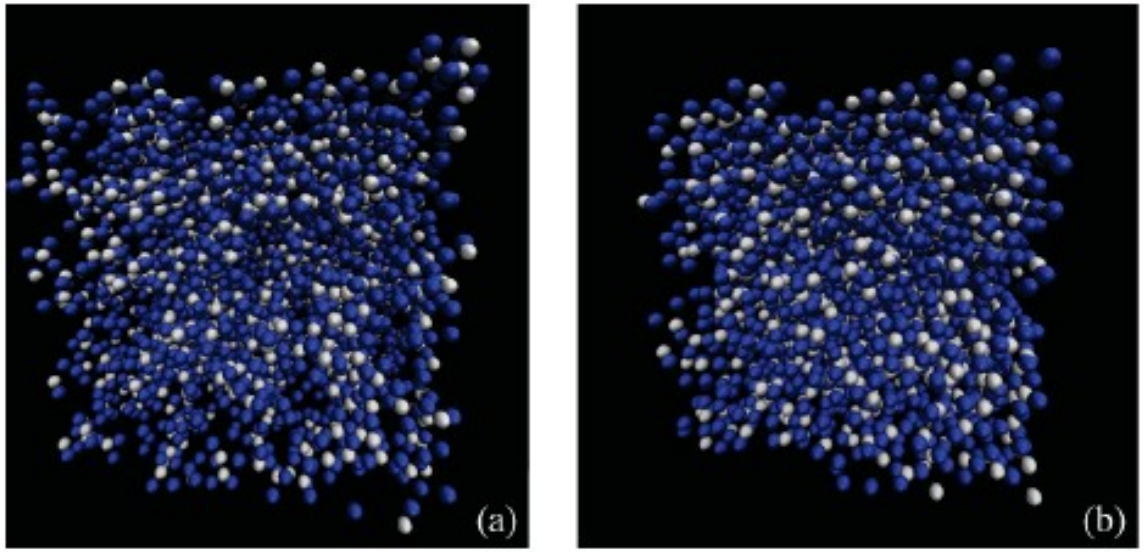

FIG. 9. (Color online) Spatial configurations formed under $T = 0.4$ MeV and $\rho = 0.045$ fm^{-3} (left) and $T = 1.0$ MeV and $\rho = 0.072$ fm^{-3} (right), both for $x = 0.3$.

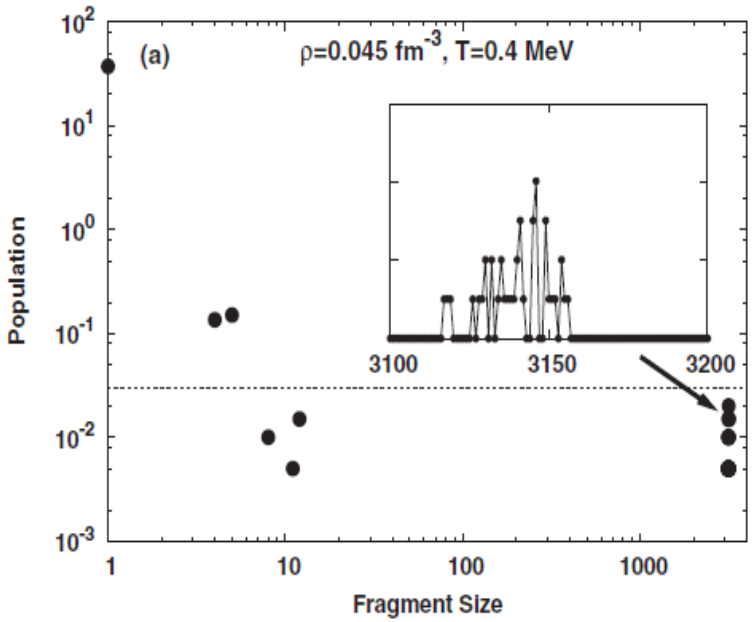

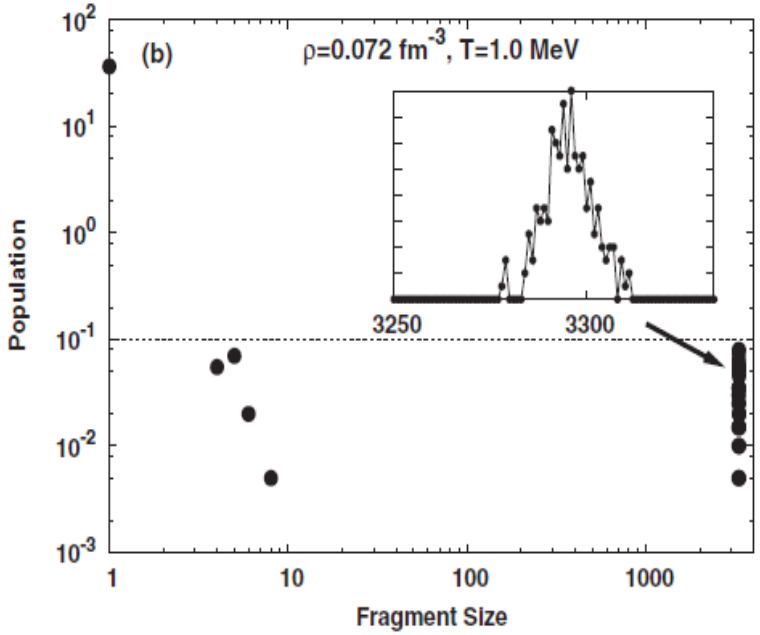

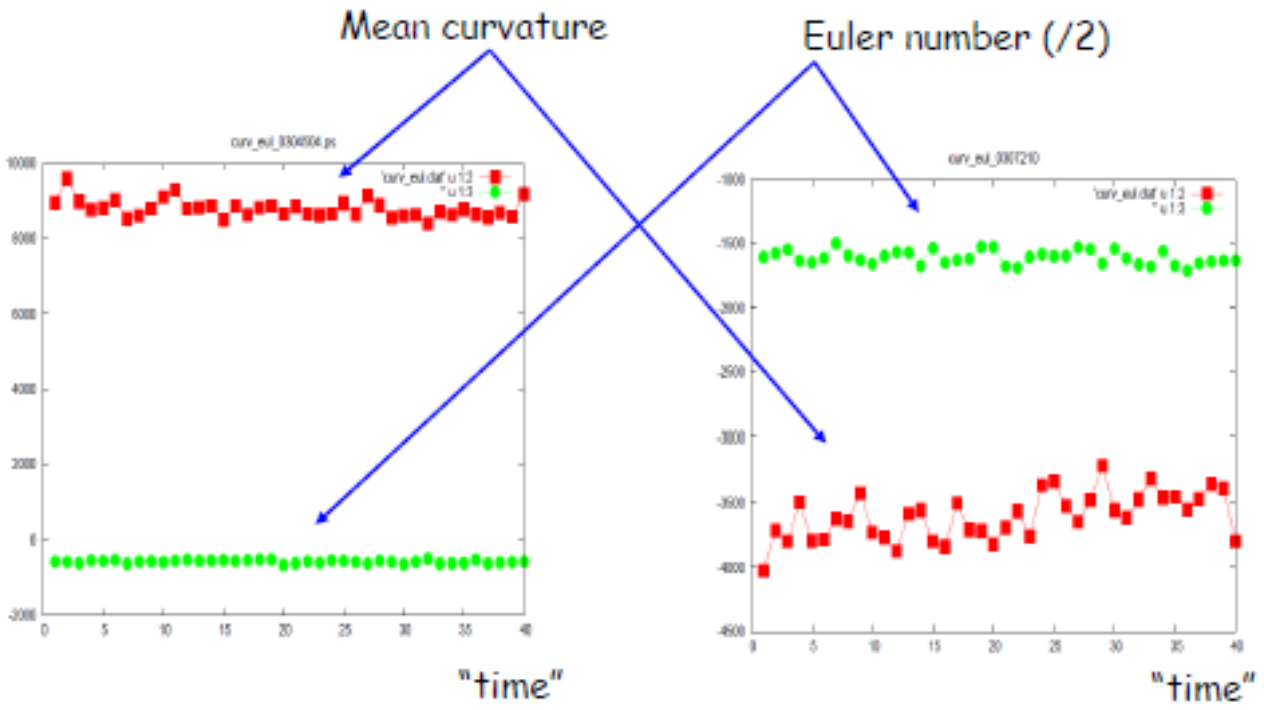

ρ =0.045

X=0.3 T=0.4

ρ =0.072

X=0.3 T=1.0

The role of coulomb

We analyze the behavior of a system driven by:

$$V\left(r_{ij},\kappa_i,\kappa_j\right)=V_{Pandha}\left(r_{ij},\kappa_i,\kappa_j\right)+\alpha\cdot V_{Coul}\left(r_{ij},\kappa_i,\kappa_j\right)$$

with $0 \leq \alpha \leq 1$

The role of coulomb

α=1 (circles)

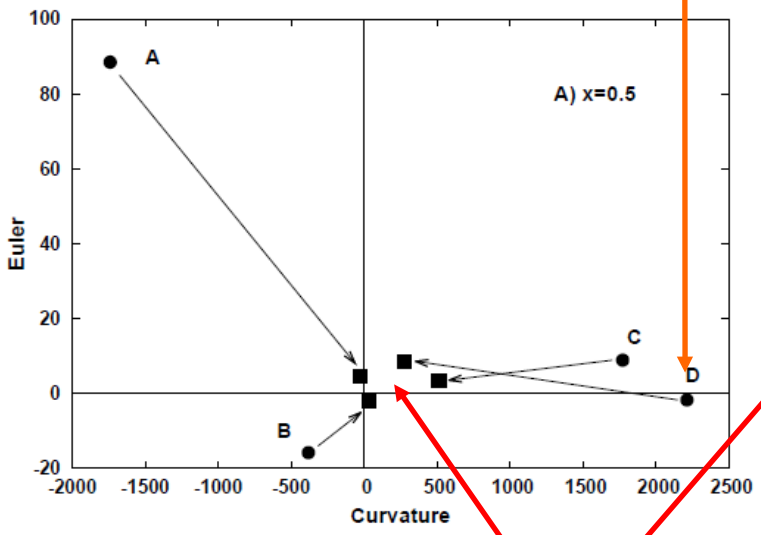

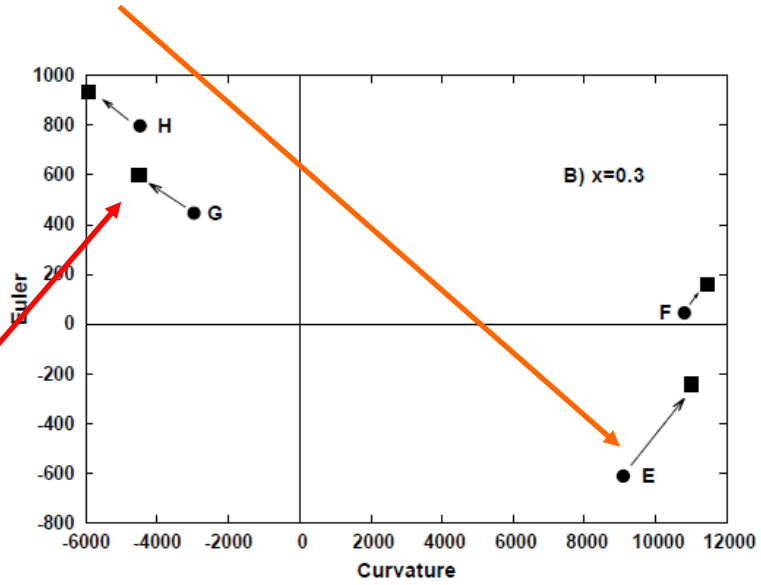

α=0 (squares)

TABLE II: Classification Curvature - Euler

	ρ (fm^{-3})	T (MeV)	$\alpha=1$ Curvature	$\alpha=1$ Euler	$\alpha=0$ Curvature	$\alpha=0$ Euler
A	0.072	1.0	-1740	89	-24	4.7
B	0.072	0.1	-382	-15.8	29.4	-1.9
C	0.015	0.1	1771	8.9	514	3.5
D	0.015	1.0	2212	-1.7	273	8.6
E	0.015	1.0	9090	-612	11011	-243
F	0.015	0.1	10804	454	11436	159
G	0.072	1.0	-2969	447	-4512	602
H	0.072	0.1	-4485	798	-5914	933

FIG. 7: Average values of the Curvature and Euler numbers of the structures listed in Table II; circles correspond to structures with Coulomb and squares to structures without Coulomb, arrows indicate the average displacement of the structures as α goes from 1 to 0.

This suggests that there is pasta even without Coulomb!

Nuclear Matter CMD

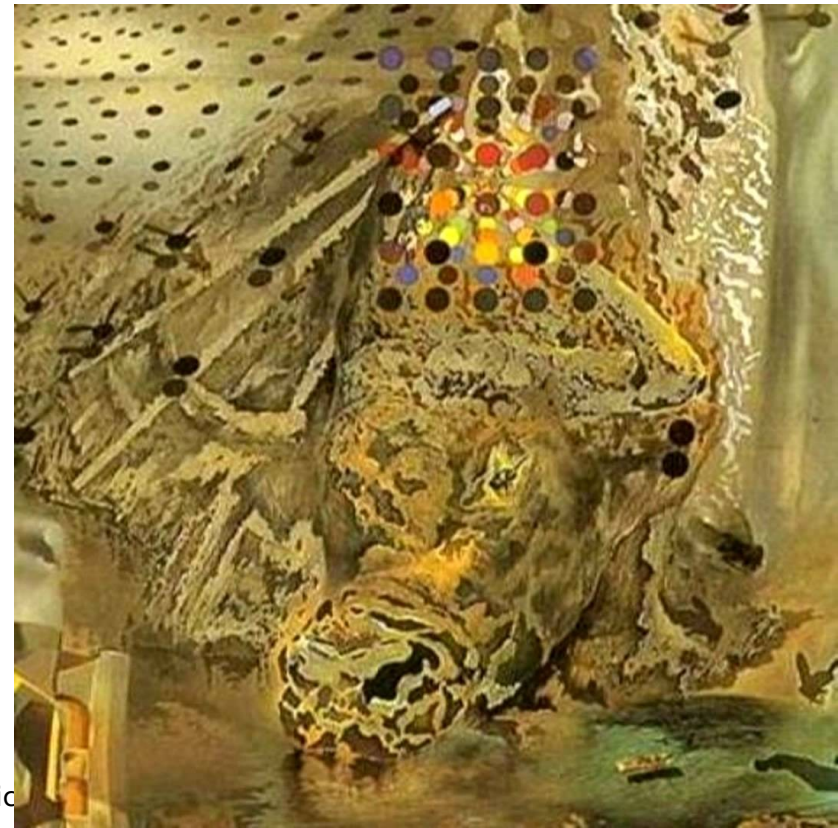

Simulations of cold nuclear matter at subsaturation densities
P. A. Giménez Molinelli, J. Nichols, J. A. López & C. O. Dorso; Nuclear Physic

Back to CMD

Illinois Potential Medium

$$V_{np}(r) = V_r\,[exp(-\mu_r r)/r - exp(-\mu_r r_c)/r_c] -$$
$$- V_a\,[exp(-\mu_a r)/r - exp(-\mu_a r_c)/r_c]$$
$$V_{nn}(r) = V_0\,[exp(-\mu_0 r)/r - exp(-\mu_0 r_c)/r_c]$$

Nuclear Matter

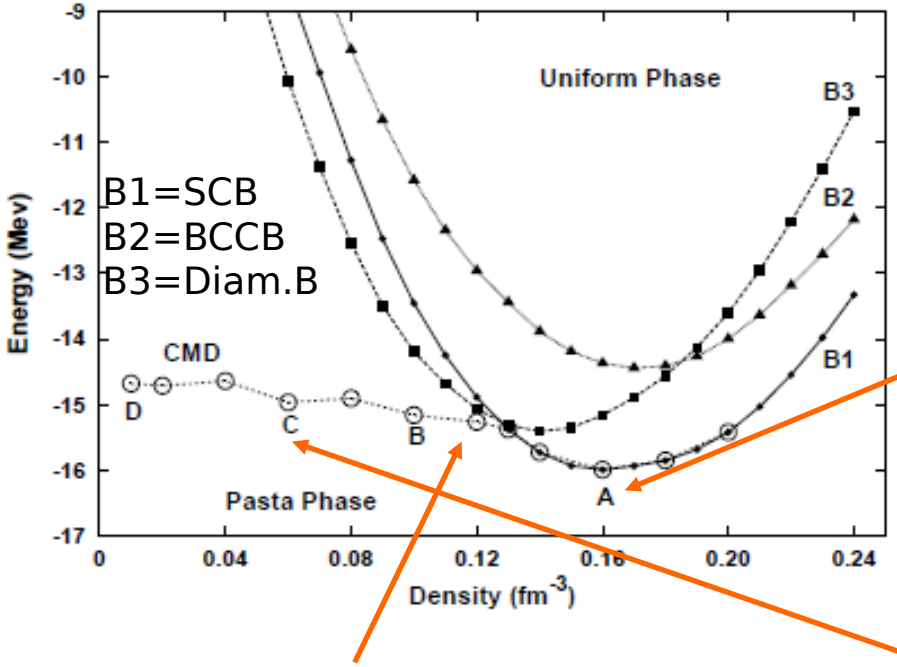

FIG. 1. Binding energies per nucleon for systems obtained with the Pandharipande medium potential for crystalline lattices with $B1$, $B2$ and $B3$ crystal geometries, and using molecular dynamics at $T = 0.001\ MeV$ (CMD). The structures corresponding to the four labeled points ("A" through "D") are shown in Figure 2.

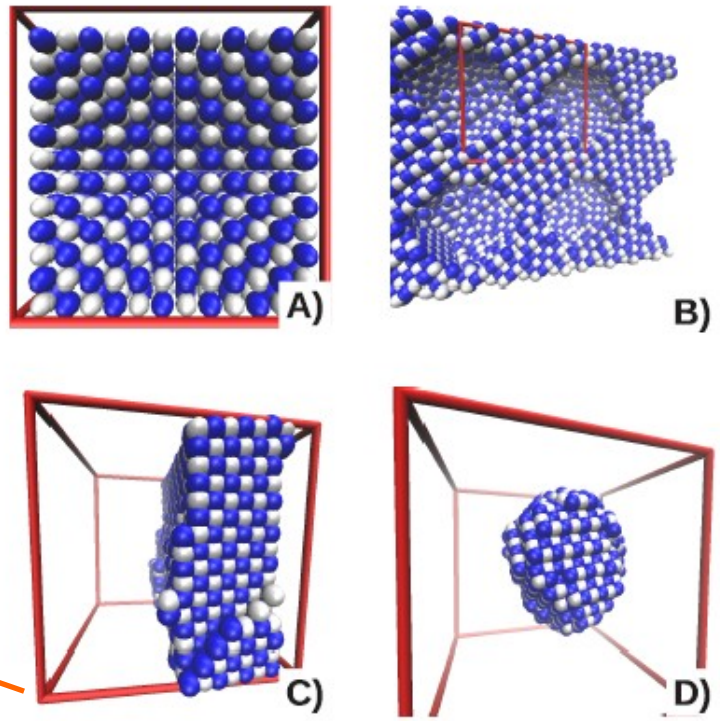

FIG. 2. (Color online) Structures corresponding to the labeled points of Figure 1. Point A corresponds to a formation in the regular $(B1)$ lattice, while the rest of the points are non-homogeneous structures.

Illinois Potential Medium

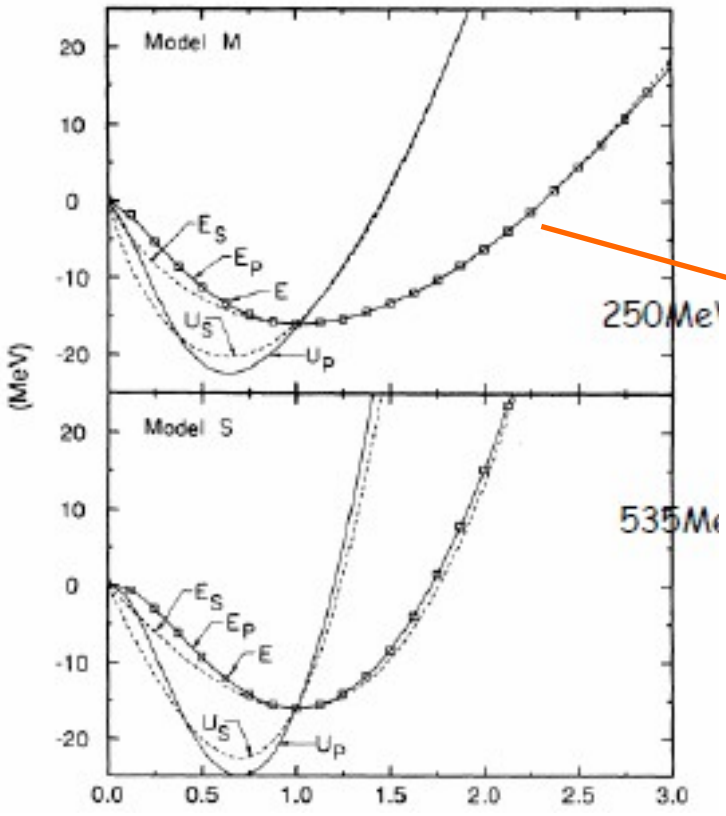

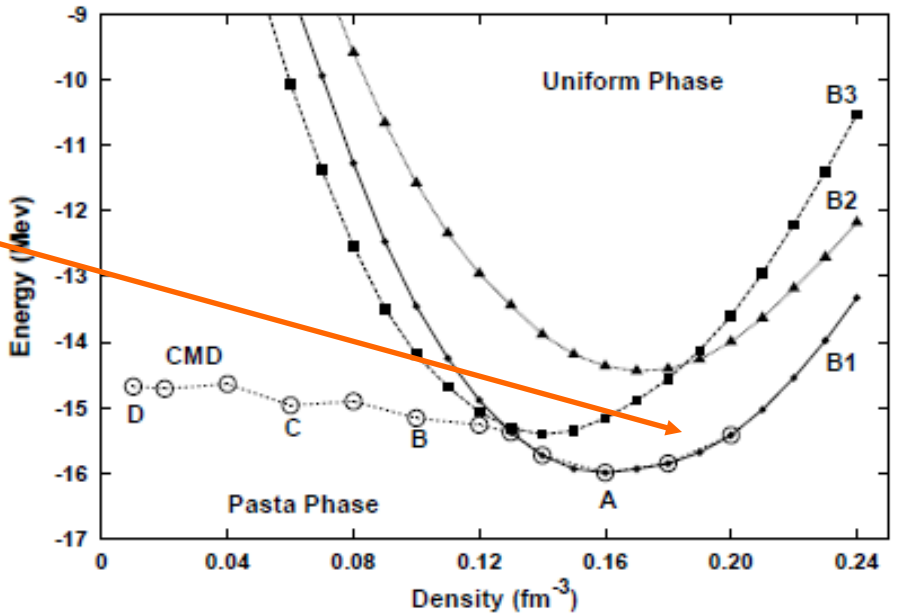

FIG. 1. Binding energies per nucleon for systems obtained with the Pandharipande medium potential for crystalline lattices with $B1$, $B2$ and $B3$ crystal geometries, and using molecular dynamics at $T = 0.001\ MeV$ (CMD). The structures corresponding to the four labeled points ("A" through "D") are shown in Figure 2.

Illinois Potential Medium

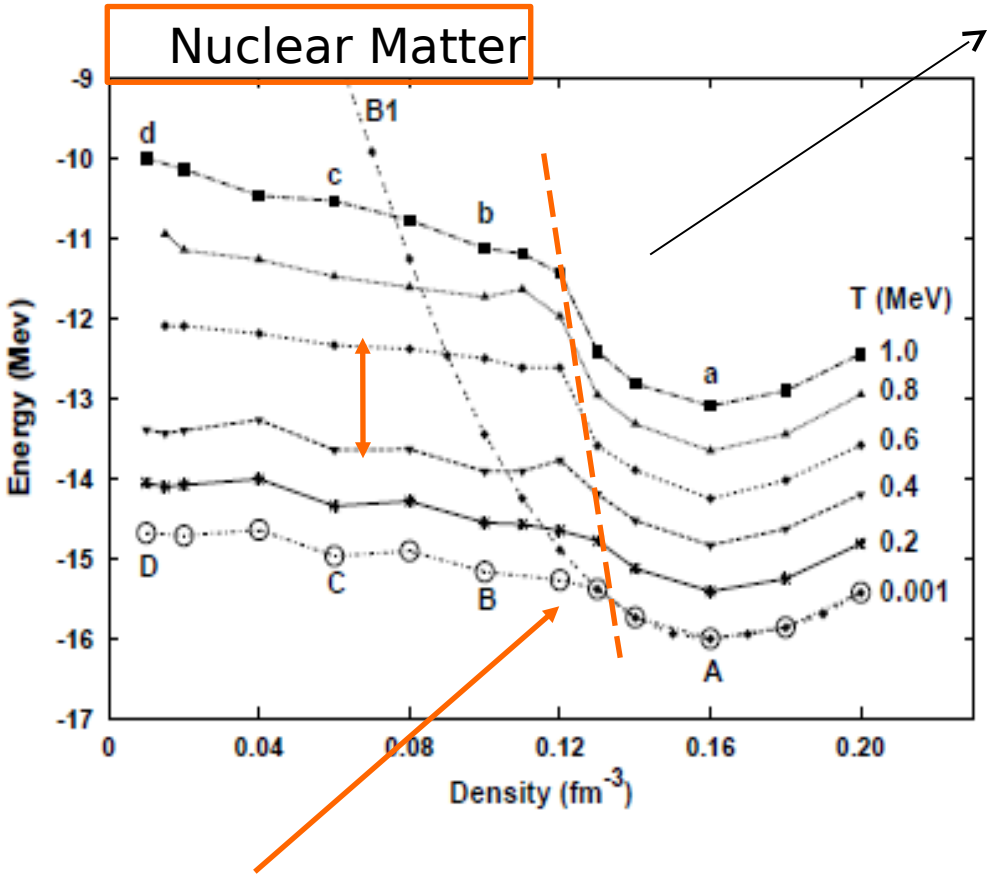

FIG. 3. Binding energies per nucleon for systems obtained with the Pandharipande medium potential at the listed temperatures.

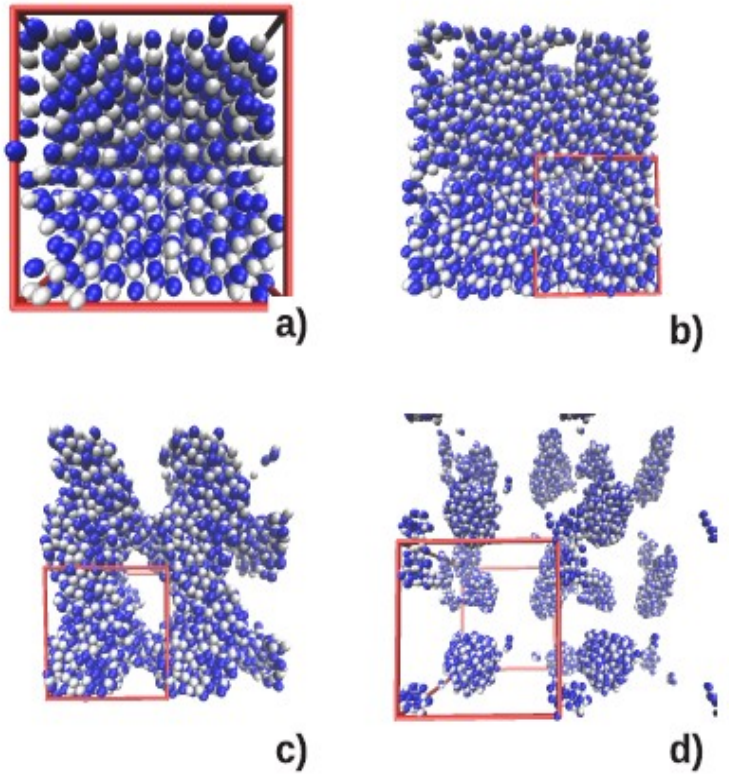

FIG. 4. (Color online) Structures corresponding to the labeled points of Figure 3 obtained with the Pandharipande medium potential at $T = 1.0\ MeV$.

Low T structures

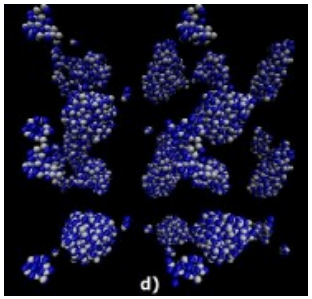

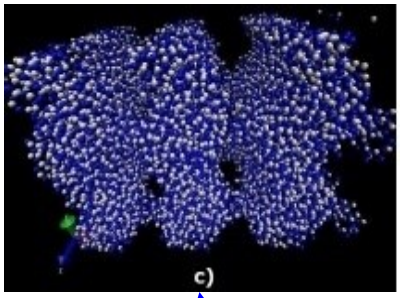

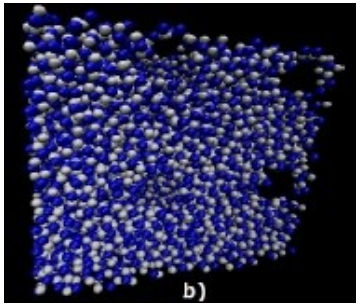

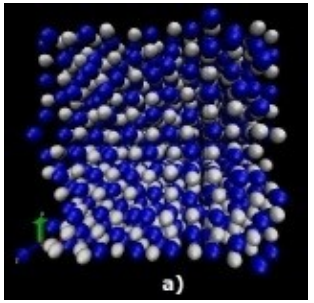

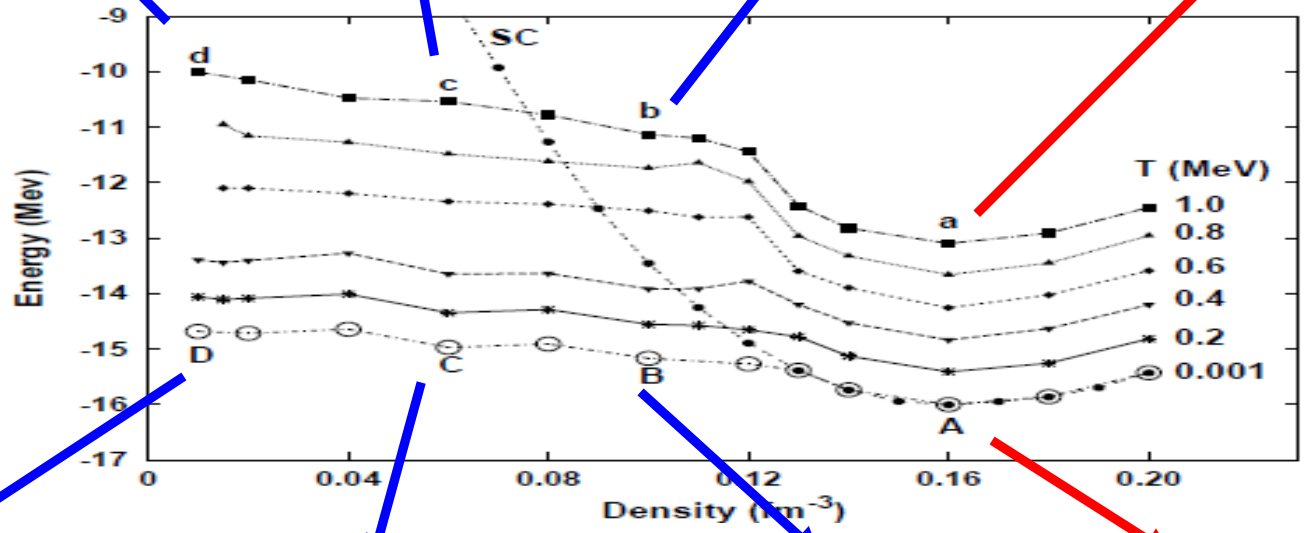

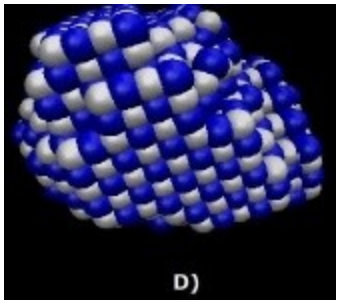

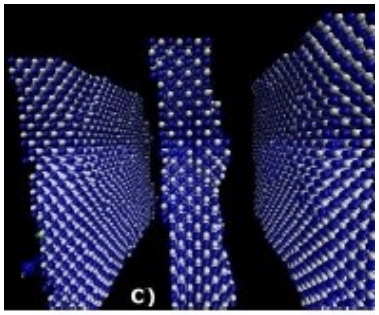

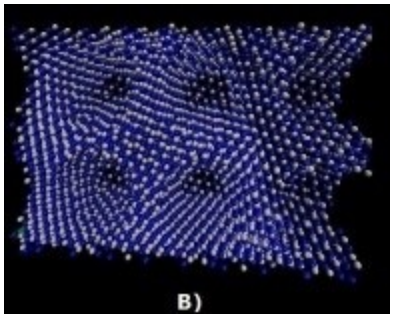

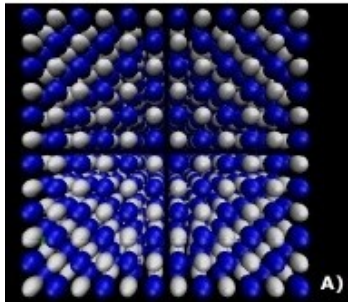

What is the role of Coulomb?

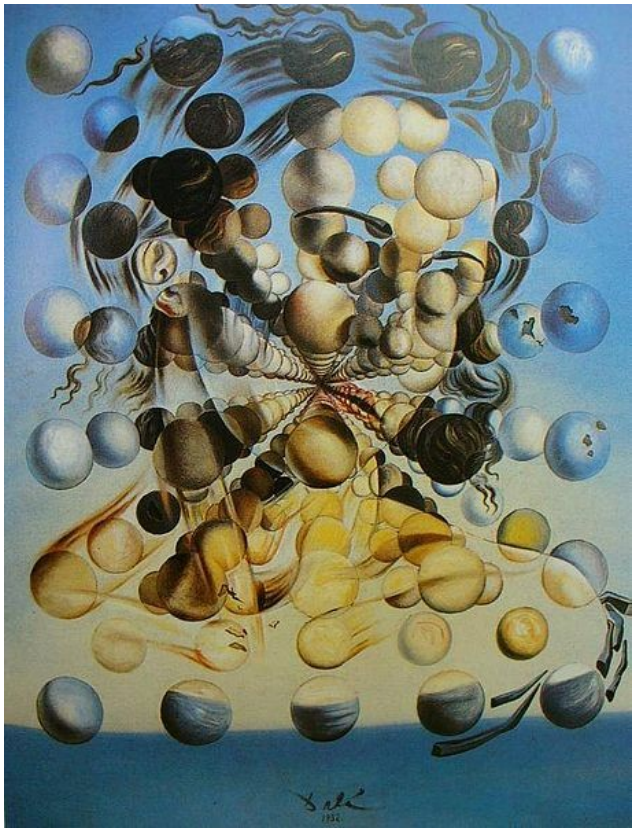

Effect of Coulomb screening length on nuclear ``pasta'' simulations
P. N. Alcain, P. A. Gimenez Molinelli, J. I. Nichols & C.O.Dorso Phys. Rev.C (2014)

What is the role of Coulomb?

Lennard Jones + Coulomb

Illinois potential is rather complicated because :

$$V_{np}(r) = V_r\left[\exp(-\mu_r r)/r - \exp(-\mu_r r_c)/r_c\right] - V_a\left[\exp(-\mu_a r)/r - \exp(-\mu_a r_c)/r_c\right]$$

$$V_{nn}(r) = V_0\left[\exp(-\mu_0 r)/r - \exp(-\mu_0 r_c)/r_c\right]$$

$$V_{pp}(r) = V_0\left[\exp(-\mu_0 r)/r - \exp(-\mu_0 r_c)/r_c\right] + \exp\left(-\frac{r}{\lambda}\right)\cdot\left(\frac{\nu_c}{r}\right)$$

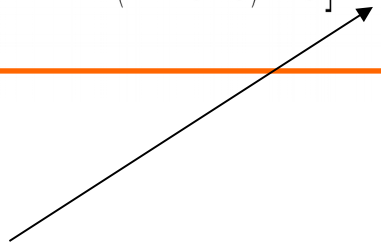

Lennard Jones +coulomb

$$V(r) = V_0\left[\left(\frac{\sigma}{r}\right)^{12} - \left(\frac{\sigma}{r}\right)^{6}\right] + \exp\left(-\frac{r}{\lambda}\right)\cdot\left(\frac{v_c}{r}\right)$$

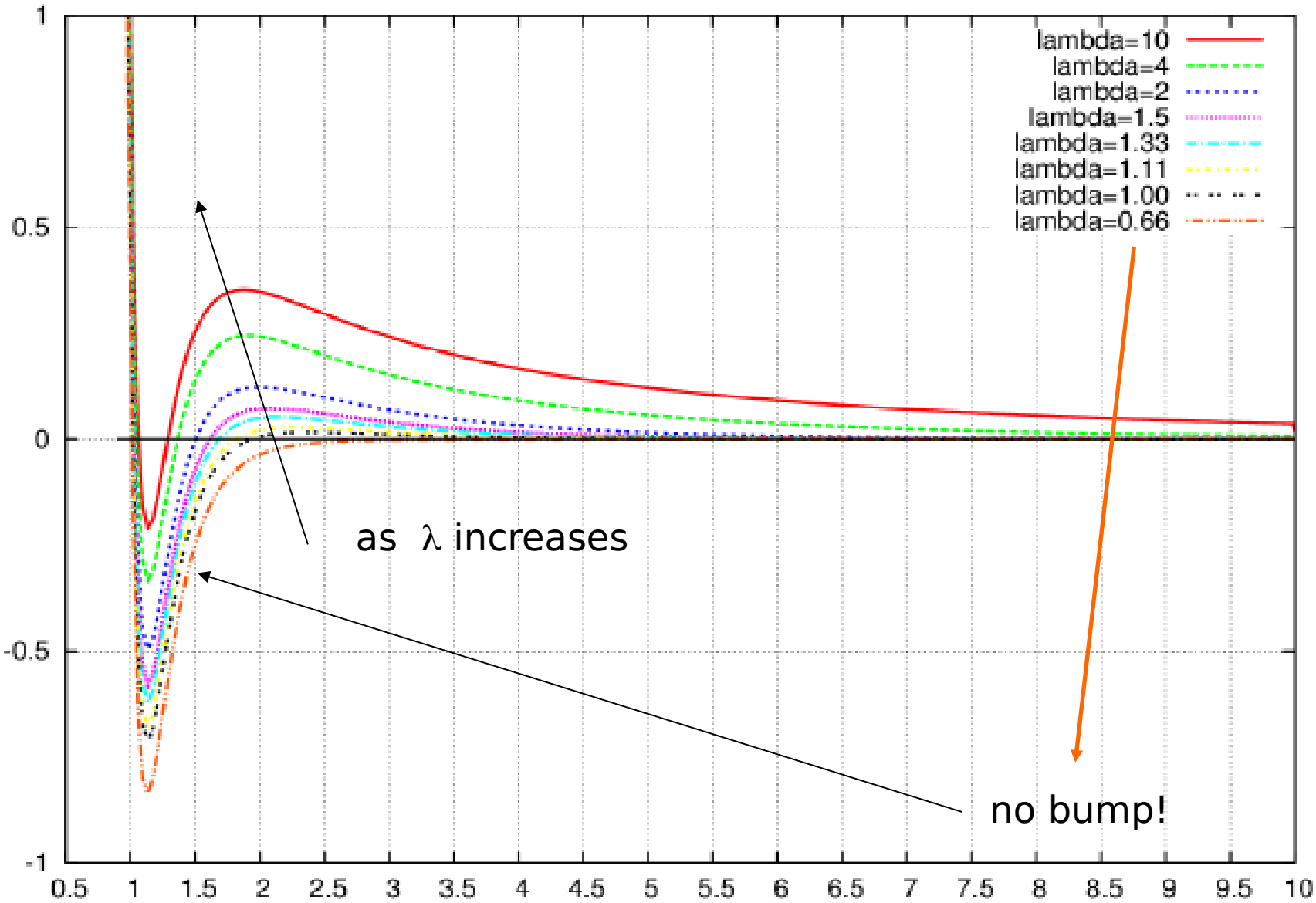

The role of coulomb (2 dimensions)

N=800

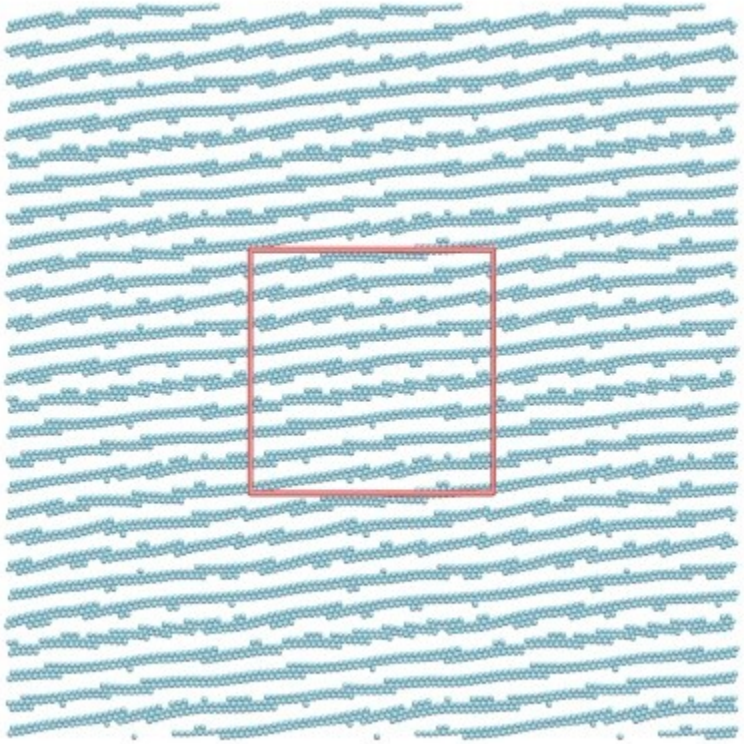

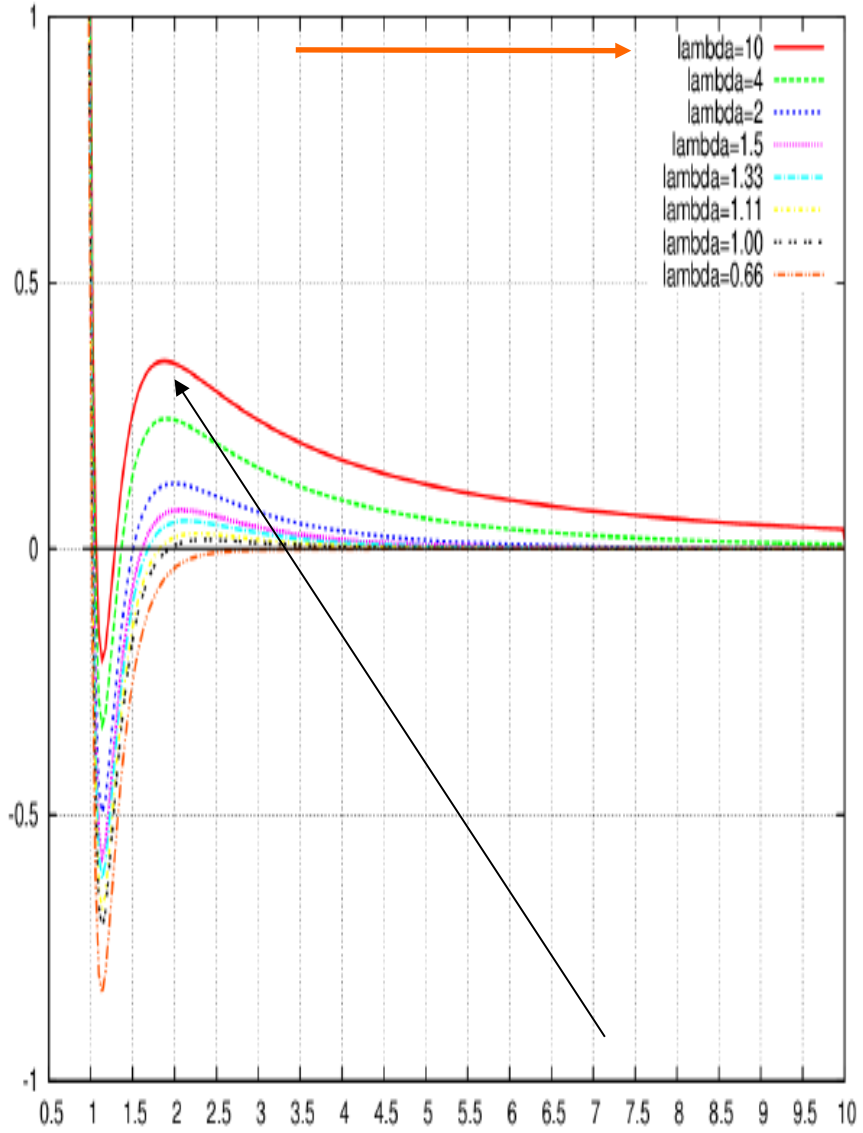

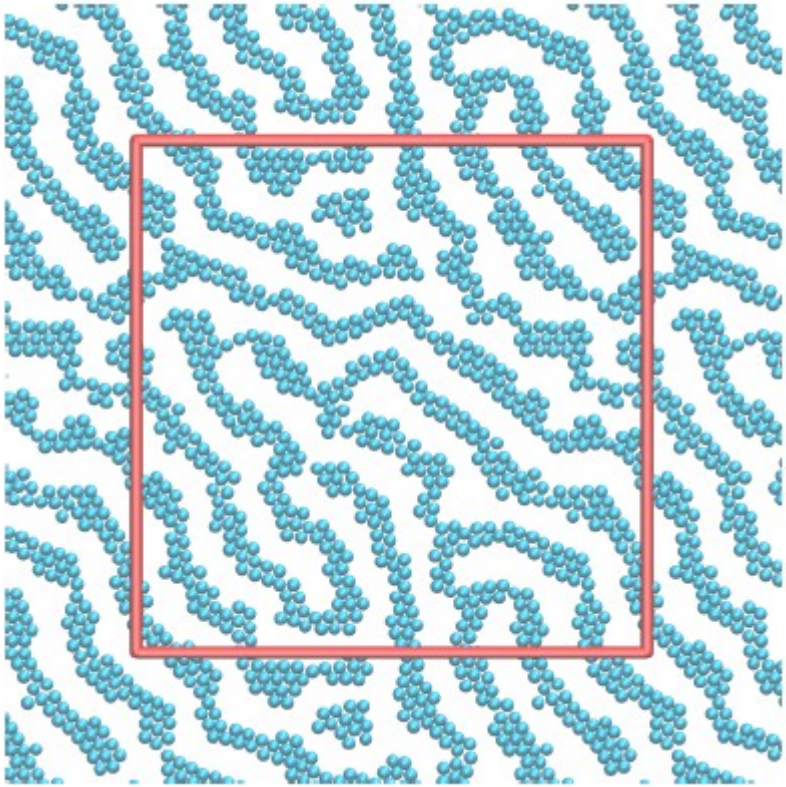

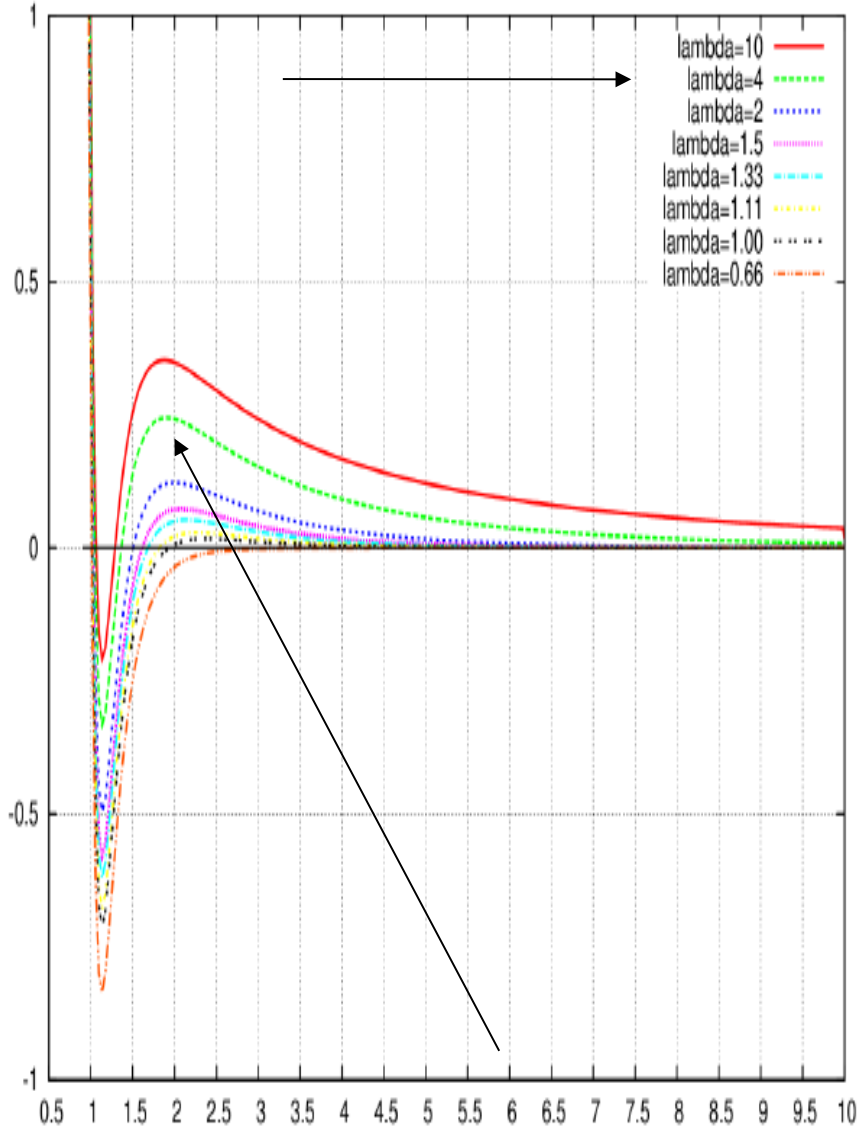
lambda=10
lambda=4
lambda=2
lambda=1.5
lambda=1.33
lambda=1.11
lambda=1.00
lambda=0.66
1
0.5
0
-0.5
-1
0.5
1
1.5
2
2.5
3
3.5
4
4.5
5
5.5
6
6.5
7
7.5
8
8.5
9
9.5
10

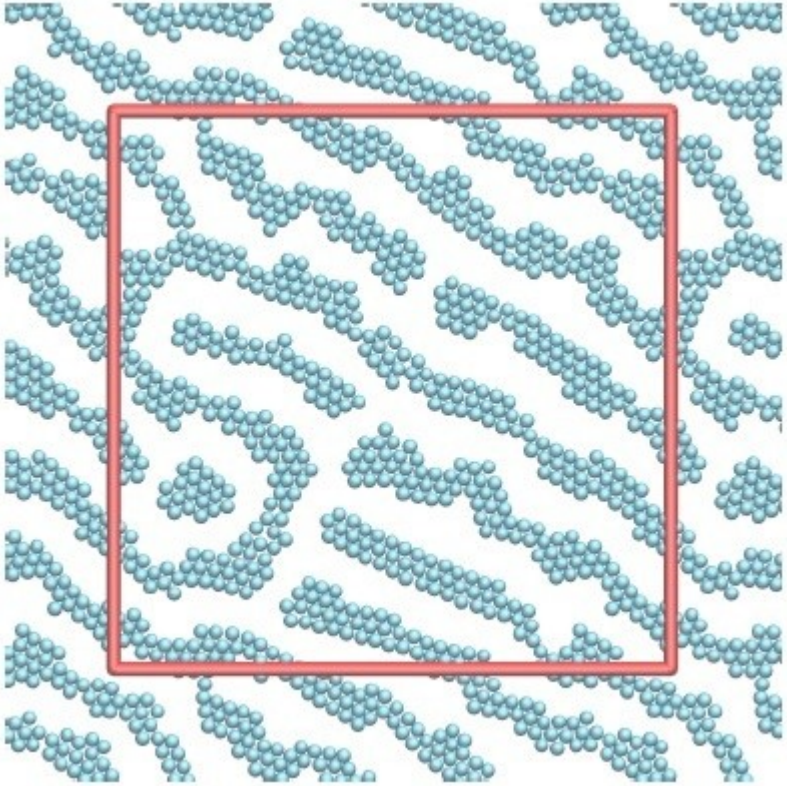

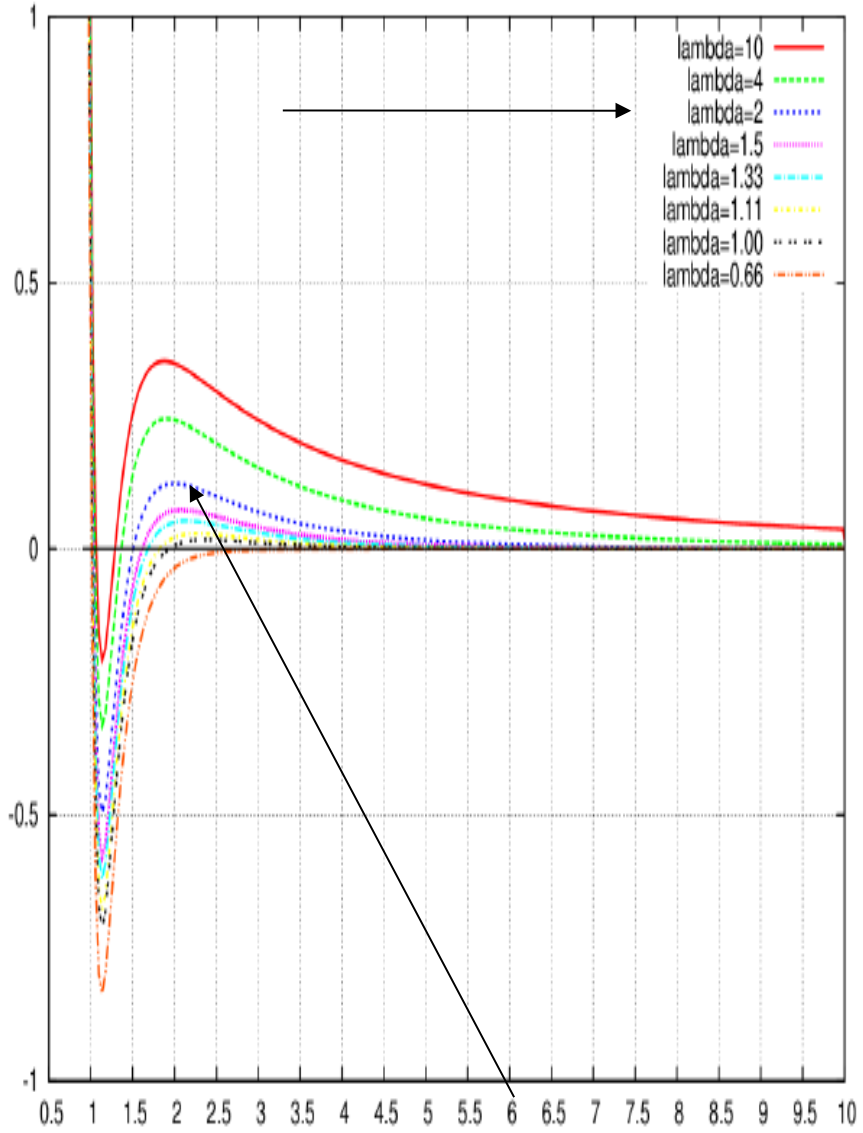
lambda=10
lambda=4
lambda=2
lambda=1.5
lambda=1.33
lambda=1.11
lambda=1.00
lambda=0.66
1
0.5
0
-0.5
-1
0.5
1
1.5
2
2.5
3
3.5
4
4.5
5
5.5
6
6.5
7
7.5
8
8.5
9
9.5
10

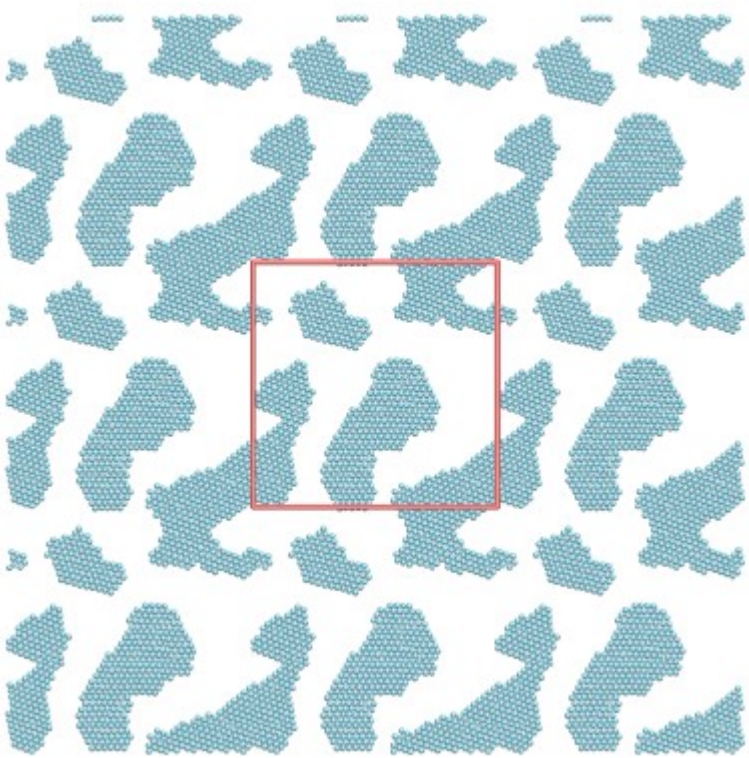

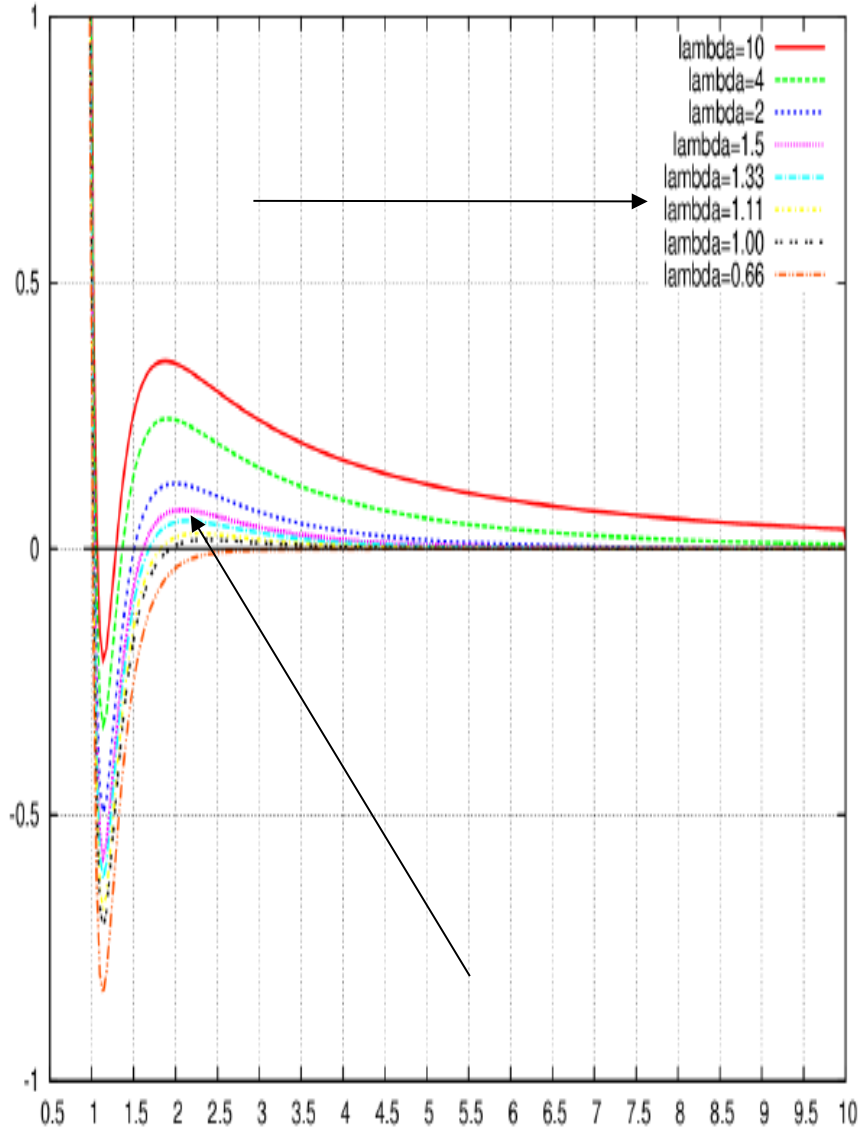
lambda=10
lambda=4
lambda=2
lambda=1.5
lambda=1.33
lambda=1.11
lambda=1.00
lambda=0.66
1
0.5
0
-0.5
-1
0.5
1
1.5
2
2.5
3
3.5
4
4.5
5
5.5
6
6.5
7
7.5
8
8.5
9
9.5
10

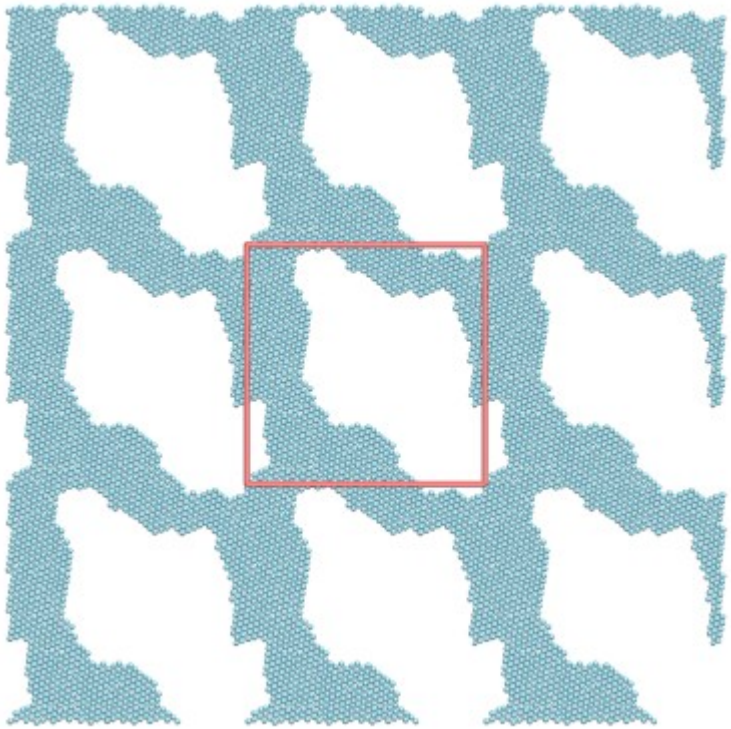

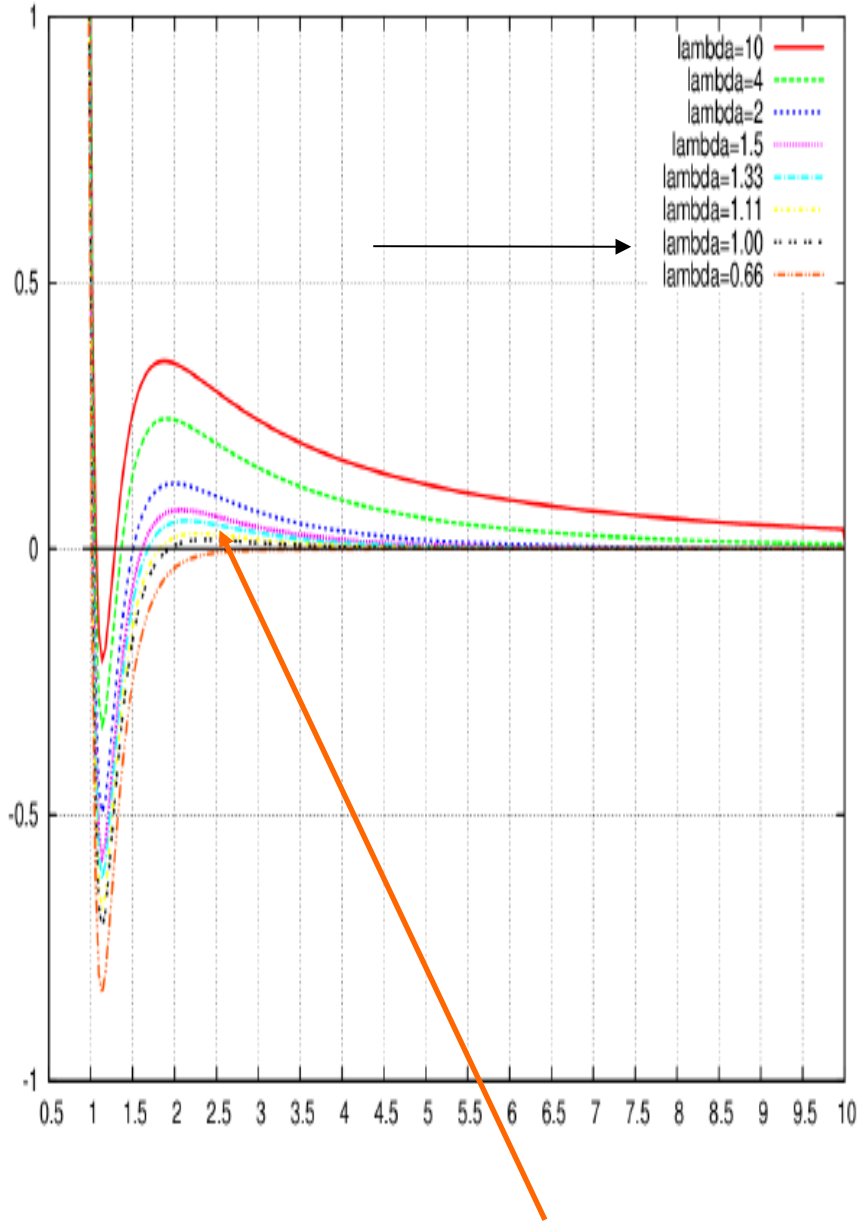
lambda=10
lambda=4
lambda=2
lambda=1.5
lambda=1.33
lambda=1.11
lambda=1.00
lambda=0.66
1
0.5
0
-0.5
-1
0.5 1 1.5 2 2.5 3 3.5 4 4.5 5 5.5 6 6.5 7 7.5 8 8.5 9 9.5 10

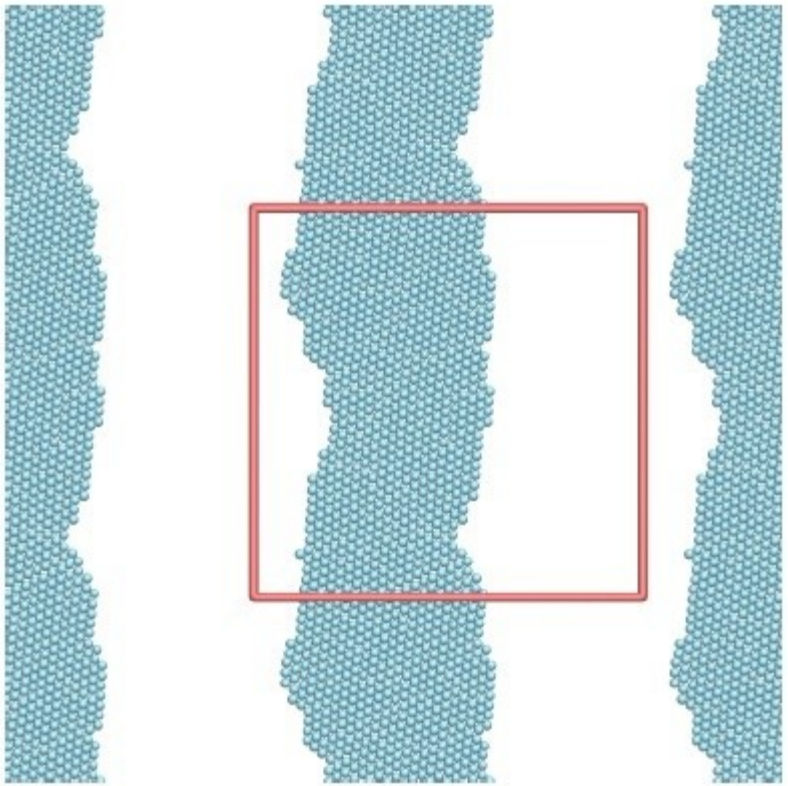

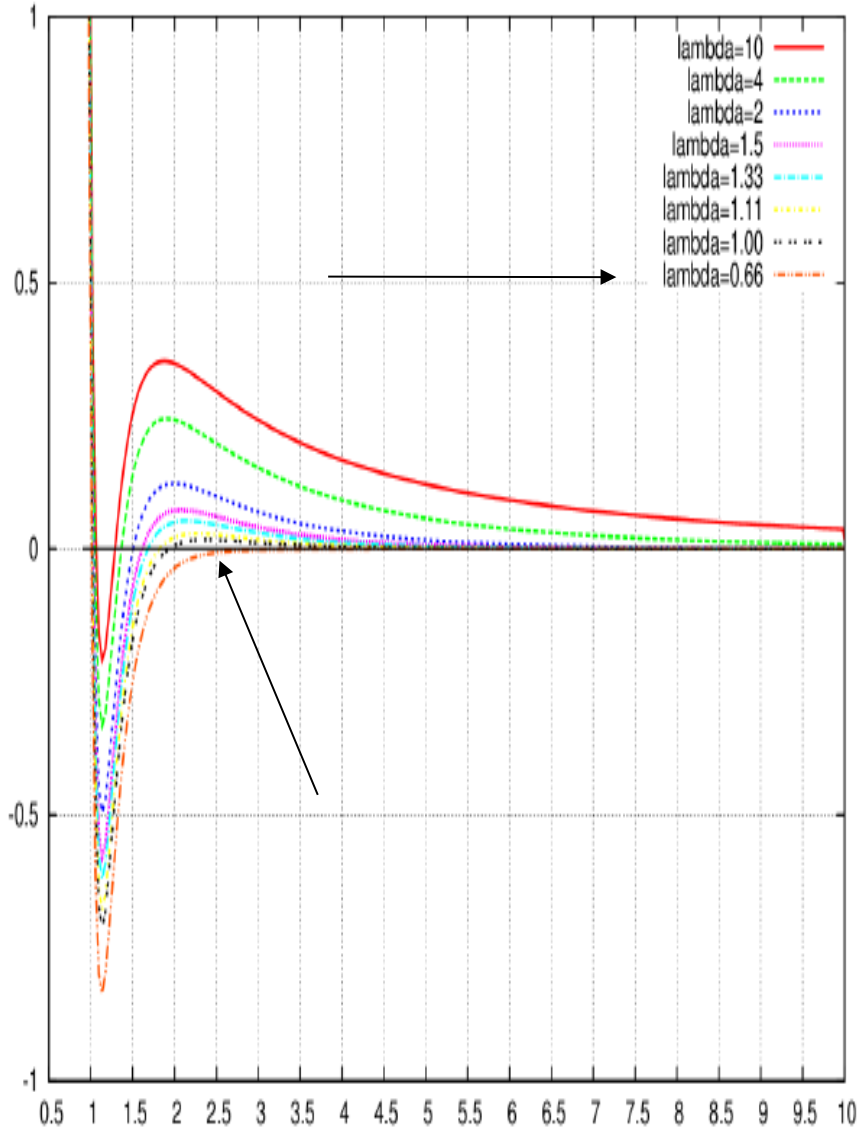

no bump, still get ‘pasta’

In 3 dimensions, no coulomb, Lennard Jones

$$V_{LJ}(r) = 4\epsilon\left[\left(\frac{\sigma}{r}\right)^{12} - \left(\frac{\sigma}{r}\right)^{6}\right]$$

1 structure per cell

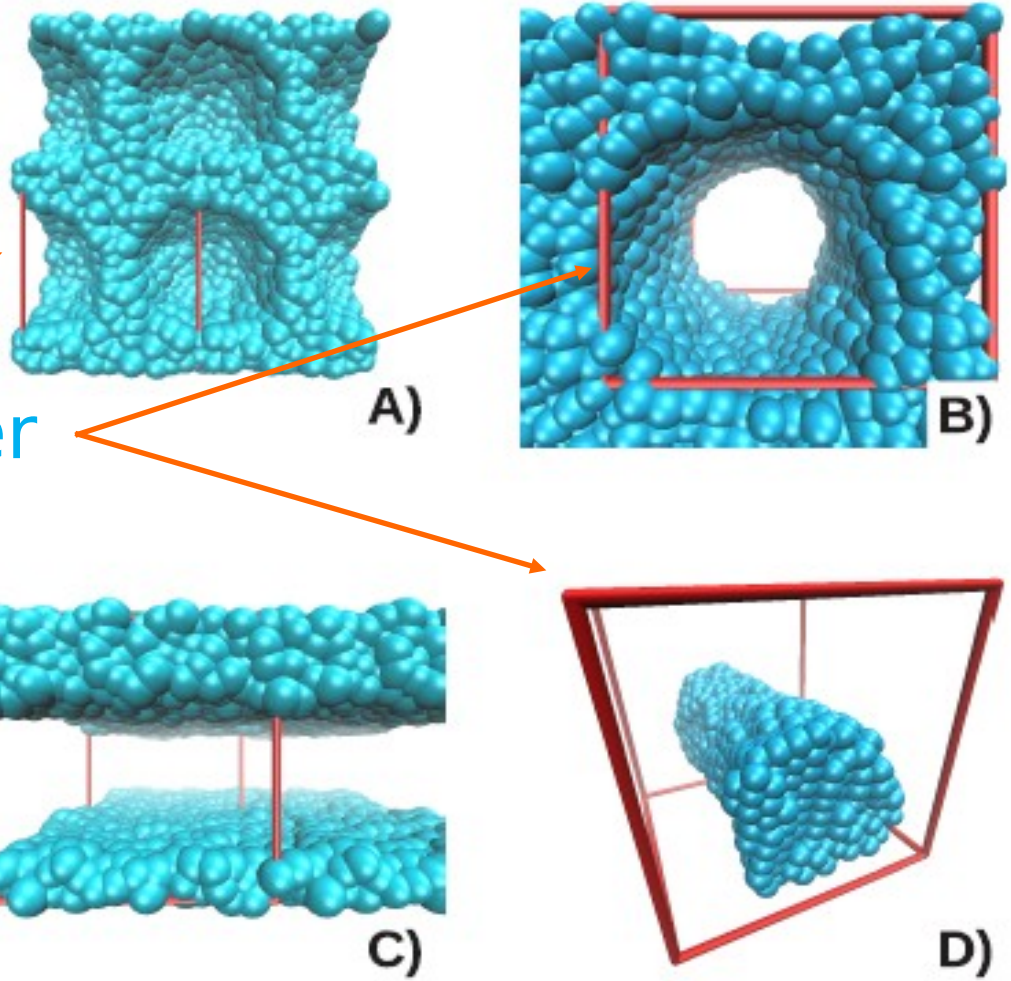

In the absence of coulomb we still get “Pasta” but just one structure per cell

The scale is fixed by the cell

When coulomb is switched on and λ is above the “critical value” (next) we get “True Pasta”, multiple structures per cell

The scale is fixed by the potential

Finite size, periodic boundary conditions and the appearance of “Pasta” without Coulomb

The system is infinite (PBC), particles interact by a short range potential

Given a configuration we can write

$$E = E_{bulk} + E_{surf}$$

$$S_{sphere} = 4\pi \left(\frac{3}{4\pi}\right)^{\frac{2}{3}} \times u^{\frac{2}{3}} \times L^2$$

$$S_{rod} = 2\,(\pi)^{\frac{1}{3}} \times u^{\frac{1}{3}} \times L^2$$

$$S_{slab} = 2 \times L^2$$

Free Surfaces within cell

$$A = E - TS$$

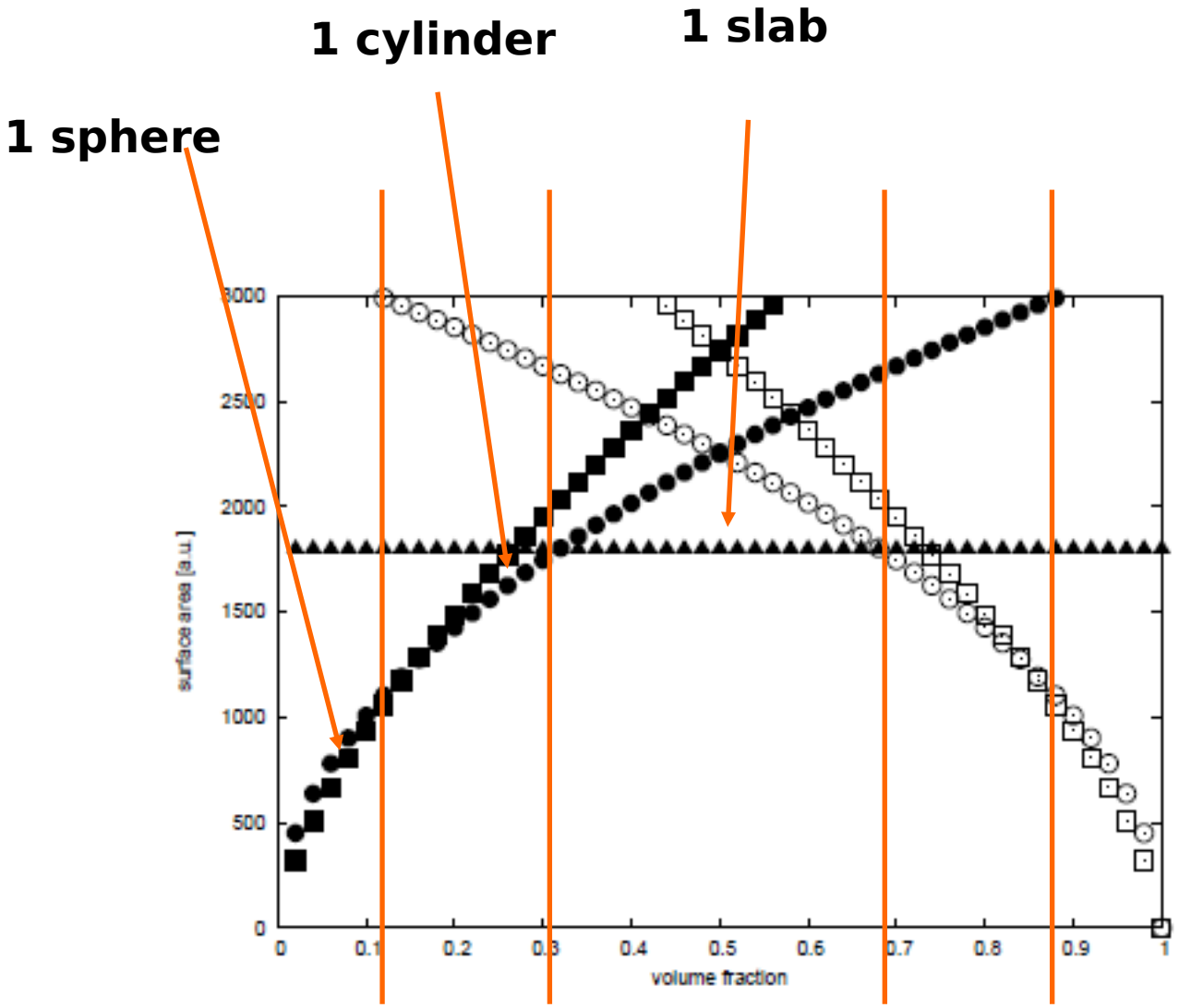

FIG. 12. Surface area of various simple shapes as a function of volume fraction for a cell of $L = 30$. The shapes are: Sphere (full squares), Cilindrical rod (full circles), slab (full triangles), cilindrical bubble (empty circles) and spherical bubble (empty squares)

MINI CONCLUSION

Same as in 2D Lennard Jones for $\lambda < \lambda_c$

Without Coulomb (i.e. Nuclear Matter)

all of the “Nuclear Potentials” Display

“1 cell Pasta”

Illinois potential + screened Coulomb

NS Matter?

We now explore:

The effect of varying λ

The effect of varying the temperature

Clusters as a function of T

Pressure

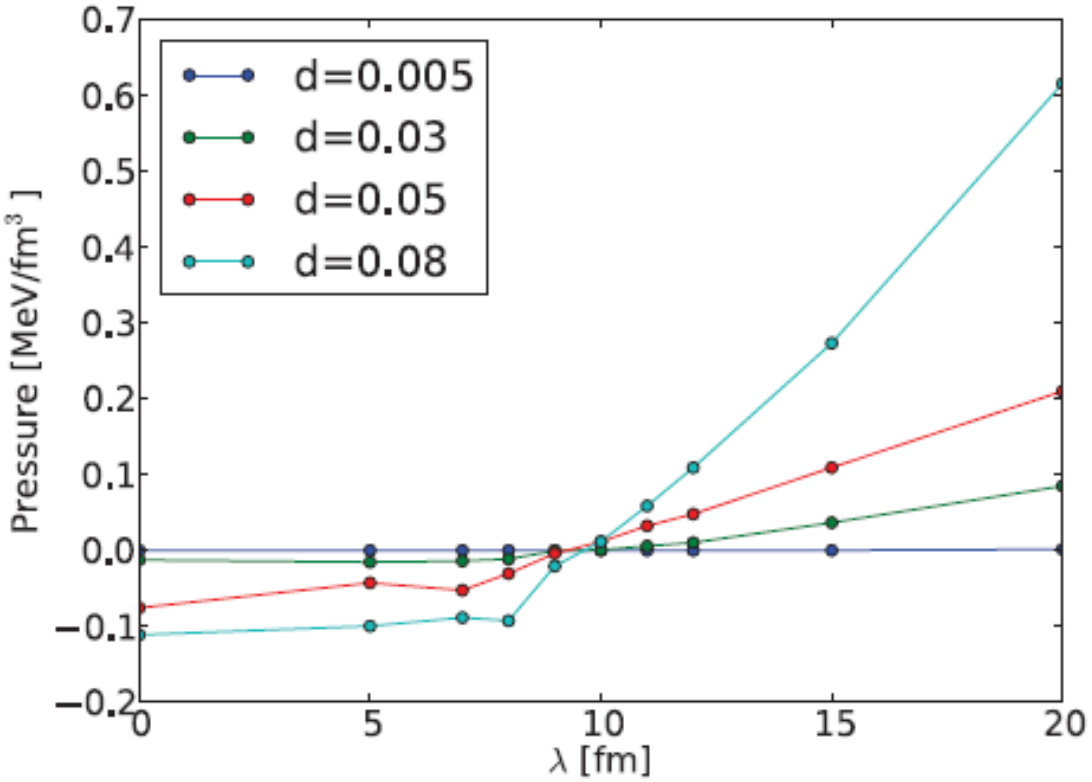

FIG. 1. (Color online) Pressure as a function of λ for different densities. We see that, for $\lambda < 10$ fm, the pressure is negative, implying that periodic boundary conditions are affecting the morphology of the solution.

The pressure is computed by the virial formula

$$P = \frac{Nk_BT}{V} + \frac{1}{3}\frac{\Sigma_i^N \mathbf{r}_i \cdot \mathbf{F}_i}{V},$$

As before we fix the density and then we vary λ in order to see at which point the solution goes to a single structure per cell

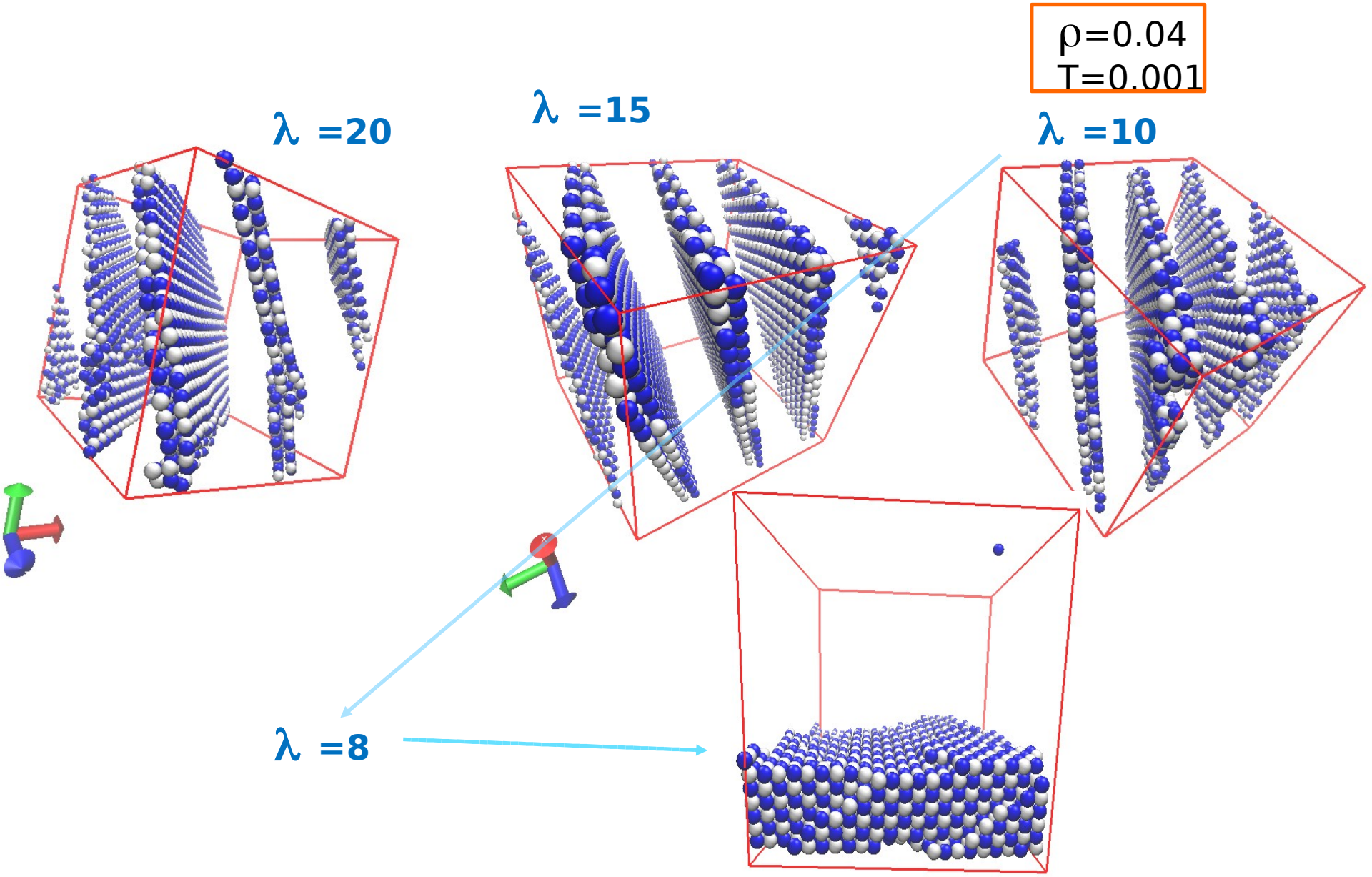

Minkowski functionals

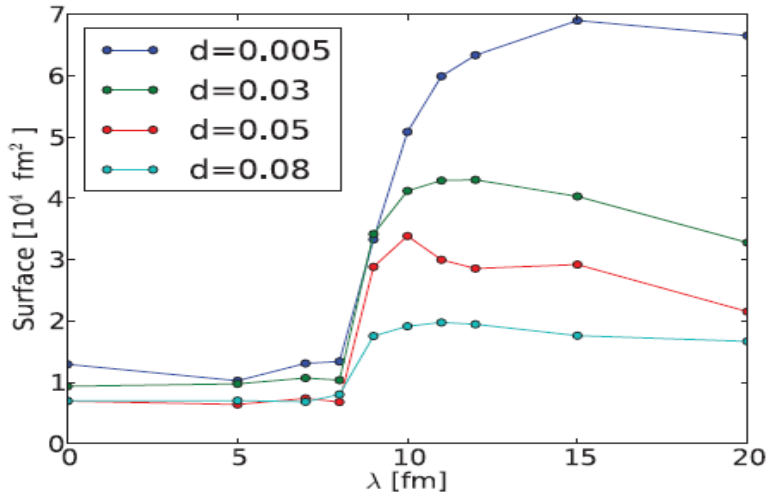

(a) Surface

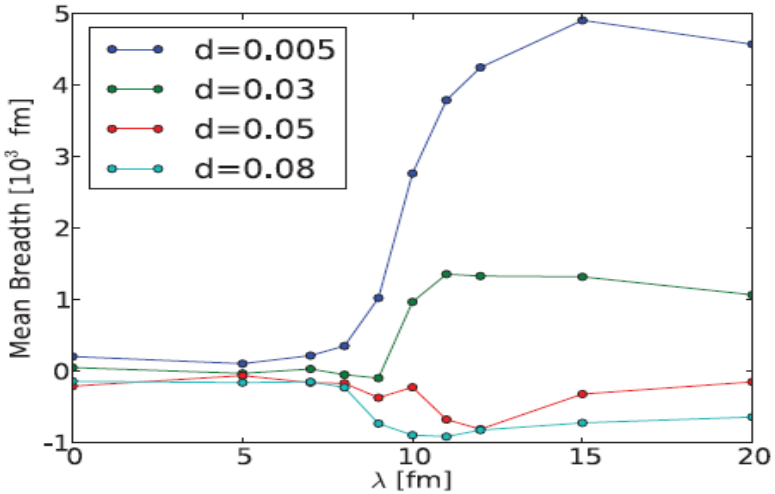

(b) Mean Breadth

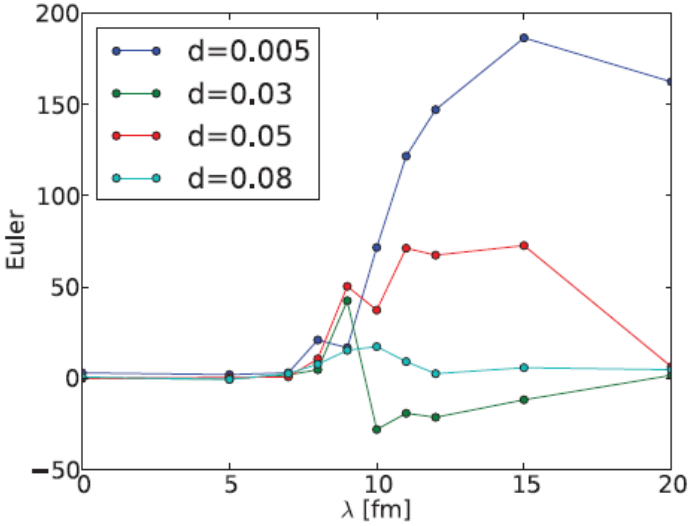

(c) Euler number

FIG. 2. (Color online) Minkowski functionals dependence on λ. We can see that there is a transition regime between $\lambda = 7$ fm and $\lambda = 15$ fm where the Minkowski functionals are changing.

If we vary theTemperature…

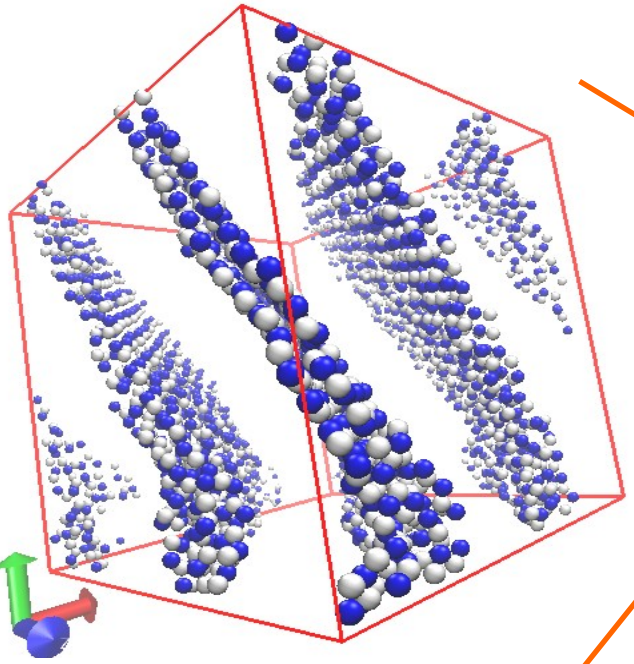

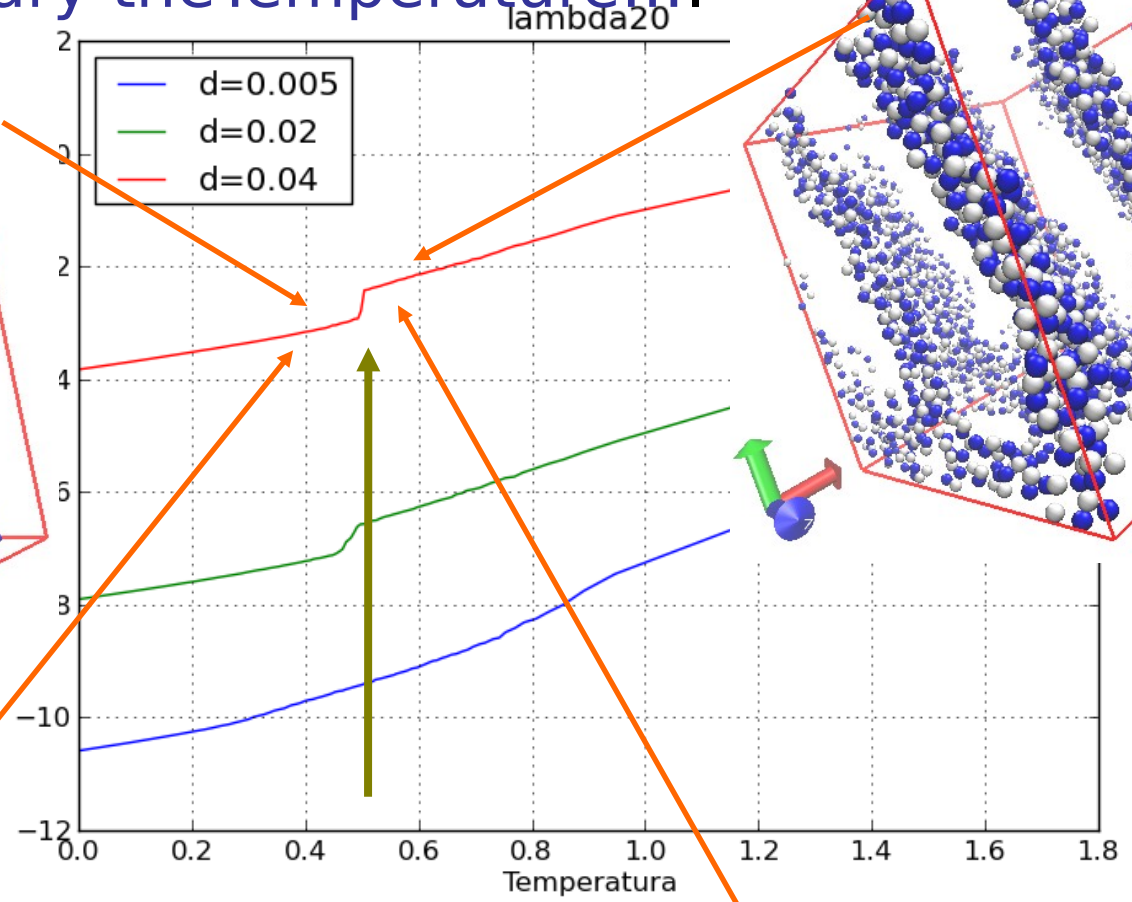

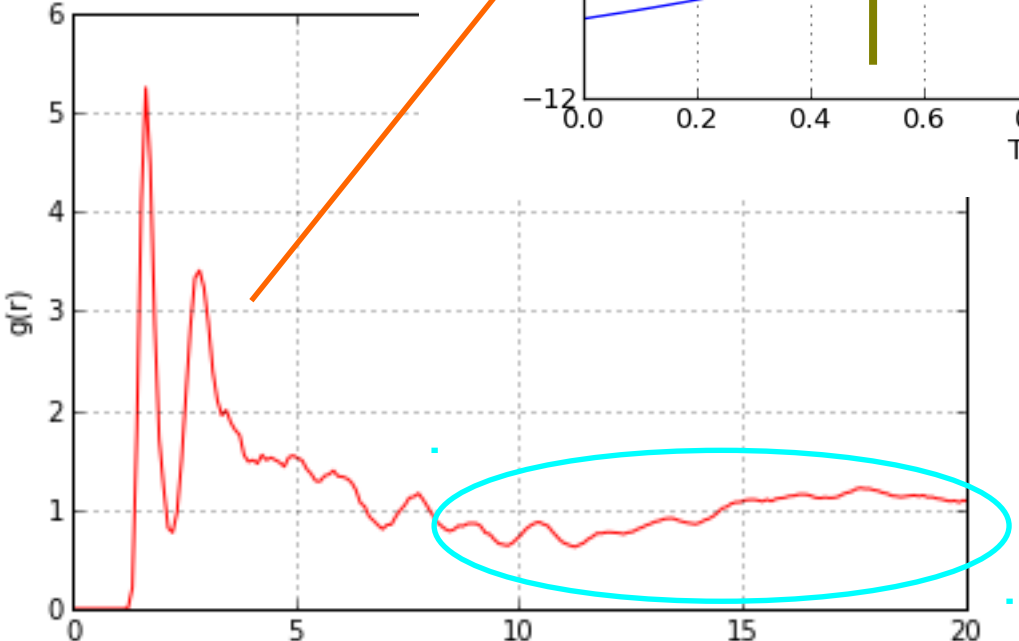

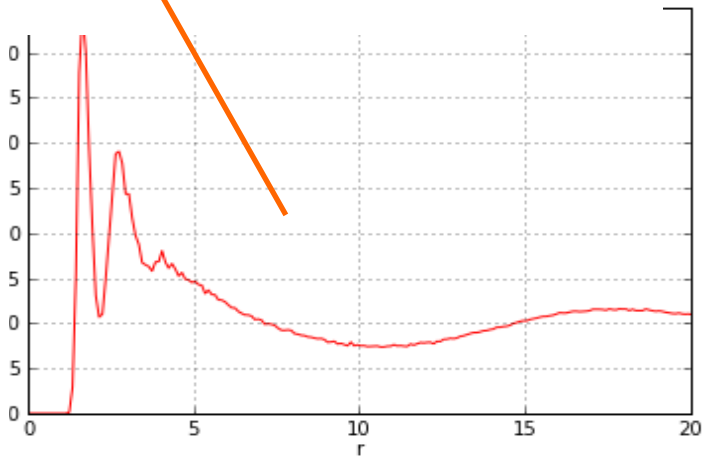

We now calculate de Lindemann coefficient

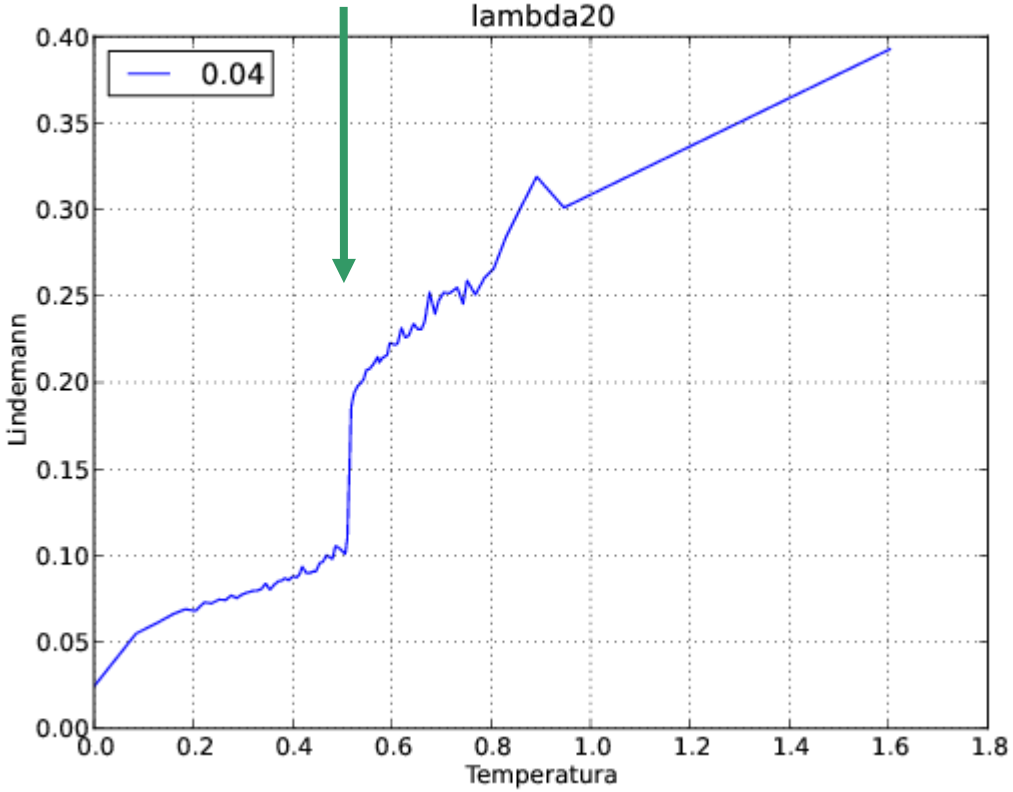

$$\Delta_L = \frac{1}{a'}\sqrt{\sum_i \left\langle \frac{\Delta r_i^2}{N} \right\rangle}$$

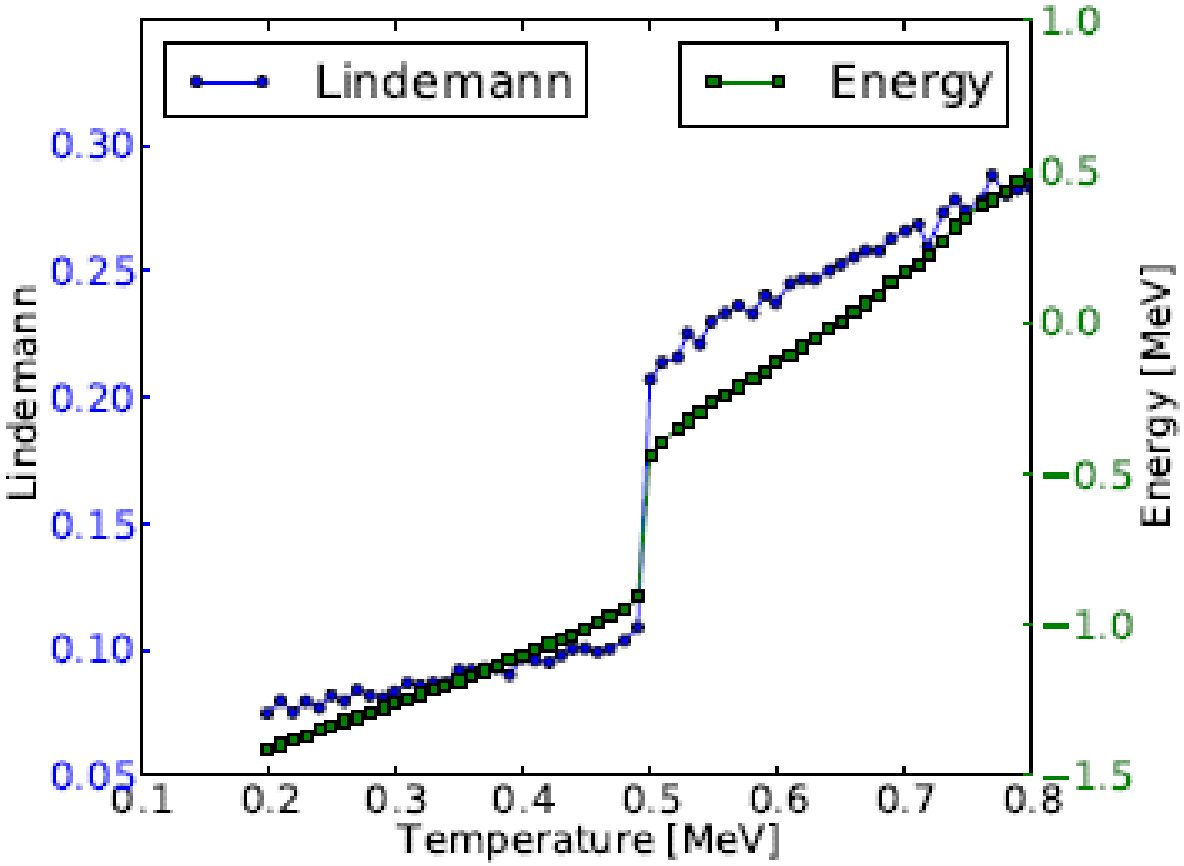

FIG. 2: Lindemann coefficient and energy as a function of temperature for a chosen density, $\rho = 0.05\,\mathrm{fm}^{-3}$. The sudden change in their value is a signal of a solid-liquid phase transition. We can see that both discontinuities are at the same temperature

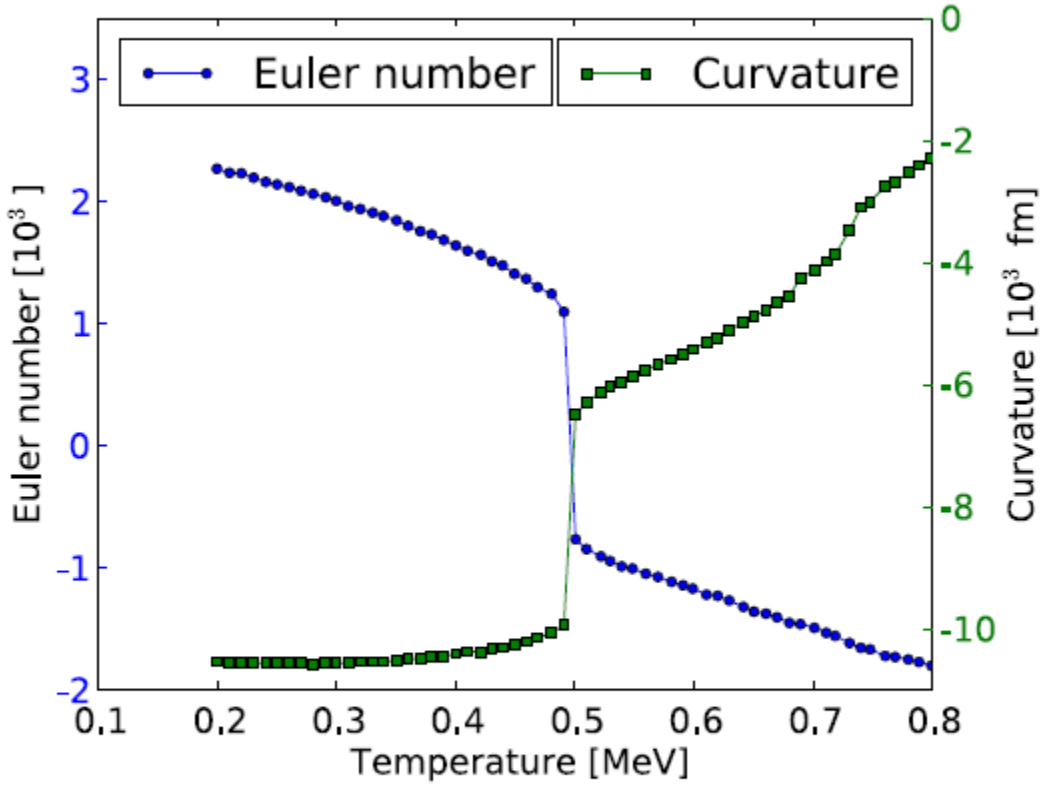

FIG. 4. (Color online) Euler number and mean breadth for $\rho = 0.05\,\mathrm{fm}^{-3}$. We observe a sharp transition for both Minkowski functionals.

Opacity

and

NS cooling

Temperature dependence of neutrino opacity of the Neutron star crust
P.N.Alcain, P.Gimenez Molinelli & C.O.Dorso,

Neutrino production in Neutron Stars

URCA process

$$n \rightarrow p + e + \overline{\nu}_e$$

$$p + e \rightarrow n + \nu_e$$

Structure Factor

$$S(q) = 1 + \rho \int_V \mathrm{d}r\, \mathrm{e}^{-i\,q\,r} g(r)$$

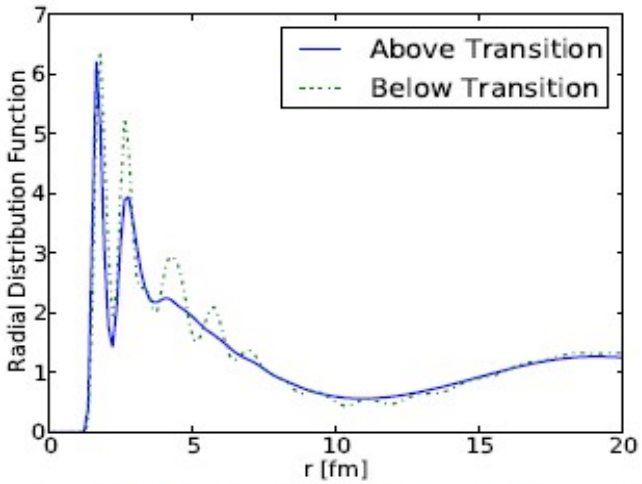

Radial distribution function for $\rho = 0.03\,\mathrm{fm}^{-3}$

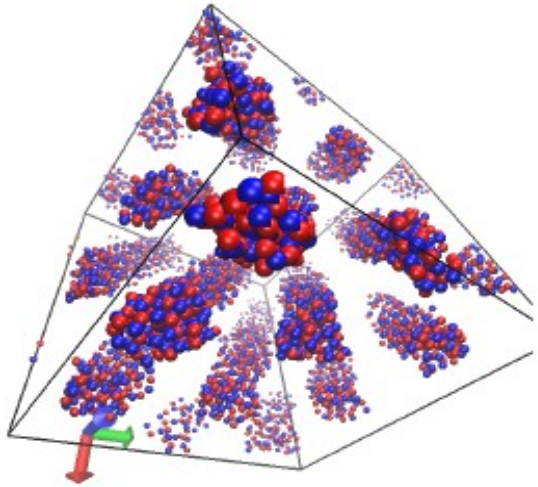

Snapshot of the system in the liquid phase for $\rho = 0.03\,\mathrm{fm}^{-3}$

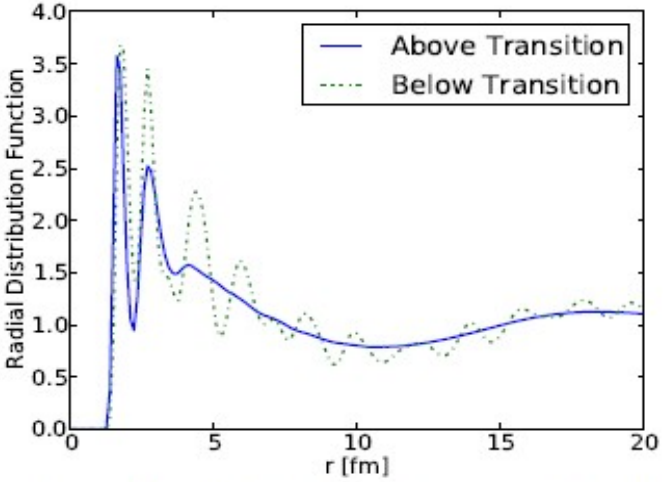

Radial distribution function for $\rho = 0.05\,\mathrm{fm}^{-3}$

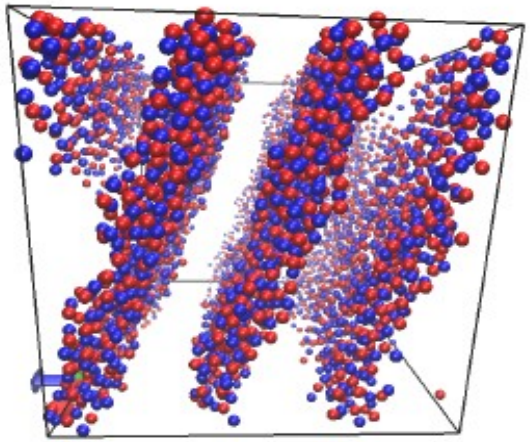

Snapshot of the system in the liquid phase for $\rho = 0.05\,\mathrm{fm}^{-3}$

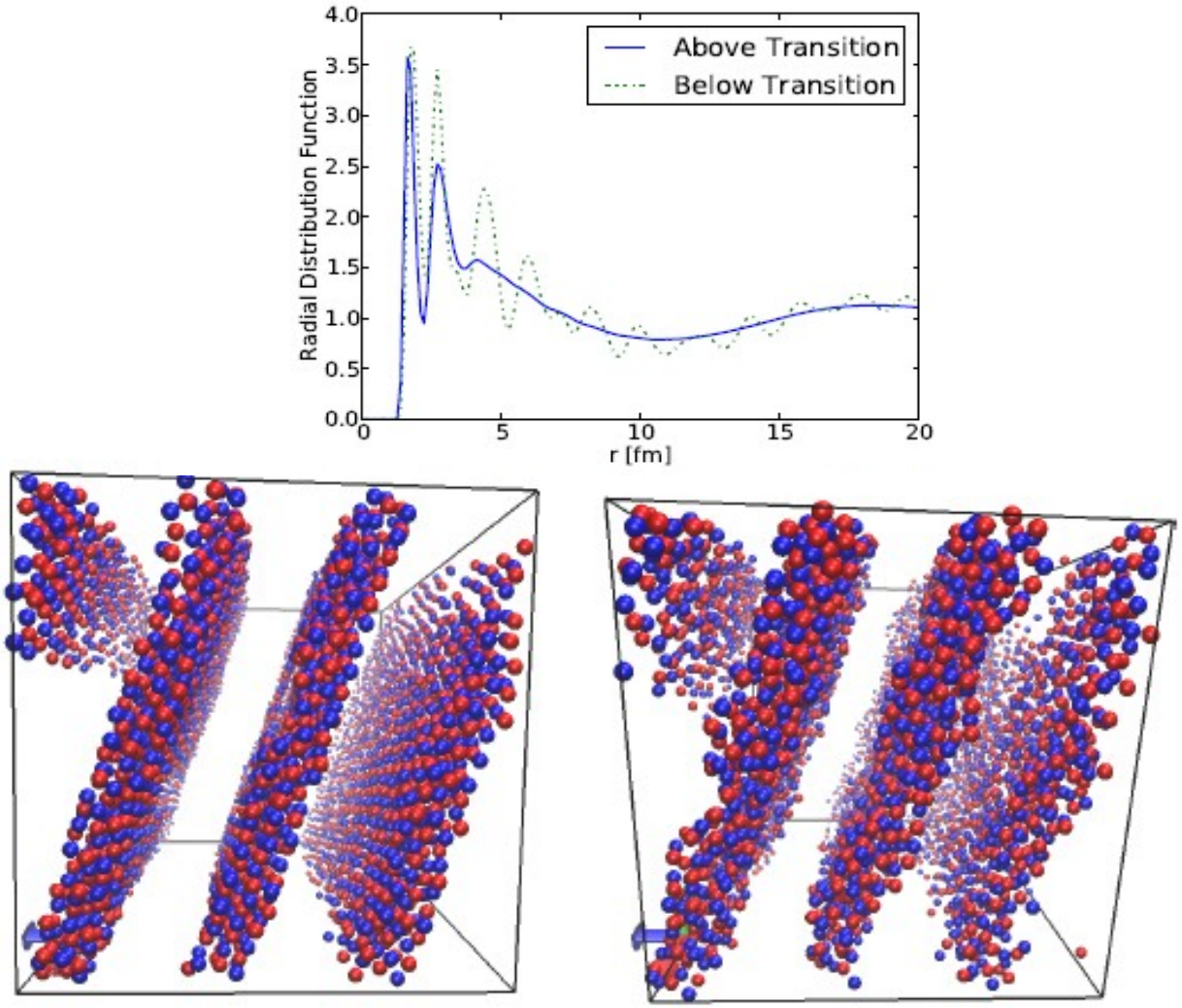

Below the transition

Above the transition

FIG. 6: Spatial distribution for $\rho = 0.05\,\mathrm{fm}^{-3}$, both above and below the transition temperature. The structures are similar, but much more disordered above the transition.

Temperature and morphology

Non traditonal pastas

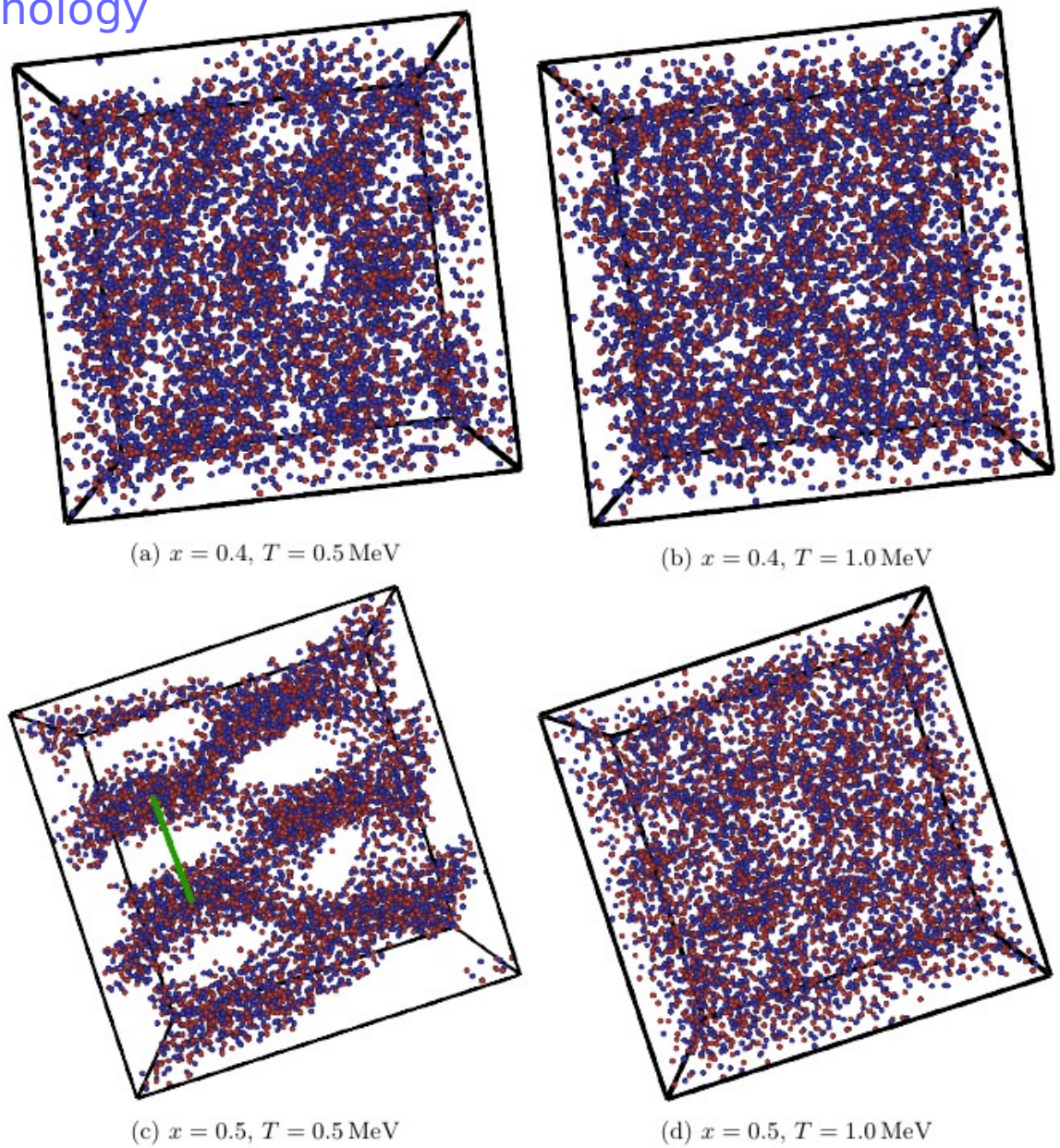

(a) $x = 0.4$, $T = 0.5\,\mathrm{MeV}$ (b) $x = 0.4$, $T = 1.0\,\mathrm{MeV}$

(c) $x = 0.5$, $T = 0.5\,\mathrm{MeV}$ (d) $x = 0.5$, $T = 1.0\,\mathrm{MeV}$

Figure 3: (Color online) Snapshots of a system with density $\rho = 0.04\,\mathrm{fm}^{-3}$ for different values of proton fraction and temperature, generated with VisIt [38]. Structures obtained at $T = 0.5\,\mathrm{MeV}$ differ substantially. Nevertheless both show inhomogeneities. We can see in panel 3c a green line marking a correlation length of $\approx 15\,\mathrm{fm}$.

Mass Max. Fragment

N ≈ 5500

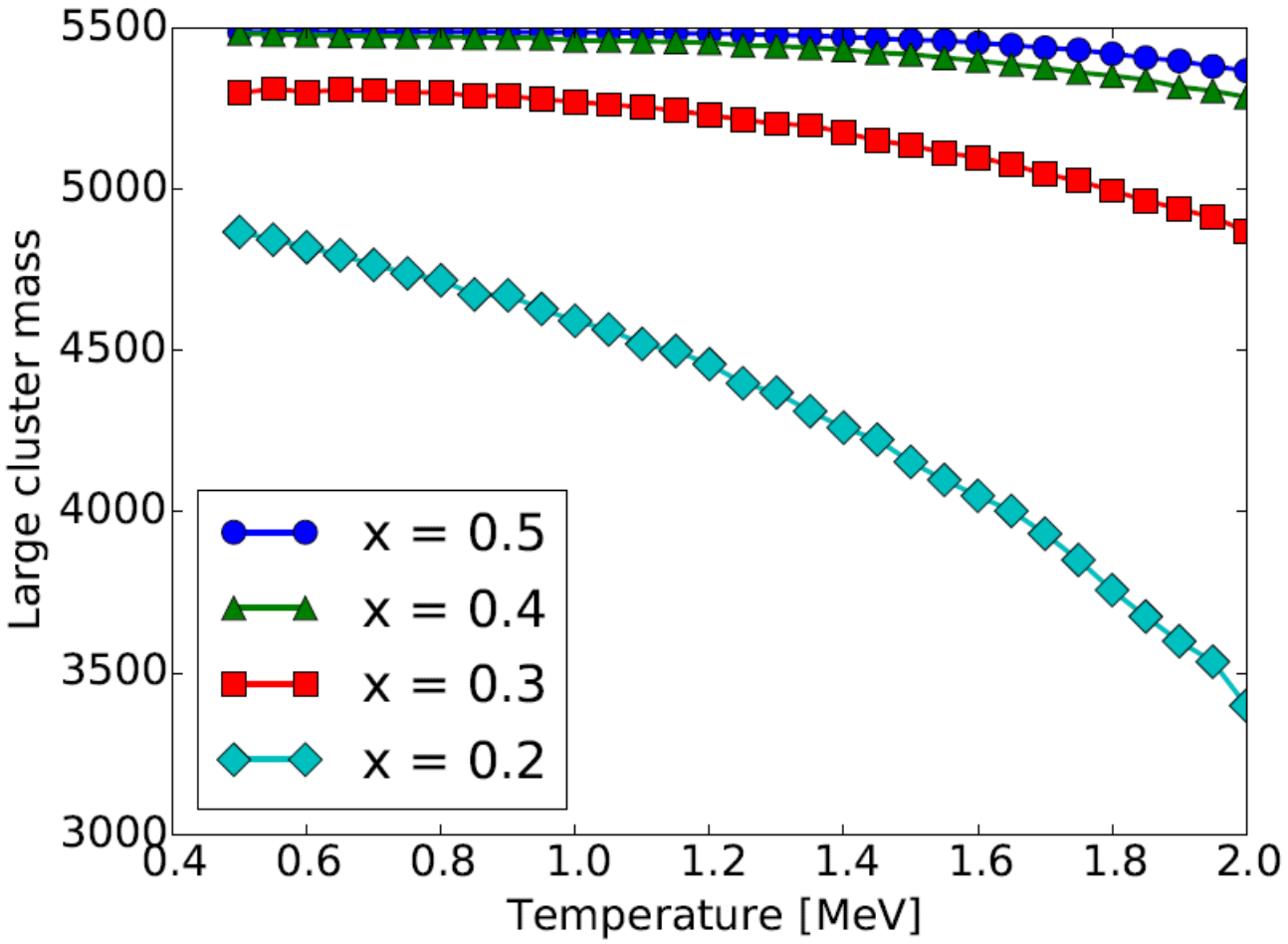

Figure 3: (Color online) Mass of the largest cluster for $\rho = 0.04\,\mathrm{fm}^{-3}$ for different values of x.

T=2.0MeV

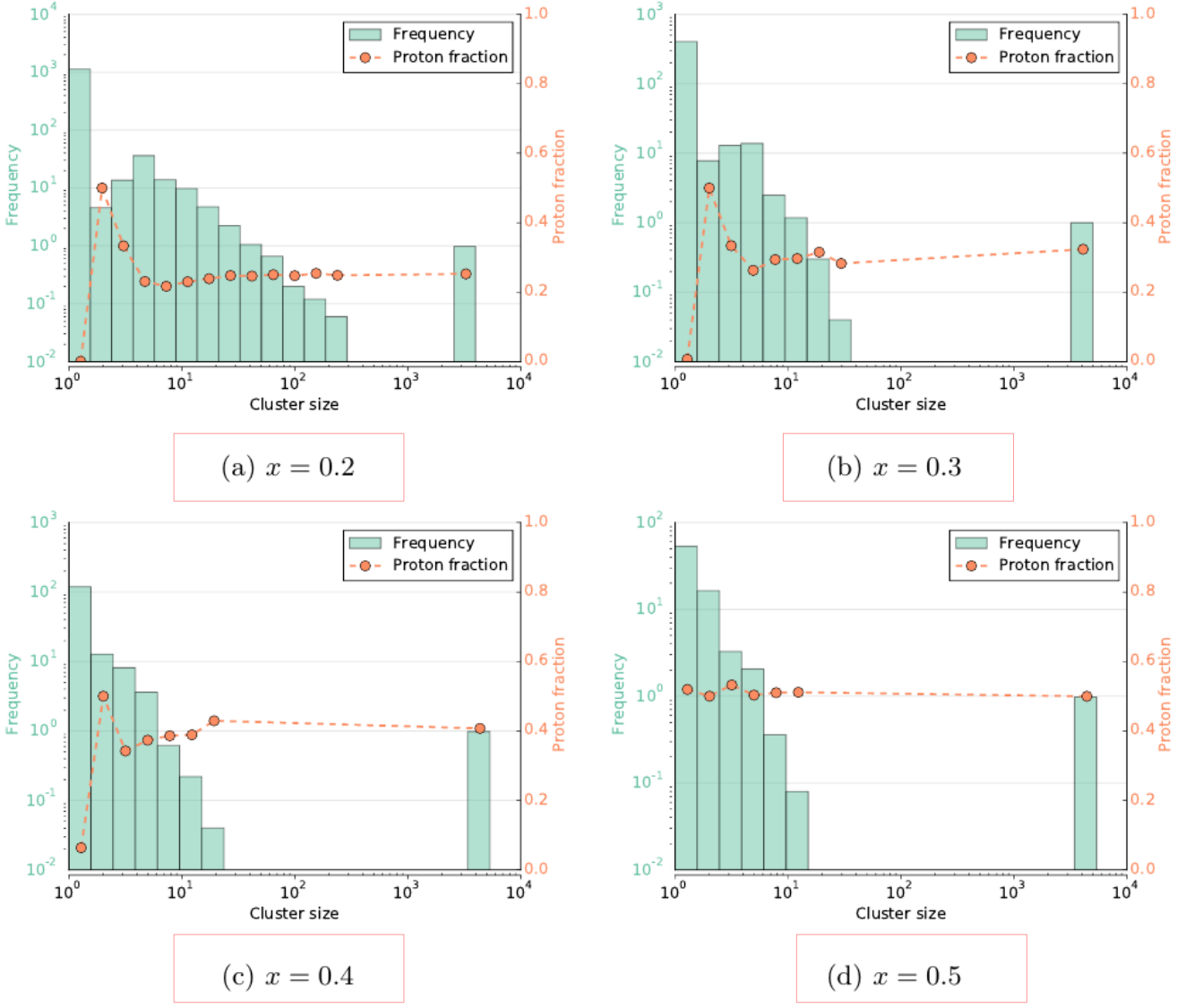

(a) $x = 0.2$

(b) $x = 0.3$

(c) $x = 0.4$

(d) $x = 0.5$

Figure 4: (Color online) Cluster distribution with MSTE algorithm for temperature $T = 2.0\,\mathrm{MeV}$, density $\rho = 0.04\,\mathrm{fm}^{-3}$ and different proton fractions. For the lowest of the studied proton fractions, $x = 0.2$, the large cluster has a higher proton fraction (about 30% higher) and there are many isolated neutrons. Please note that the scales are different for each graph.

Radial Distribution function

X=0.5
T=0.5
ρ=0.05

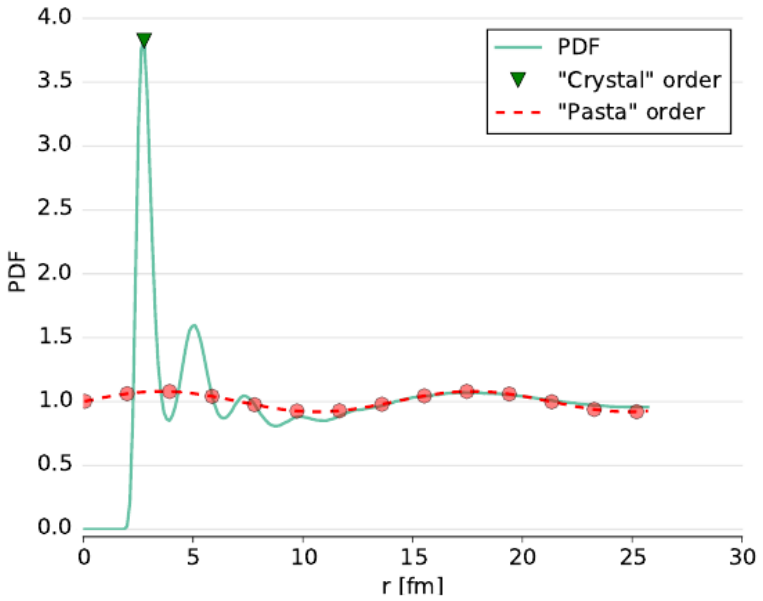

(a) Pair distribution function.

Structure Factor

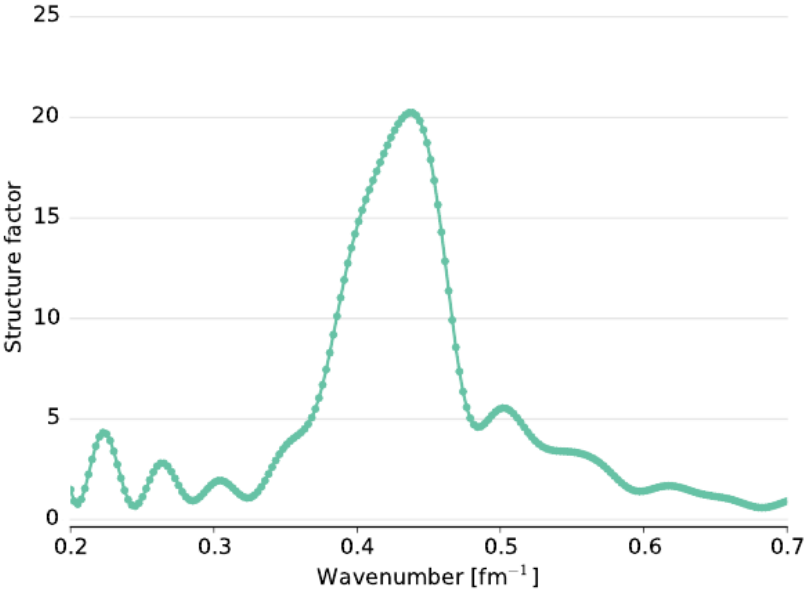

(b) Static structure factor.

Figure 6: (Color online) 6a Pair distribution function and 6b static structure factor for a system with proton fraction $x = 0.4$, density $\rho = 0.04\,\mathrm{fm}^{-3}$ and temperature $T = 0.5\,\mathrm{MeV}$. The first peak in the $g(r)$ due to crystalline structures is marked with ▼, while the very long range order is marked with a dashed line – –. In the structure factor we can see the peak located at $q_{\mathrm{peak}} = 0.43\,\mathrm{fm}^{-1}$ with a width of about $\mathrm{FWHM} = 0.08\,\mathrm{fm}^{-1}$. The ripples for low wavenumbers are due to finite size effects.

Absorption peak wavelength

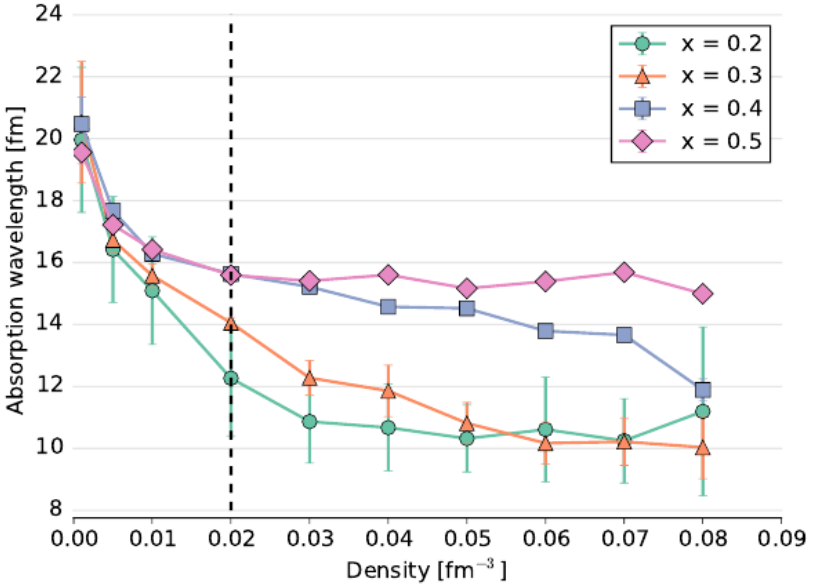

(a) Absorption peak wavelength

Absorption peak height

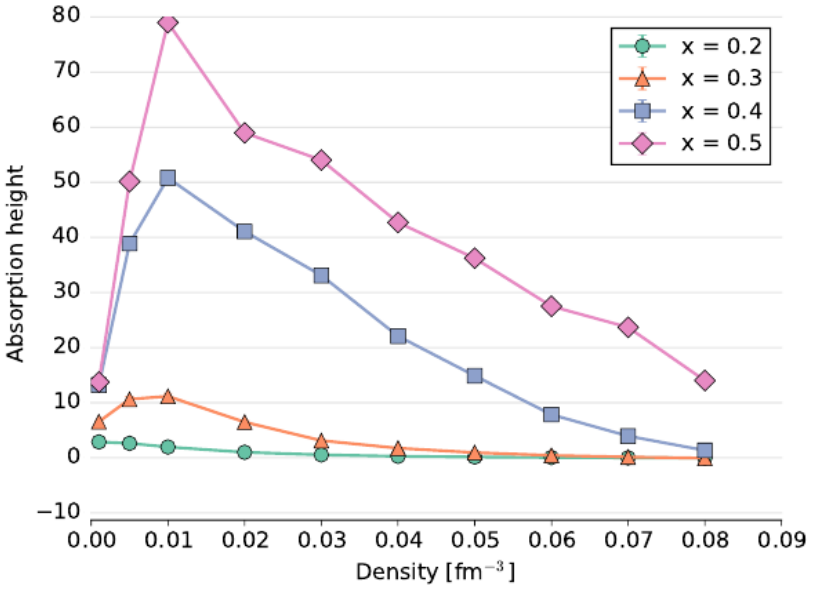

(b) Absorption peak height

Absorption peak 7a wavelength and 7b height for low temperature ($T = 0.5\,\mathrm{MeV}$) as a function of density for different proton fractions. We can see the wavelength changing rapidly for $\rho < 0.02\,\mathrm{fm}^{-3}$ (*gnocchi* phase) and stabilizing for higher densities.

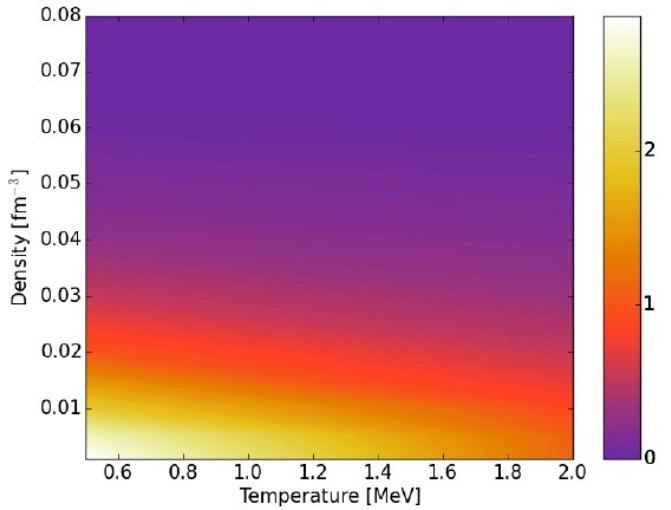

(a) $x = 0.2$

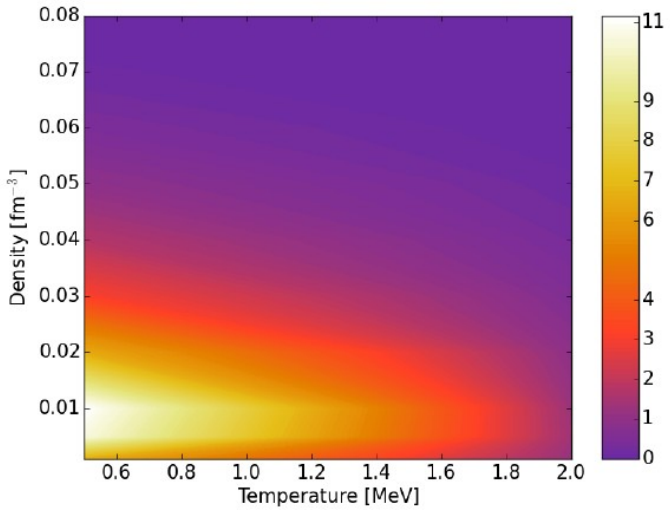

(b) $x = 0.3$

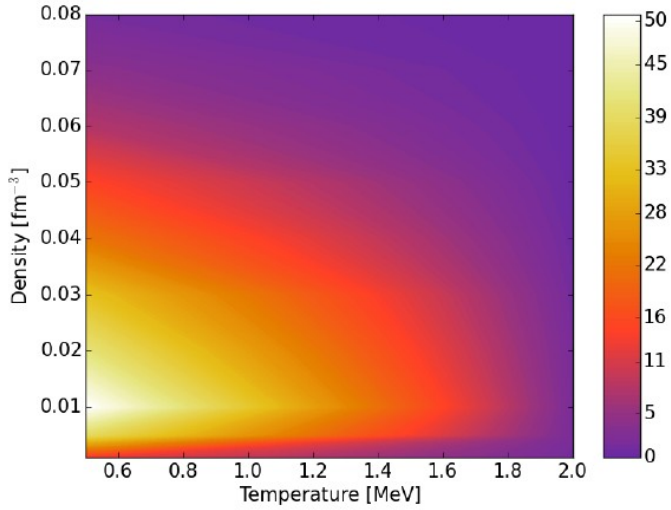

(c) $x = 0.4$

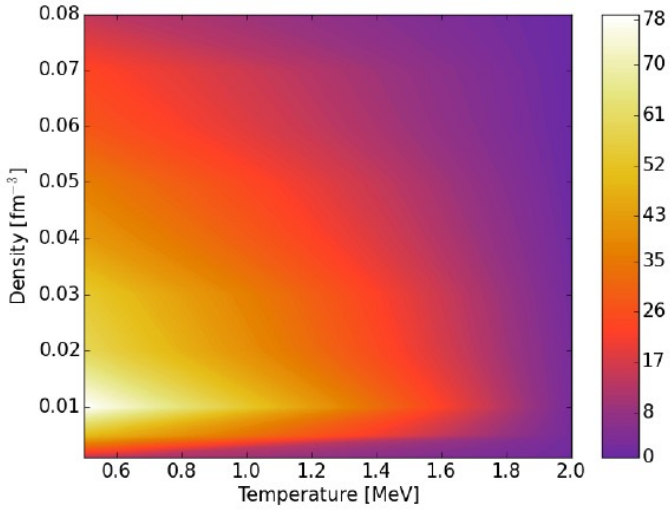

(d) $x = 0.5$

Figure 9: (Color online) Absorption peak in the Urca wavelength for different proton fractions as a function of temperature and density. It can be seen that the absorption decreases drastically for $T \gtrsim 0.8\,\mathrm{MeV}$. We also show here that the absorption is affected by the proton fraction, as can be noted by the scales on the color bar. Also note that the absorption for $x = 0.2$ and $x = 0.3$, the results are governed by noise.


WORK IN PROGRESS

Fragmentation of

Expanding Neutron Star Matter

Preliminary Results

Infinite expanding system

The microscopic Big Bang

$$\mathbf{P}_i^{\mathrm{coll}} = h \frac{\mathbf{R}_i}{\rho_0^{-1/3}} P_{\mathrm{F}},$$

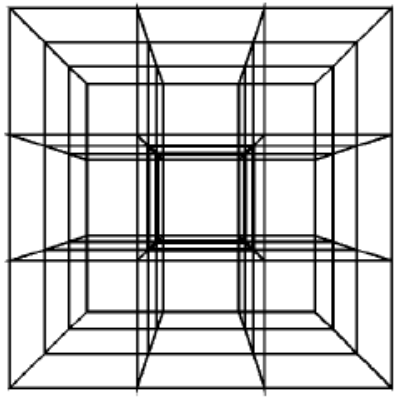

FIG. 1. A schematic picture of the periodic boundary. The primitive cell marked by thick lines is surrounded by 26 replica cells.

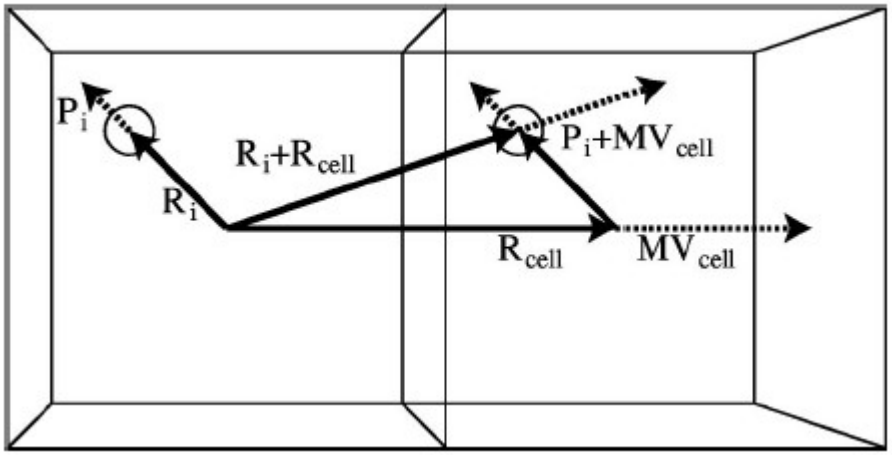

$$L(t) = L_0(1 + \eta\, t)$$

C. O. Dorso and A. Strachan, Phys. Rev. B **54**, 236 (1996).

Cluster Models

$$i \in C_n^{\mathrm{MST}} \Leftrightarrow \exists j \in C_n \mid r_{ij} < r_{cut}$$

$$i \in C_n^{\mathrm{MSTE}} \Leftrightarrow \exists j \in C_n : V_{ij} + K_{ij} \leq 0$$

$$\epsilon_n = \sum_{i \in C_n} K_i^{CM} + \sum_{i,j \in C_n} V_{ij}$$

Infinite MST-Cluster

Recognition

We developed an algorithm for the recognition of infinite clusters across the boundaries. We explain here in detail the implementation for MST clusters in 2D, being the MSTE and 3D extension straightforward. In figure 6 we see a schematical representation of 2D clusters recognized in a periodic cell, labeled from 1 to 6 (note that these clusters don't connect yet through the periodic walls).

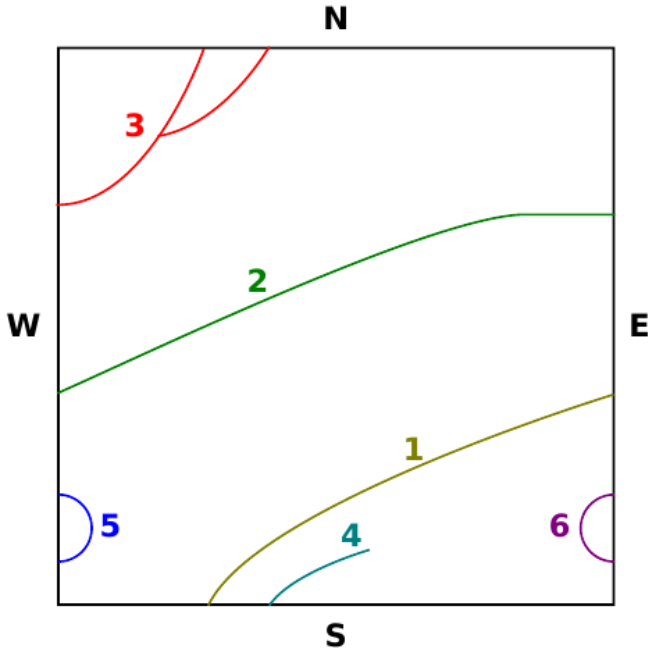

Figure 6: (Color online) Schematical representation of 2D clusters, recognized only in the cell and not through the periodic walls, labeled as N, S, W, E. The clusters inside the cell are labeled from 1 to 6,

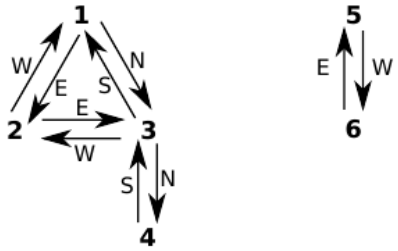

Figure 7: Graph of the clusters with connections labeled by the wall of the boundary they connect through. The graph can be divided in 2 subgraphs that don't connect: 1–2–3–4 and 5–6. Each of these subgraphs is as cluster when periodic boundary conditions are considered.

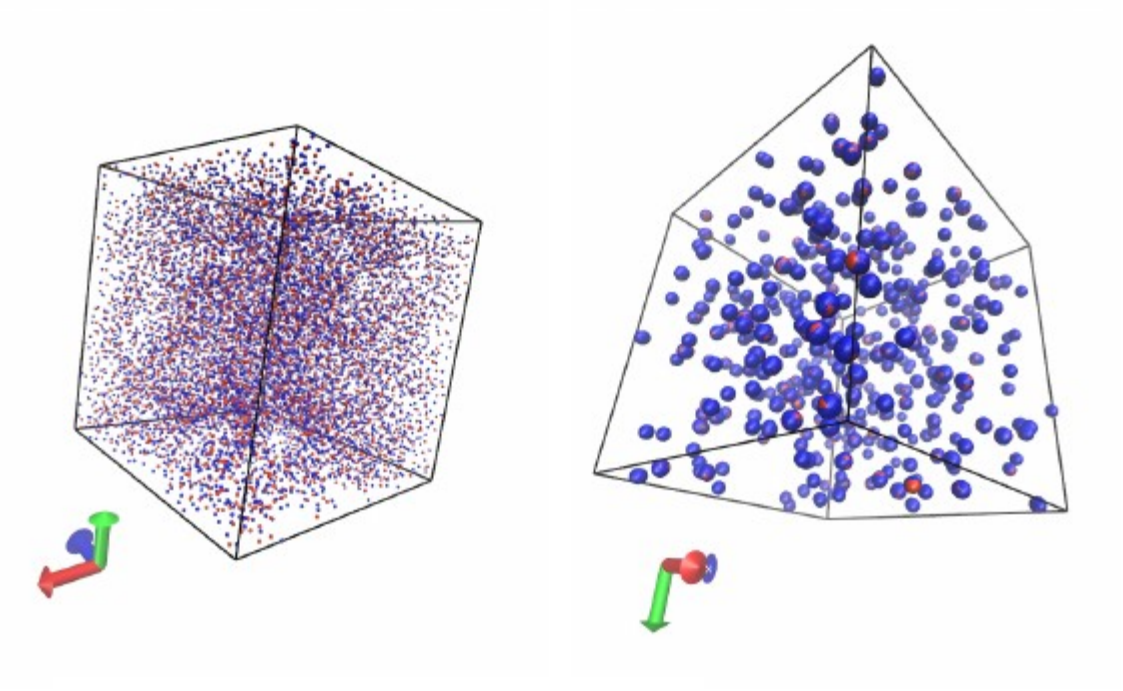

N=11000

$\eta = 0.0005\,\mathrm{fm/c}$

Snapshots of a system in the initial configuration a and the final expanded system b In the expanded system we see clearly formed *gnocchi* clusters

Dens : 0.05; Temp : 0.5; X : 0.1

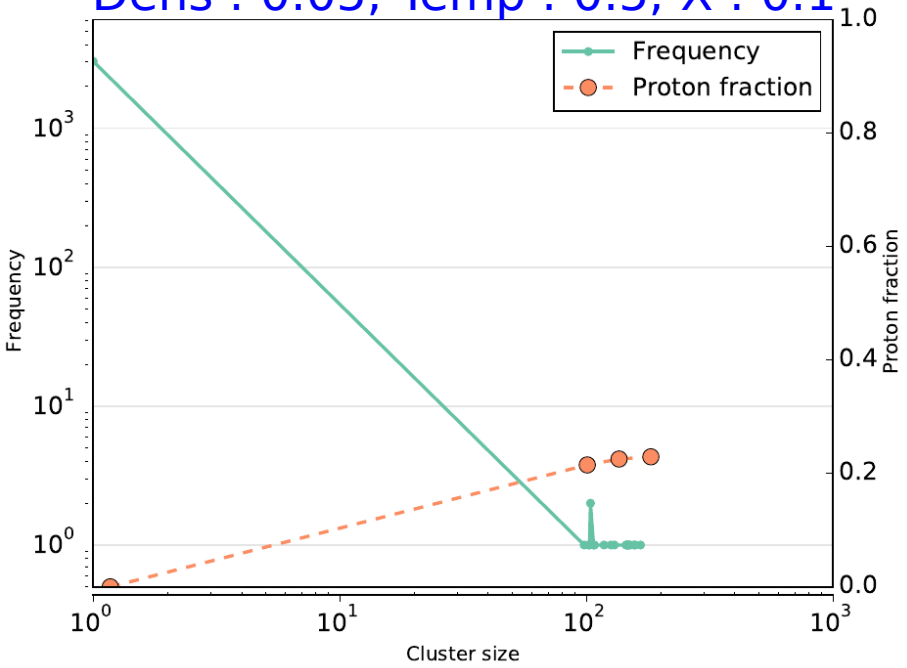

Dens : 0.05; Temp : 0.1; X : 0.4

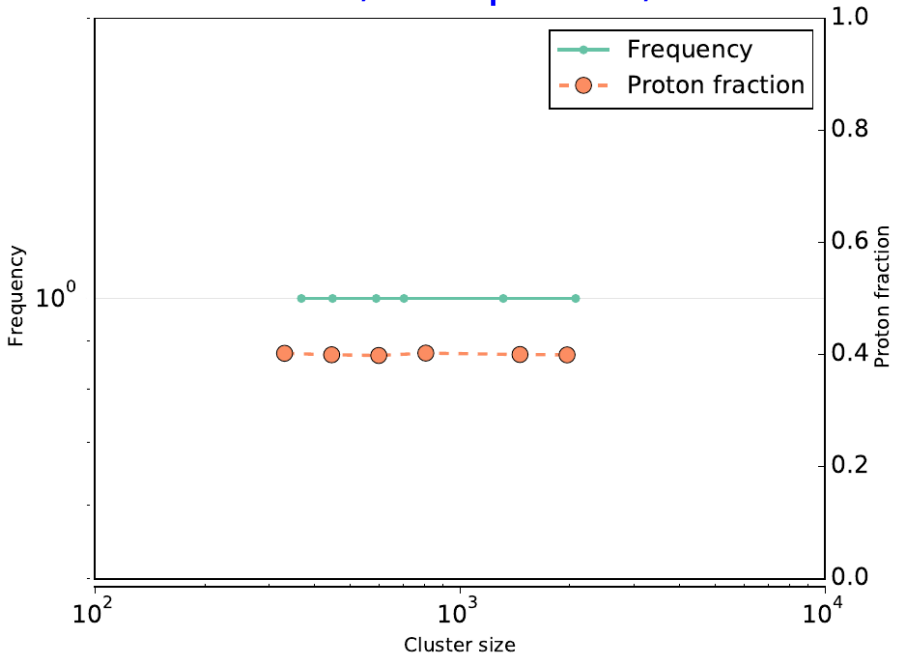

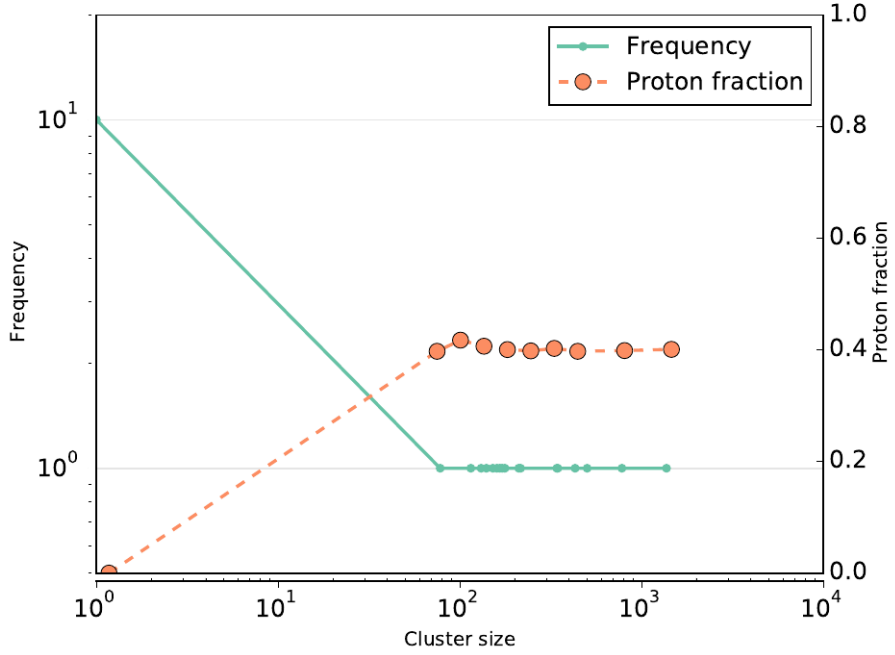

Dens : 0.05; Temp : 0.5; X : 0.4

Thermal Conductivity of Nuclear “Pasta”

Preliminary Results

In Collaboration with A.Strachan & J Dunn (Purdue)

Methodology

Muller-Plathe Method:

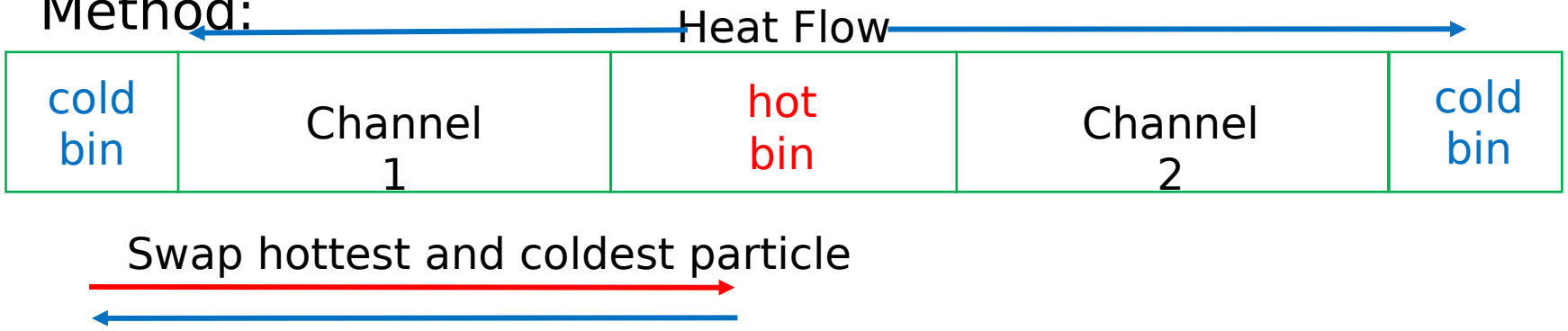

- Continuously swapping the hottest particle in the cold bin with the coldest particle in the hot bin imposes a temperature gradient on the system, which also generates a continuous heat flow
- Thermal conductivity is then calculated using Fourier's Law:

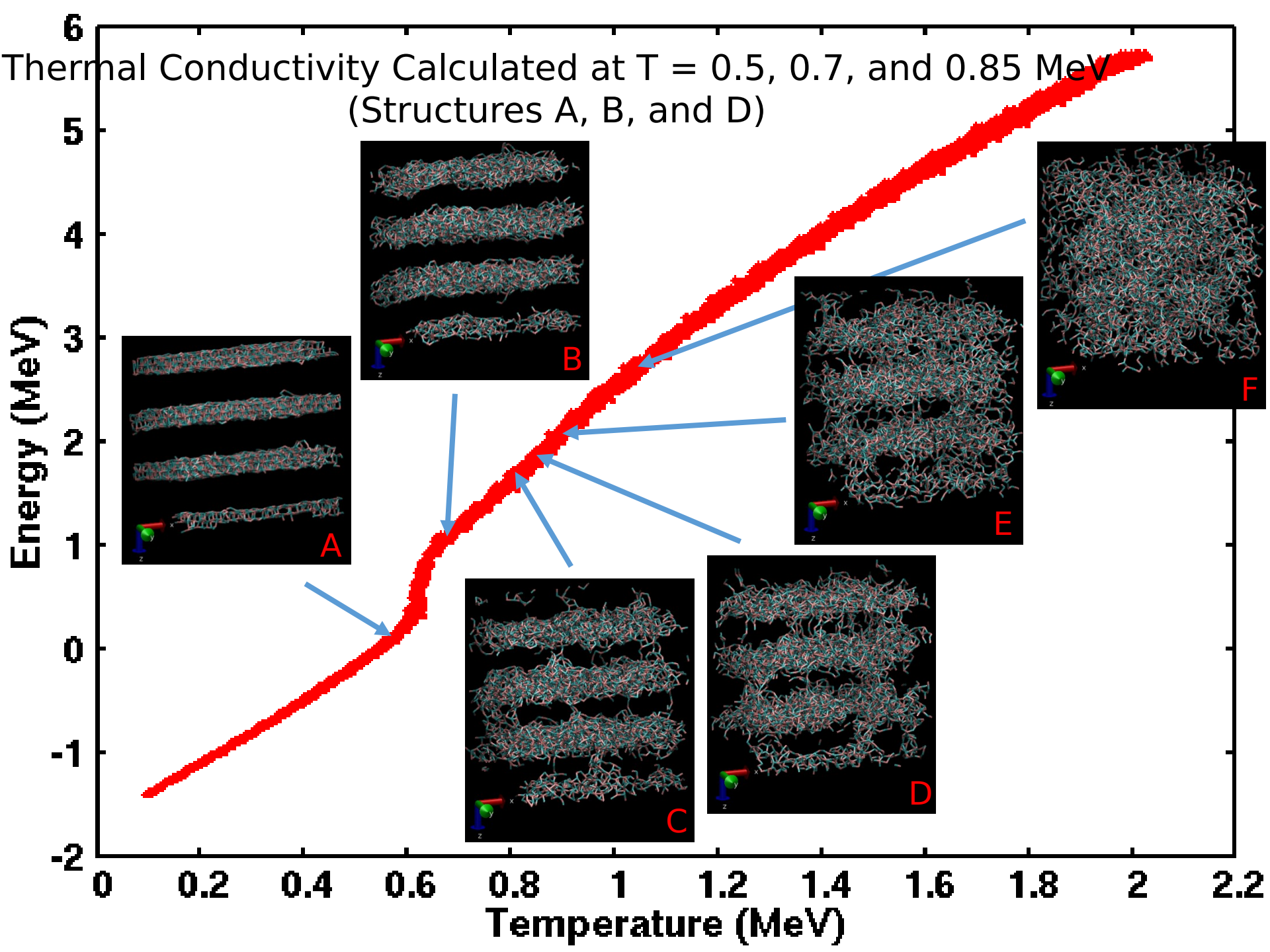
Thermal Conductivity Calculated at T = 0.5, 0.7, and 0.85 MeV
(Structures A, B, and D)
Energy (MeV)
Temperature (MeV)
6
5
4
3
2
1
0
-1
-2
0
0.2
0.4
0.6
0.8
1
1.2
1.4
1.6
1.8
2
2.2
A
B
C
D
E
F

Preliminary Results for Thermal Conductivity

Along with heat flux and temperature gradient

•The difference in temperature between the hot and cold bins are too high in these calculations, so simulations with a slower swapping have been submitted.

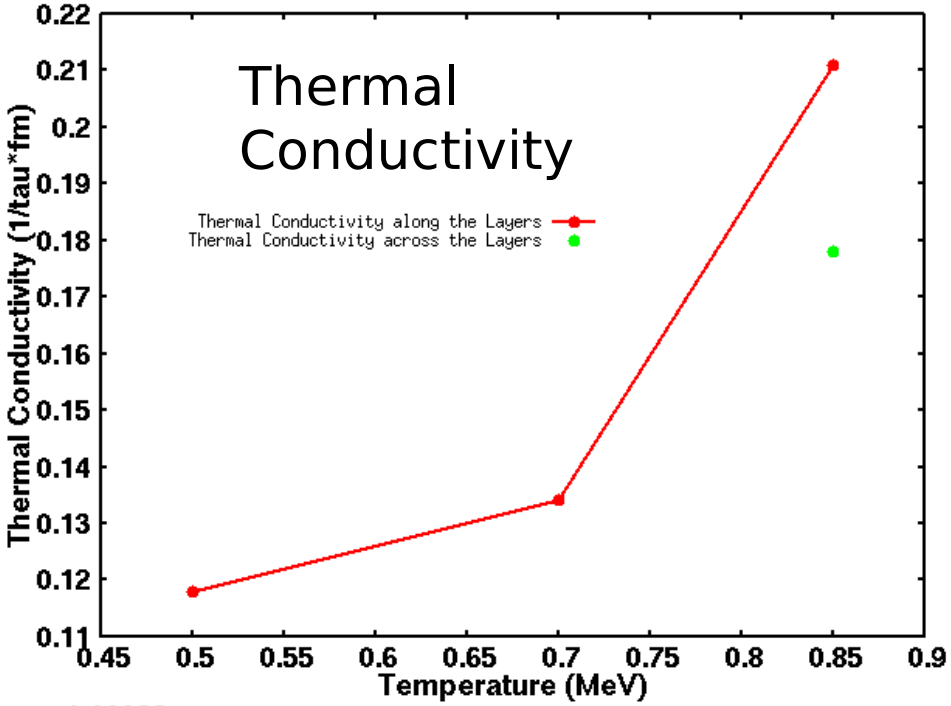

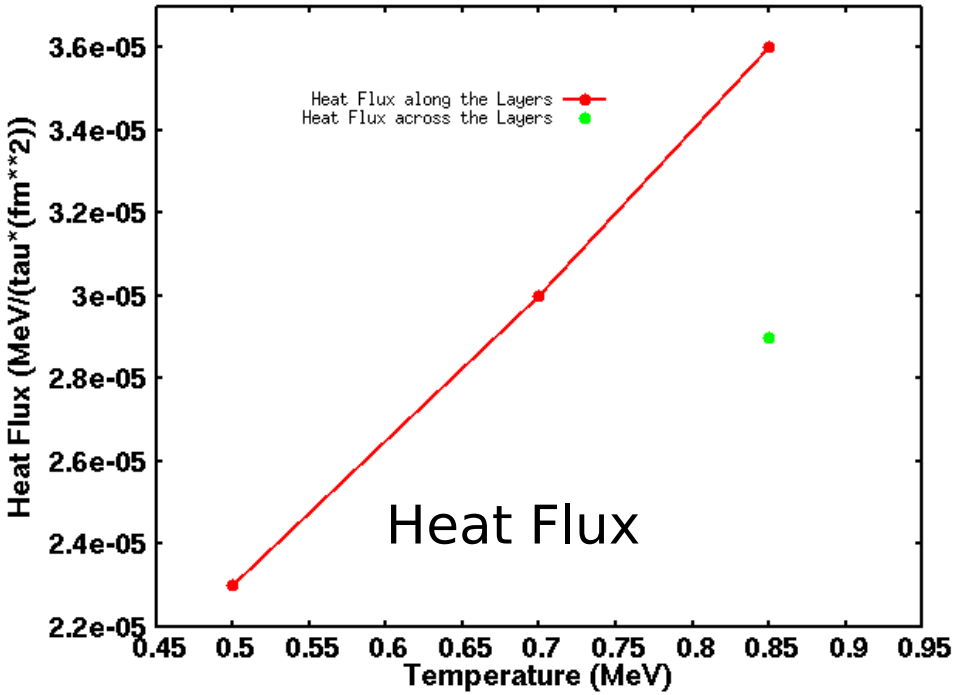

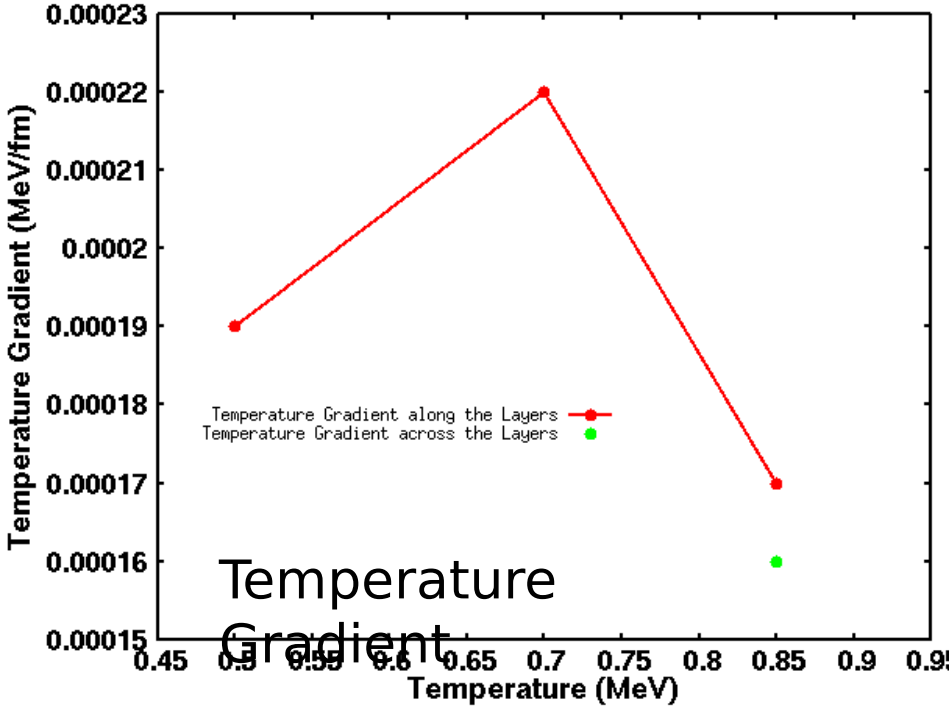

Structure at 0.5 MeV

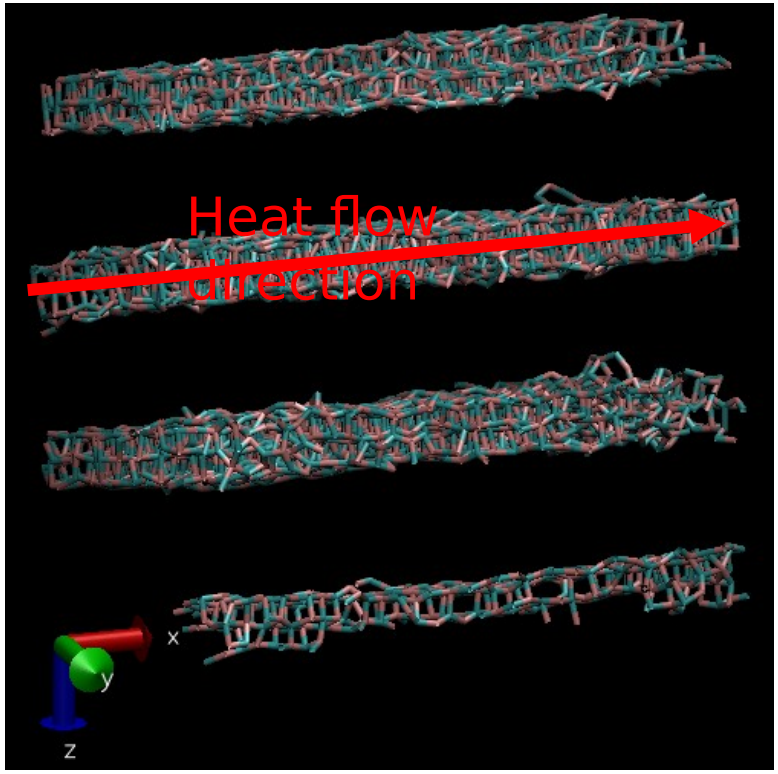

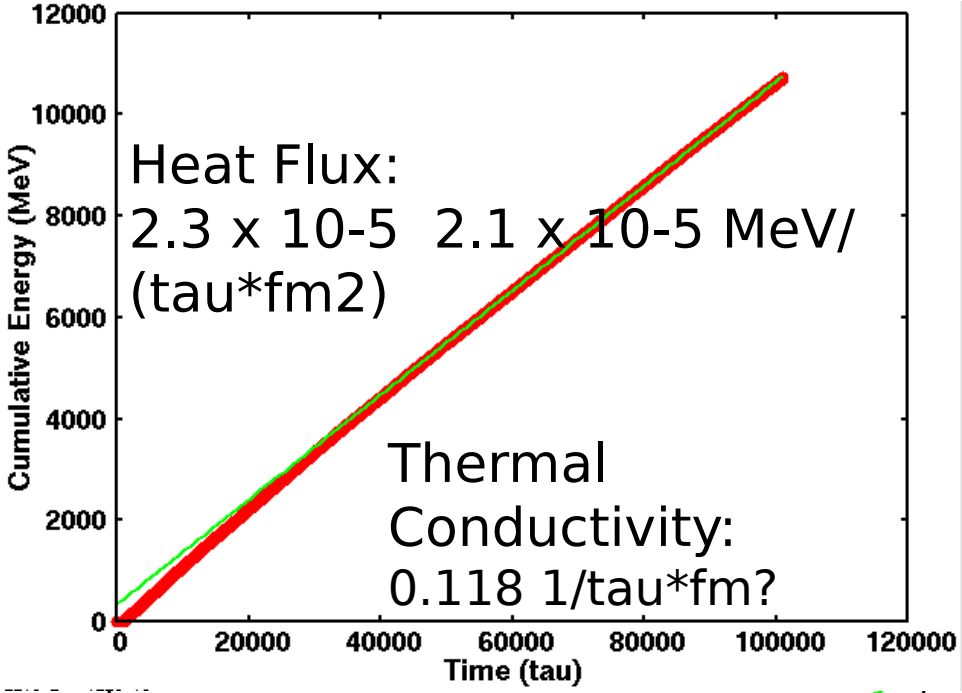

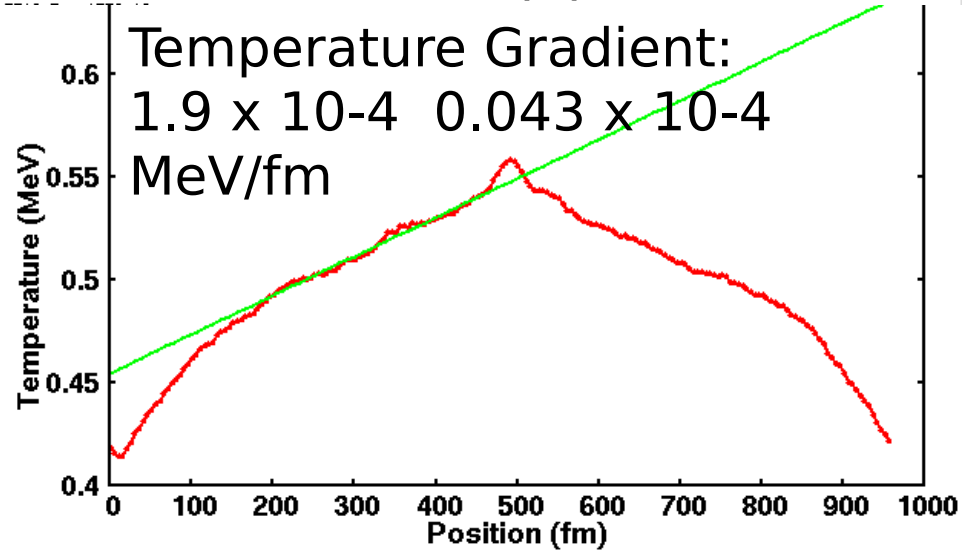

Simulation Details:
Timestep: 0.1
Swap rate: 1 time every 400 timesteps
Equilibrated for 10,000 timesteps
Ran Muller-Plathe for 1,000,000 timesteps
Averaged results over last 500,000 timesteps

Structure at 0.7 MeV

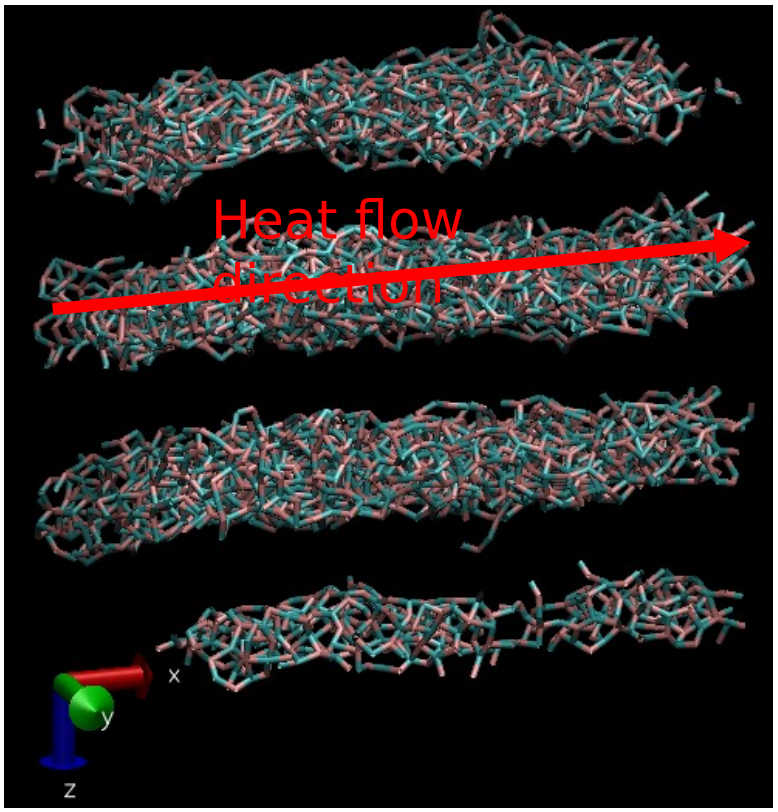

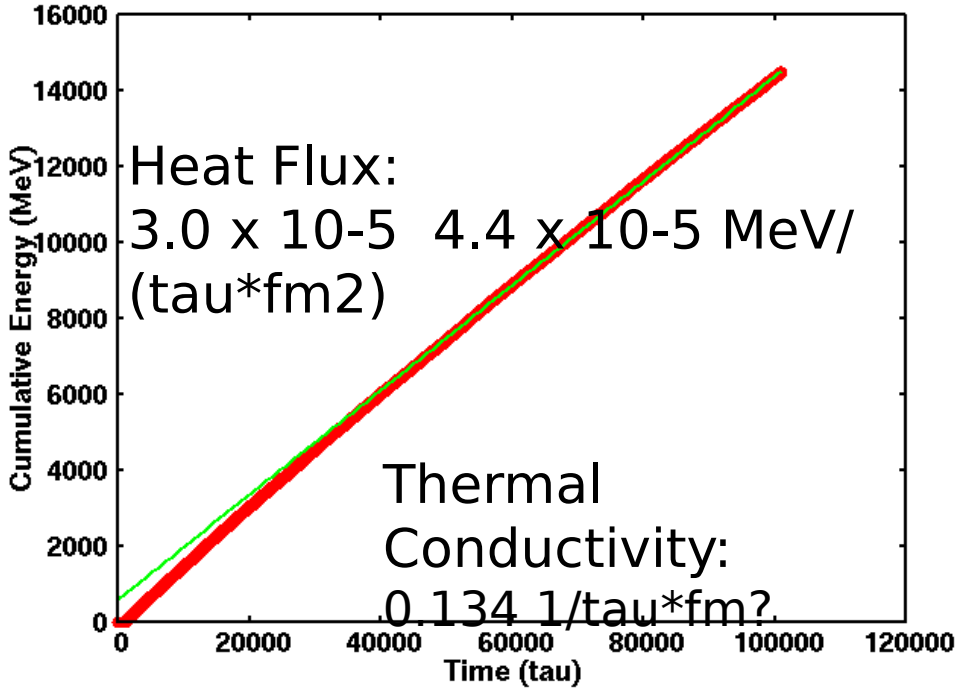

Simulation Details:
Timestep: 0.1
Swap rate: 1 time every 400 timesteps
Equilibrated for 10,000 timesteps
Ran Muller-Plathe for 1,000,000 timesteps
Averaged results over last 500,000 timeste

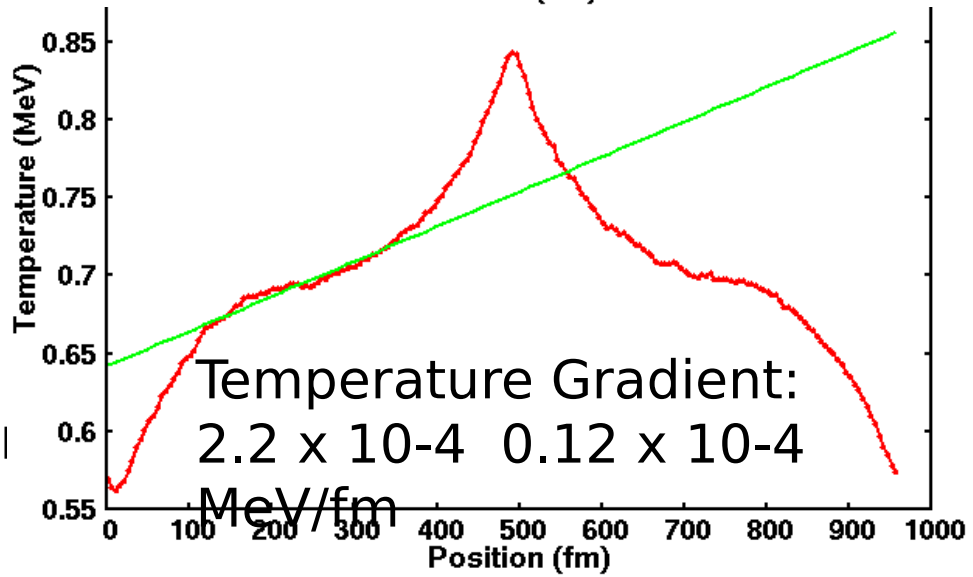

Structure at 0.85 MeV

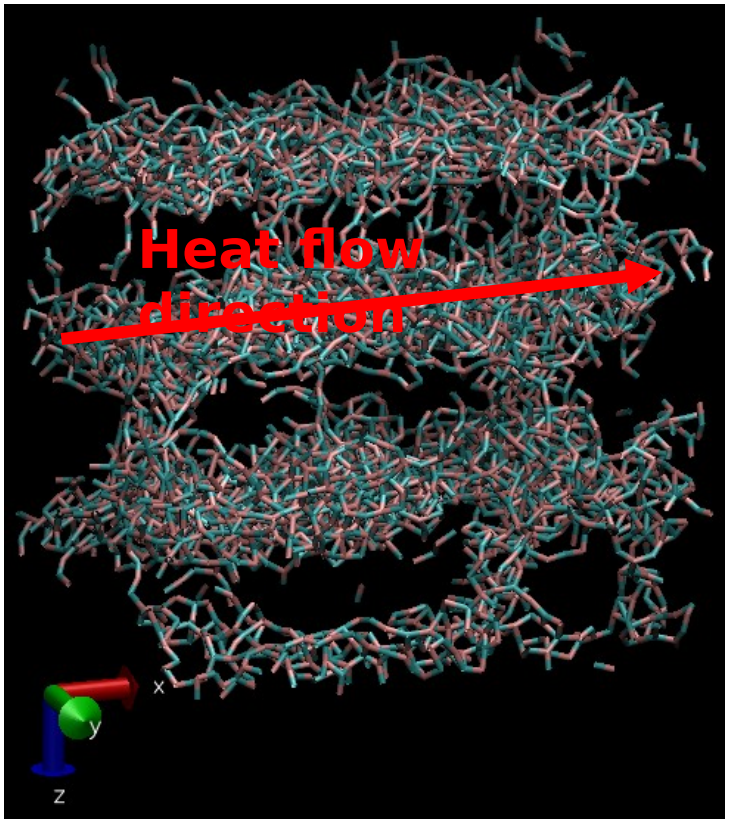

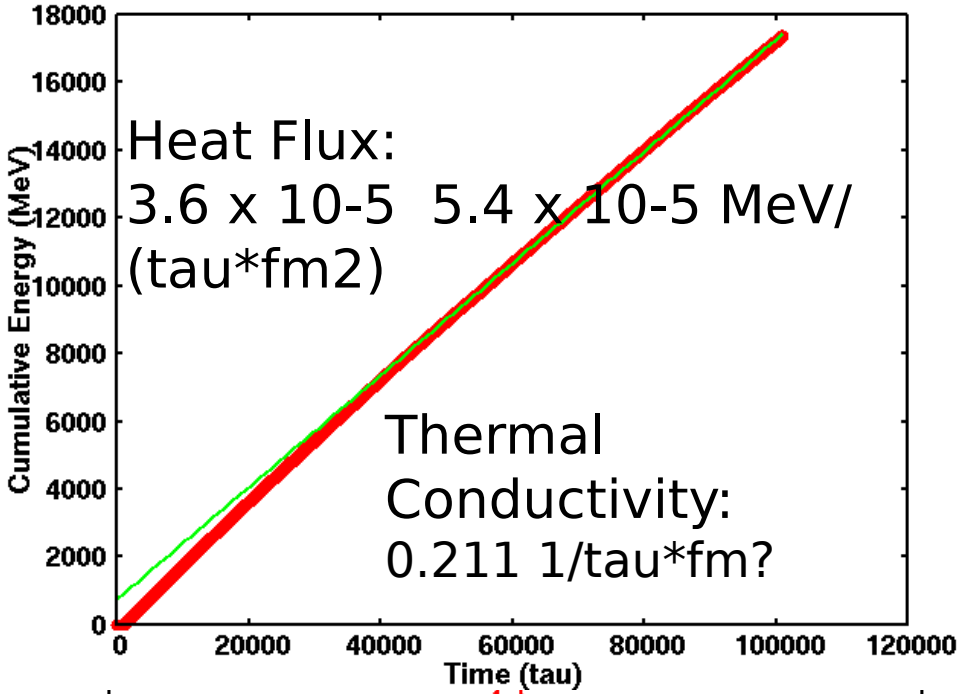

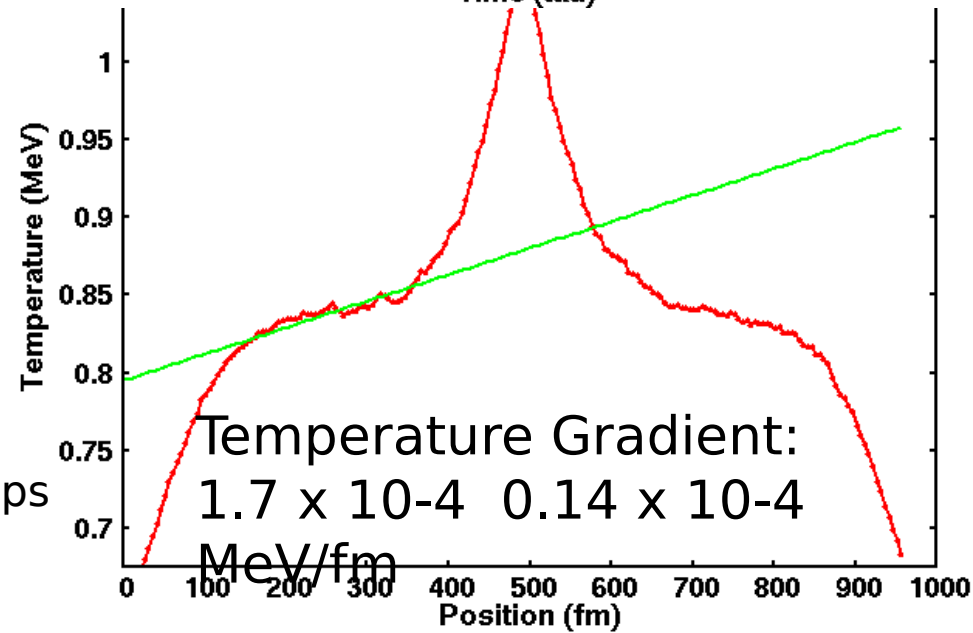

Simulation Details:
Timestep: 0.1
Swap rate: 1 time every 400 timesteps
Equilibrated for 10,000 timesteps
Ran Muller-Plathe for 1,000,000 timesteps
Averaged results over last 500,000 timesteps

Structure at 0.85 MeV (heat flow across layers)

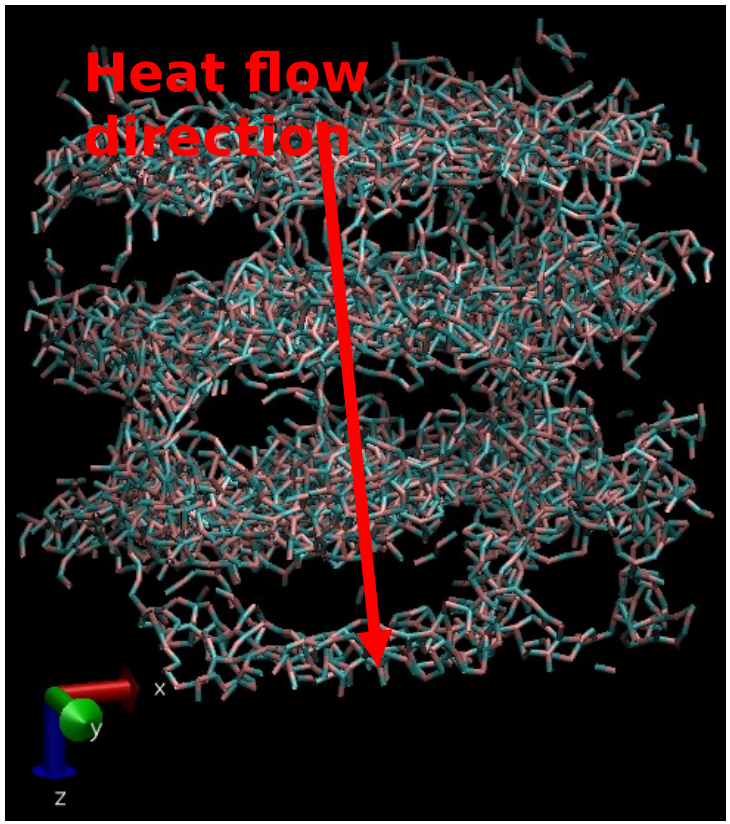

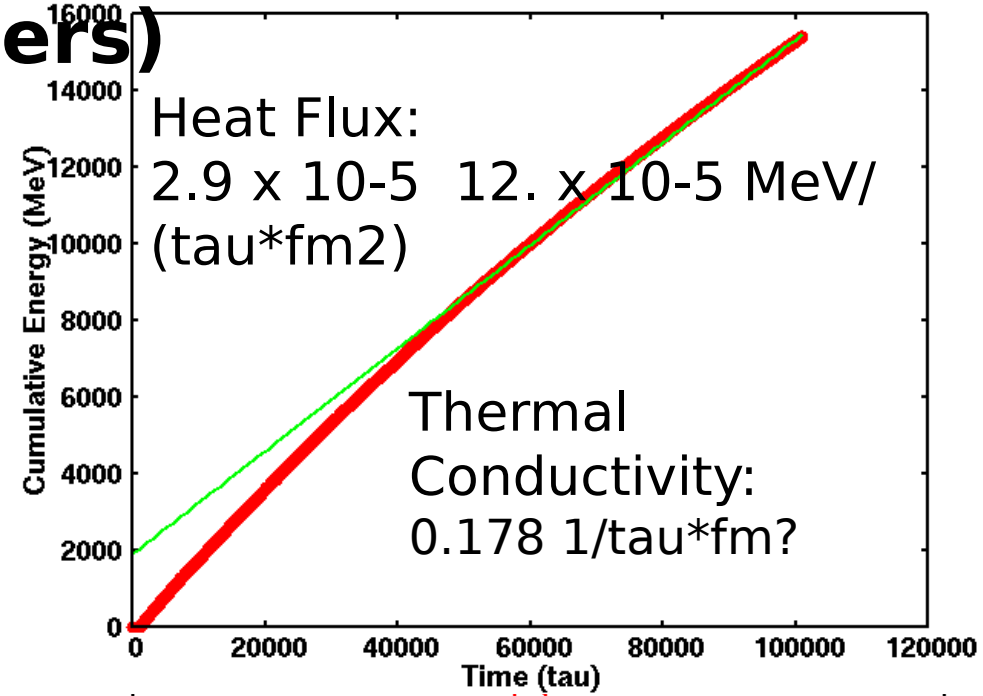

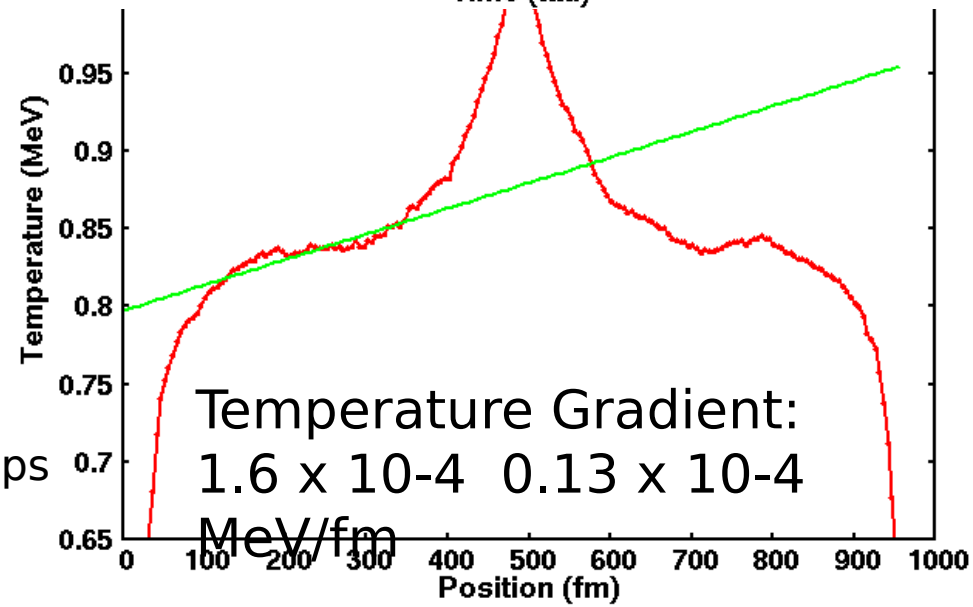

Simulation Details:
Timestep: 0.1
Swap rate: 1 time every 400 timesteps
Equilibrated for 10,000 timesteps
Ran Muller-Plathe for 1,000,000 timesteps
Averaged results over last 500,000 timesteps

Conclusions

Systems with competing interactions undergo “pasta” formation at Low temperatures

Systems with hc + attractive interactions (i.e. LJ) display “1 per cell pasta” at Low Temperatures

This systems can be properly described by

- Minkowsky functionals
- Correlation functions
- Fragments mass distributions

When the long range part of the potential is of the form Coulomb+Debye screening there is a λ_c such that below it, the systems moves into the “1 per cell pasta” regime

A jump in energy when increasing T associated with morphological change has been detected, Also in the Lindemann coefficient

At low temperatures well defined pastas (well ordered)

As temperature rises solid-liquid phase transitions within pastas

At higher Temperatures Pasta→Pastasciuta

Neutrino opacity for Nuclear Pastas

Neutrino opacity for non traditional Pastas (pastasciuta)

Fragmentation of expanding infinite Neutron Star Matter (N~51000)


Thank you